COMPUTER AIDED PRODUCT AND PROCESS DESIGN SYSTEM FOR AXISYMMETRIC DEEP DRAWING

By

P. V. Vijayakumar

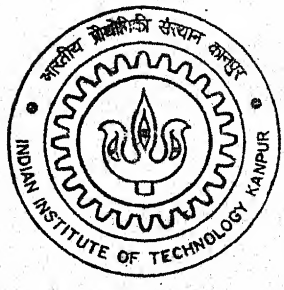

DEPARTMENT OF MECHANICAL ENGINEERING

Indian Institute of Technology Kanpur

MARCH, 2003

COMPUTER AIDED PRODUCT AND PROCESS DESIGN SYSTEM FOR AXISYMMETRIC DEEP DRAWING

A Thesis Submitted
In Partial Fulfilment of the Requirements
for the Degree of
Master of Technology

by

P. V. VIJAYAKUMAR

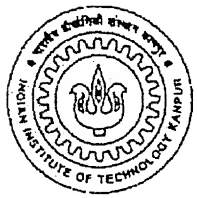

to the

DEPARTMENT OF MECHANICAL ENGINEERING
INDIAN INSTITUTE OF TECHNOLOGY KANPUR
INDIA

March, 2003

CERTIFICATE

It is certified that the work contained in the thesis entitled "***Computer Aided Product and Process Design System for Axisymmetric Deep Drawing***", by ***Mr. P. V. Vijayakumar*** , has been carried out under our supervision and that this work has not been submitted elsewhere for a degree.

Dr. G.K. Lal
Professor
Dept. of Mechanical Engineering and
I.I.T Kanpur

Dr. N.V. Reddy
Asst. Professor
Dept. of Mechanical Engineering
I.I.T. Kanpur

March, 2003

Dedicated to My Parents and Teachers

Acknowledgments

I express my sincere gratitude, regards and thanks to my supervisors Dr. N. V. Reddy and Prof. G. K. Lal for their excellent guidance, invaluable suggestions and generous help at all the stages of my research work. Their interest and confidence in me was the reason for all the success I have made.

I would like to thank to all my friends and colleagues for their smile and friendship making the life at I.I.T. Kanpur enjoyable and memorable.

I gratefully acknowledge the financial assistance from Department of Science and Technology, India for carrying out my work.

Last but not the least I am thankful to the All Mighty for giving me enough perseverance, patience and strength to rise after every debacle.

Vijayakumar

Abstract

Designing process sequences for deep drawing of axisymmetric components has traditionally been a trial and error process. Designers have to rely on the previous experience in laying out the process sequence for a particular part. The design and manufacture of dies /tools for producing deep drawing components is extremely costly and time consuming. It is necessary to cut down the time for developing, designing and producing the dies and punches to increase the production rate of sheet metal components. This can be accomplished by developing a computer aided system which generates process sequences using the knowledge of formability limit, i.e. the limiting drawing ratio.

Present work is an attempt towards developing a computer aided product and process design system that can generate a set of feasible forming process parameters for the purpose of process design by taking the input as the required finished part. A feature based parametric product design module is developed to automate the input of geometric information to the process design system. Process analysis model developed by Sonis et al. [2003] is modified by considering bending and unbending along die arc radius, the same is used to determine the limiting drawing ratios for the first as well as subsequent draws. Predictions of the same model are validated by comparing with the available experimental results [Thorp, 1973; El-Sebaie and Mellor, 1972; Lange, 1985 and Leu, 1999].

Required database are developed for the properties of commonly deep drawn metals and the tribological data. Commonly followed practices related to tool design and process sequence, reported in handbooks, research papers and industrial practices are incorporated into the system in the form of design rules. Process sequencing module is developed and it consists of geometrical design module and rectification module. The process sequence generated using the geometrical design module may not be feasible, as the formability of the material is not taken into consideration. Adding new intermediate stages to the geometric sequence wherever the process analysis module predicts formability violation modifies process sequence. Feasible sequence module is developed to generate alternative process sequences considering annealing between stages. The capabilities of the developed system is tested with process sequences available in the literature [Jones, 1951; Eshel et al., 1986; Sitaraman et al., 1991; ASM hand book,1992; Park et al.,1998]. Many case studies are presented to demonstrate the capabilities of the present system.

Contents

List of Figures

List of Tables

Nomenclature

C_1, C_2, C_3, C_4, C_5	constants
D_0	initial blank diameter
D_p	punch diameter
DR	drawing ratio
F_w	flange width
F	drawing force
F_h	blank-holding force
H	final height of the cup
K	material constant
$L_i : i = 1, 2, 3..$	length around the axis of rotation for the cup elements
LDR_0	limiting drawing ratio for the first draw
$LDR_i : i = 1, 2, 3..$	limiting drawing ratio for redraw
P_c	critical drawing force
$P_i : i = 1, 2, 3..$	path of center of gravity for the cup elements
R	initial radius of the annular ring
$\bar{R}$	normal anisotropy value
R_0	initial blank radius
R_1, R_2	intermediate radius on initial blank
R_i, $R_{i+1} : i = 1, 2, 3..$	intermediate radius on the bottom of the cup
SA	surface area
$d_{c_i} : i = 1, 2, 3..$	cup diameter after redraws
p_{BH}	blank holder pressure
t	instantaneous thickness
t_0	initial blank thickness
r	radius of the partially drawn cup corresponding to R
r_b	blank holder corner radius
r_d	die arc radius
r_0	radius of the partially drawn cup corresponding to R_0
r_{c0}	cup radius after the first draw
$r_{c_i} : i = 1, 2, 3..$	cup radius after redraws
r_{cd}	die opening radius

v	velocity of punch
n	strain hardening exponent
ϵ_1, ϵ_2, ϵ_3	strains at points 1, 2 and 3 respectively
ϵ_p	previous strain
μ	coefficient of friction
ϵ_r, ϵ_θ, ϵ_z	strains in the r, θ & z directions respectively
$\bar{\epsilon}$	generalised strain
$\bar{\epsilon}^0$	strain induced during first draw
$\bar{\epsilon}^i : i = 1, 2, 3..$	strain induced during redraws
$d\epsilon_r$, $d\epsilon_\theta$, $d\epsilon_z$	strain increments in the r, θ & z directions respectively
σ_0	yield stress
σ_b	bending stress along the die profile during first draw
σ_{b1}	bending stress along the blank holder profile during redraws
σ_{b2}	bending stress along the die profile during redraws
$\sigma_{critical}$	critical drawing stress
σ_e	generalised stress
σ_f	frictional stress
σ_r, σ_θ, σ_z	stresses in the r, θ & z directons respectively
σ_{total}	total drawing stress in the cup wall
σ_u	ultimate tensile strength
$\sigma_{r_{cd}}$	total drawing stress at the radius r_{cd}
$\sigma_{r_{co}}$	total drawing stress at the radius r_{co}
$\bar{\sigma}$	generalised stress
$\bar{\sigma_1}$	mean flow stress at the blank holder profile during redraws
$\bar{\sigma_1}$	mean flow stress at the die profile profile during redraws

Chapter 1

Introduction and Literature Survey

1.1 Introduction

Deep Drawing is one of the most important sheet metal forming process. Deep drawn components form a significant part of manufacturing activity, and they are widely used in various industries like automobile, tractor, aerospace, defense, machine tools, refrigeration, air conditioning and many other industrial fields. The design and manufacture of dies/tools for producing deep drawing components is extremely costly and time consuming. It is necessary to cut down the time for developing, designing and producing the dies/tools for the production of sheet metal components so as to stay competitive in the global economy. The high cost and long lead-times of die design development and manufacture are mainly due to the traditional trial and error procedures used by skilled die designers and makers to obtain the correct tooling shape and forming conditions that will yield the desired part shape and properties. The design phase for a given component involves several calculations and subsequent decisions are based on heuristics and existing trade practices in industry. A process designer may have to spend a lot of time in analyzing the given problem and/or in consulting the handbooks for various relations to arrive at the desired solution. Also, problems in designing dies/tools arise when tool designer is confronted with new materials where previous deep drawing experience or forming data does not exist.

To overcome the above-mentioned problems and to sustain competitiveness, there is a need for an intelligent aid to the process designers. Development of a computer aided knowledge based process designing system will help process designers in developing and evaluating process sequences and in predicting possible defects/problems before the actual dies/tools are manufactured. Ability to predict and prevent problems will allow prior modification of the process sequence/tool design with obvious financial and time saving. Additional advantages are that more accurate and consistent designs can be generated and skilled process designers are not needed. For generating an automatic process sequence design, there is a need for the development of such a computer model that captures the design knowledge and the properties such as stress-strain characteristics, anisotropy data, ultimate tensile value etc. Process design for deep drawing needs understanding the process and its parameters as the sheet metal is transformed

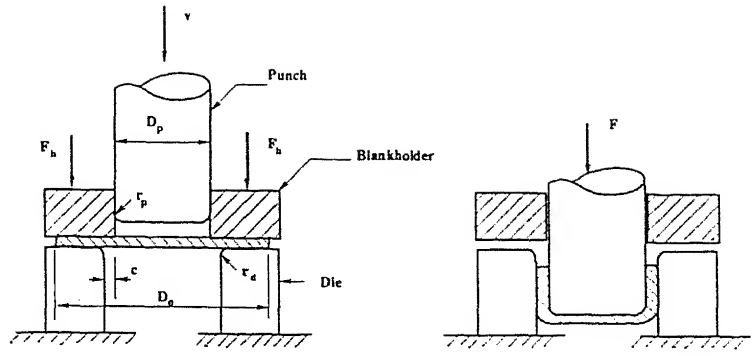

Figure 1.1: Drawing of a cup-shaped part: Symbols c = clearance, D_0 = blank diameter, D_p = punch diameter, r_d = die arc radius, r_p = punch corner radius, F = drawing force, F_h = blank-holding force [Groover, 1995].

from a flat sheet to a hollow body. Without the complete knowledge of the influence of the process variables such as material property variations, friction conditions, punch/die geometry and work piece geometry on the process mechanics, it will not be possible to predict and prevent the defects, or to design the equipment adequately. Stage design and process sequencing for the manufacture of sheet metal components by single and multi-stage deep drawing requires knowledge of limiting drawing reduction (LDR).

Number of approximate methods of analysis have been developed and applied to various metal forming processes. The most well known methods are the slab method, slip line field method, upper bound method and finite element method. From the literature [Leu, 1999] it is evident that the slab method can predict limiting drawing ratios close to the predictions of finite element analysis as well as experimental results. Therefore in the present work a model based on the force equilibrium method has been used to estimate the limiting drawing ratio. Present work is an attempt to develop a computer aided product and process design system by combining both analytical and empirical knowledge of the deep drawing to help the process designers. It incorporates the object modeling (feature based geometric description) to design the required product, process analysis model to estimate the limiting drawing ratio for single and multi-stage deep drawing considering various aspects such as anisotropy, plastic instability, material property variation, etc. of the given material.

1.2 Deep Drawing Process

Deep drawing is a sheet-metal-forming operation in which a piece of sheet metal or blank usually held down flat against a die by a blank holder, is forced into and/or through the die opening by means of a punch to form a hollow component. A blank of diameter D_0 is drawn into a die by means of a punch of diameter D_p. The punch and die have corner radii, r_p and r_d. The sides of

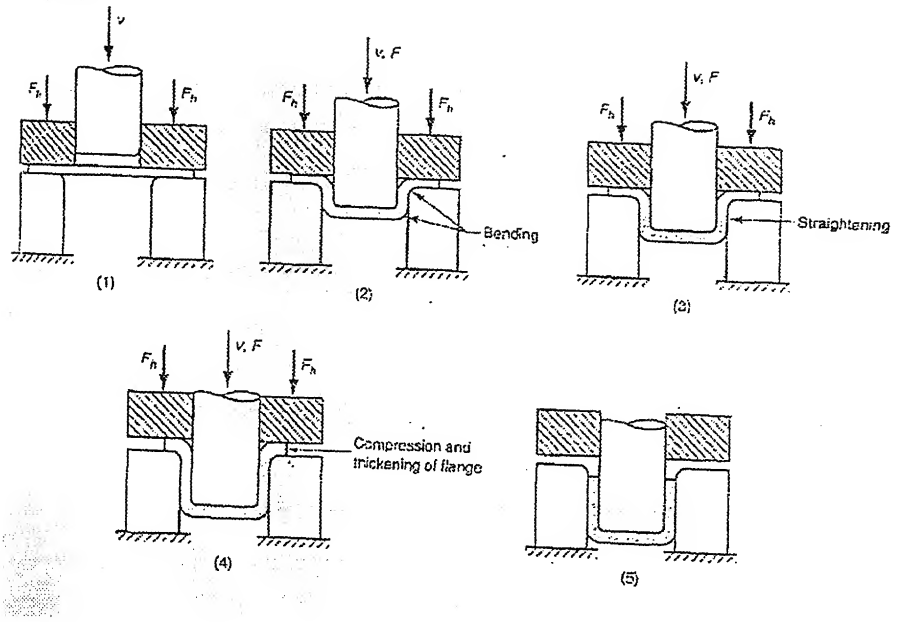

Figure 1.2: Stages in deformation of work in deep drawing: (1) punch makes initial contact with work, (2) bending, (3) straightening, (4) friction and compression, and (5) final cup shape showing effects of thinning in the cup walls. (V = velocity of punch, F = punch force, F_h = blank-holding force)[Groover, 1995]

punch and die are separated by a clearance, which is about 10% greater than the stock thickness. The punch applies a downward force F to accomplish the deformation of metal, and a downward holding force F_h is applied by the blank holder to prevent wrinkling, as shown in the Fig. 1.1. As the punch proceeds downward towards its final bottom position, the work experiences a complex sequence of stresses and strains as it is gradually formed into the shape defined by the punch and die cavity. The stages in the deformation process are illustrated in Figure 1.2. As the punch first begins to push into the work, the metal is subjected to bending operation. The sheet simply bent over the corner of punch and the corner of the die, as in the Figure 1.2(2). The outside perimeter of blank moves in toward the center in this stage, but only slightly.

As the punch moves further down, a straightening action occurs in the metal that was previously bent over the die radius, as shown in Figure 1.2(3). The metal at the bottom of the cup as well as along the punch radius, moves downward with the punch. But the metal that was bent over the die radius is straightened to form the wall of the cylinder. At the same time, more metal must be added to replace that which is now being used in the cylindrical wall. The metal in the flange portion of the blank is pulled or drawn toward the die opening to re-supply the previously bent and straightened metal now forming the cylinder wall. During this stage of the process, the friction and compression play roles in the flange of the blank. Initially static friction is involved until the metal starts to move and then, sliding friction governs the process. Magnitude of the

holding force applied by the blank holder as well as the friction conditions at the two interfaces are determining factors in the drawing operation. Lubricants are generally used to reduce friction forces. In addition to friction, compressive forces also occur on the outer edge of the blank. As the metal in this portion of the blank is drawn toward the center, the outer perimeter becomes smaller. As the volume of metal remains constant, the metal is squeezed and becomes thicker at the flange edge. This often results in wrinkling of the remaining flange of the blank, especially when thin sheet metal is drawn or when the blank holder force is too low. It is a condition that cannot be corrected once it has occurred. The friction and compression effects are illustrated in Figure 1.2(4).

The holding force applied by the blank holder also plays an important role in deep drawing. If it is too large, it prevents the metal from flowing properly toward the die cavity, resulting in stretching and possible tearing of the sheet metal. Determining the proper holding force involves a delicate balance between these opposing factors. Progressive downward motion of the punch results in a continuation of metal flow caused by drawing of cylinder wall, as shown in the Figure 1.2(5).

Redrawing

Often multi-stage drawing is necessary to produce the final part as complete reduction may not be possible in a single draw. The second drawing stage, and any further drawing stages if needed are referred to as redrawing. A redrawing operation is illustrated in Figure 1.3.

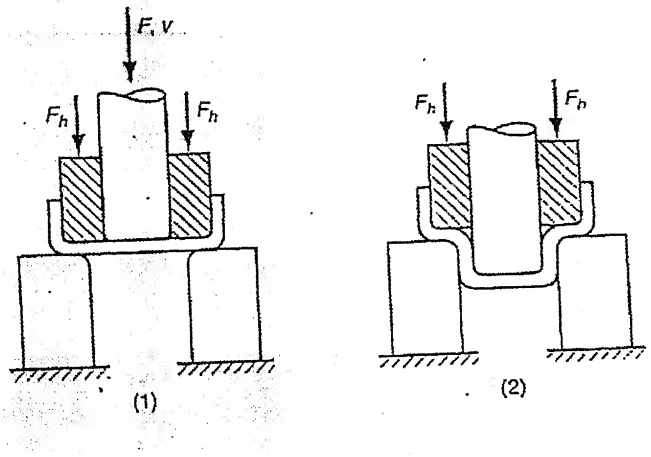

Figure 1.3: Redrawing of a cup: (1) start of redraw and (2) end of stroke. (v = velocity of punch, F = punch force, F_h = blank-holding force) [Groover, 1995]

Several different conditions exists during redrawing:

- As the metal flows it must be compressed, but only between the old punch radius and the new die radius. This is where wrinkling may occur, so a tubular blank holder is used

between the punch and the drawn cup inside diameter.

- The cylindrical wall and the top edge of the drawn cup simply slip downward on the blank holder. No work hardening occurs at this time.
- The drastic change is that the cylindrical wall must be bent to the blank holder radius and then straightened. This is in addition at the later bending to the die radius and straightening.

The percentage of reduction in diameters for all redraw operations are considerably less than that for the first draws due to the following reasons:

- The new cup side wall area taking the tensile loading is much smaller and will tear at lower punch loads. This new load-bearing metal was formed from the soft metal bottom of the drawn cup and has no strength advantage from previous work hardening.
- The additional bending to the blank holder radius and straightening means that less compressive load is permitted to prevent tearing.
- The metal in the drawn-cup cylindrical wall is already work hardened and has lower ductility for the redraw.

1.3 Drawability

Drawability of any material is expressed in terms of a Limiting Drawing Ratio (LDR) or Percentage Reduction. LDR is defined as the ratio of diameter D_0 of the largest blank that can be successfully drawn without fracture to the diameter of the punch D_p. Therefore,

$$LDR = \frac{D_0}{D_p}$$

and the Percentage Reduction is given by

$$\% \text{ Reduction} = \frac{D_0 - D_p}{D_0} \times 100$$

In an idealized forming operation deformation occurs in the flange and over the die lip. No deformation takes place over the nose of punch. The drawability of metal depends on two factors:

1. The ability of the material in the flange region to flow easily in the plane of the sheet under shear.
2. The ability of the side wall material to resist deformation in the thickness direction.

1.4 Literature Survey

Deep drawing, with *press working, stamping* and *die forming* being commonly used synonyms, is an experienced-based technology. A natural procession of investigation starts with an experimental study from which analytical models can be developed. 'Know-how' has been accumulated largely by trial and error, since the process was introduced in 18th century, though a massive thrust to understand the process started only in 1920's.

Chung and Swift [1951] measured changes in the thickness undergone by a uniformly thin blank when drawn into a cup and tried to predict the drawing force. They carried out a comprehensive experimental and analytical investigation at the University of Sheffield in 1950. They drew 4 inch diameter cups of varying blank sizes, thickness, wall recess radii, materials and operating conditions, with each undergoing a total of 500 to 900 measurements. The analytical treatment utilized some of Hill's [1950] predictions as applied to the strains developing in radial drawing. They also developed a model for bending over the die profile radius. They were, however unable to extend their solution to the punch nose region. Wallace [1960] carried out experiments with finished punch and knurled punch, with and without lubrication in order to observe the increment in limiting drawing ratio. He obtained an increase in limiting drawing ratio from 2.325 with a polished and lubricated punch to 2.550. These experiments were carried out on E.D.D. (Extra Deep Drawing) quality and D.D. (Deep Drawing) quality steels.

Wright [1962] studied the effect of mechanical properties (ultimate tensile strength, % elongation, strain hardening and normal anisotropy) on deep drawability and stretch formability for various materials viz. commercial aluminium, copper, zinc and titanium and its alloys. He concluded that relationship between deep drawability and the four mechanical properties cannot be expressed in terms of a product/quotient type of empirical formula.

Woo [1968] presented the analysis of the deep drawing of a cylindrical cup, including the drawing and stretch-forming parts. In the analysis, he calculated the strains due to drawing near the die lip and used them as the boundary values for the analysis of the stretch-forming region. He also analyzed the effect of anisotropy using the Hill's theory for anisotropic material [Hill, 1950].

El-Sebaie and Mellor [1972] showed the effect of anisotropy value ($\bar{R}$) and strain-hardening exponent n-value on limiting drawing ratio. Their results indicate two instability modes, one in the cup wall and the other in the flange. Experiments were conducted on three materials viz. soft aluminium, half hard aluminium and soft 70/30 brass are drawn with smooth punch as well as rough punch to determine the limiting drawing ratio. They also developed a theoretical model based on the slab method and used the finite difference method to determine the stress and strain distributions in the cup. The predicted value of limiting drawing ratio was not close to the experimental values. Korhonen [1982] developed a model based on the slab method for estimating the maximum drawing force during deep drawing of cylindrical cups with flat-nosed

punch. He used the load maximum principle for localization of plastic flow to estimate the drawing force for two cases, one for plane stress state when thickness/punch profile radius was vanishingly small, and the other for tri-axial stress using the free body diagram (slab method). He obtained the value for press load (drawing force, P_d) as,

$$P_d = P_c \frac{DR - 1}{LDR - 1}$$

where DR is drawing ratio and P_c is the critical drawing load at LDR.

Several attempts [Yu and Johnson, 1982 and Meier and Reissner, 1983] have been made to solve the buckling problem of annular ring. Yu and Johnson [1982], proposed the critical conditions for elastic and plastic buckling of flange having circular shape, based on a two-dimensional buckling model. Oskada et al. [1995] proposed a model based on the finite element method for determining the optimal history of the blank-holding force which will not cause wrinkling and localized thinning for each deformation step. They determined the blank-holding force in deep drawing of an aluminium sheet. Ahmetoglu et al. [1995] determined the wrinkling and fracture limits. They performed experiments to show the effect of blank holding force control on fracture and wrinkling in rectangular pans. The rectangular pans were formed from aluminium alloy 2008-T4. Much of the emphasis was paid on the correlation of LDR of a sheet metal with its material properties especially with the normal anisotropy value, which indicates better drawability when its value is large. Many investigations have been carried out to evaluate the limiting drawing ratio, mainly for the first stage. Wilson et al. [1966] investigated the effect of size of blank on the load required to fracture the base of cup. The experiments were conducted on low carbon steel, α-titanium, zinc, and 3/4 hard aluminium to predict the anisotropy value from LDR values. Atkinson [1967] applied the technique of curve fitting to get the empirical relation from the experimental data for limiting drawing ratios of various materials ranging from mild steel to titanium. The general relationship between LDR and $\bar{R}$ was given by

$$8Log(\frac{D_o}{d}) = Log\bar{R} + 3$$

Emani [1984] reported that the plastic flow of anisotropic sheet during deep drawing may be regarded a two-stage deformation process, both stages occurring simultaneously. First stage deformation, taking place in the cup wall, being controlled by normal anisotropy. While the second stage deformation or asymmetric flow due to planar anisotropy, being responsible for the change in shape of rim of the flange of a partially drawn cup from circular to hypotrochoid.

Reissner and Ehrismann [1987] used the simulation technique based on the finite difference method to show extreme dependence of LDR on coefficient of friction(μ). Material was assumed to be rigid plastic with normal anisotropy and work hardening characteristics. Leu [1997] developed an expression, based on Hill's theory of anisotropic plasticity. He showed the effects of normal anisotropy ($\bar{R}$) and strain hardening exponent (n) on limiting drawing ratio and estimated the maximum drawing load at a certain drawing ratio, limiting drawing ratio (LDR) was

obtained as

$$LDR = \sqrt{e^{(2fe^{-n}\sqrt{\frac{1+\bar{R}}{2}})} + e^{(2n\sqrt{\frac{1+\bar{R}}{2}})} - 1}$$

where f is the factor of drawing efficiency varying with sheet thickness, tooling, lubrication, etc. Equation used for evaluating the drawing load was

$$\frac{P_d}{P_c} = \frac{ln(DR^2+1) - 0.7}{ln(LDR^2+1) - 0.7}$$

Leu [1999] continued his work and developed an expression for determining LDR. It normally estimates the critical blank size for a given cup radius. He has given an expression, which is a function of process parameters like normal anisotropy, strain hardening exponent, coefficient of friction, yield strength of material, etc. He showed the effect of these parameters on LDR and compared his results with the experiments for the first stage only. He neglected bending and unbending effects along punch, die profiles and wrinkling of sheet is not considered while selecting the blank holding force. Literature review for the first draw reveals that Hill's theory of anisotropic plasticity was successfully applied to calculate the stress and strain distribution in the process. It is also evident that in the deep drawing process, limiting drawing ratio depends on the characteristics of the material to be drawn. Many of the researchers reported the importance of anisotropy and strain hardening exponent on limiting drawing ratio.

Not much of the work is reported on the formulations of multi-stage drawing processes. Fogg [1968] studied bending and straightening of the unconstrained region in redrawing through a conical die by applying linearization of von-Mises yield criteria for plane stress. He showed through his experiments, bending and unbending stresses account for 23% and 47% of the total stress for redrawing ratios of 1.14 and 1.6 respectively. Parsa et al. [1994] used a rigid-plastic finite element simulation based on the theory of plasticity for slightly compressible materials to compare the limiting drawing ratio achievable by forward and reverse redrawing processes. In their analysis they used four layers of isoparametric rectangular elements and concluded that direct redrawing allows for higher total drawing ratios than reverse redrawing. Furthermore, they showed that the limiting drawing ratio for the second stage decreases and the total achievable drawing ratio increases with increasing first stage drawing ratio. Min et al. [1995] analyzed axisymmetric multi-stage deep drawing operation using rigid-plastic finite element method and bilinear quadrilateral elements. They obtained loads on punches/dies and predicted variations in thickness strains at each stage.

Sonis et al. [2003] presented a process analysis model to determine the LDR for the first draw as well as for redraws considering the effects of normal anisotropy, coefficient of friction, strain hardening, die arc radius and substantiated with available experimental results in literature. They have neglected bending and straightening effects at the punch, die profiles and no provision is given to avoid wrinkling while selecting the required blank holder force.

For designing automated process sequence, many researchers [Eshel et al., 1986; Sitaram et al., 1991; Doege and Schulte, 1992; Tisza, 1995; Esche et al., 1996; Sing et al., 1997; Park et

al., 1998 and Kang et al., 2002] have developed the Computer-Aided Engineering (CAE) systems using the rule-based knowledge and empirical formulations for the calculations of drawing load.

Eshel et al. [1986] developed rule based modeling for axisymmetrical deep drawing. They have developed AGFPO (Automatic Generation of Forming Process Outlines) system based on Generate and test-and-rectify (G&TR) strategy. They used the contemporary knowledge for single stage as well as for redrawing in rule form that can be directly utilized in an automated process-planning procedure. It incorporates empirical formulations, press working practices and plasticity knowledge. Sitaram et al. [1991] developed a hybrid Computer- Aided Engineering system for process sequence design in axisymmetric sheet metal forming. The input to the system is the final deep drawn object geometry that needs to be manufactured and output from the system is the process sequence with intermediate object geometries. However, the database constructed to check the maximum diameter reduction of the sheet blank was based on the hypothesis that materials whether they are high ductile, medium ductile or low ductile.

Tisza [1995] developed a group technology and modularity CAD/CAM system for developing deep drawing process-sequence and designing tools for the manufacture of deep drawn components having axisymmetric and rectangular cross-sections. Esche et al. [1996] developed a computer aided engineering system to design process sequences for axisymmetric deep drawn products using rule-based design module. They developed an analysis module for the first draw based on Finite Element Method (FEM) called SECTIONFORM to predict potential problems by simulating the forming processes. Esche et al. [2000] extended their work to handle forward and reverse drawing operations. They compared their punch travel and true strains results with the three-dimensional sheet forming analysis program PAM-STAMP for aluminium cups.

Sing et al. [1997] have developed a knowledge based process planning system using decision tables with fuzzy interface. They represented the knowledge of deep drawing in the form of decision tables and formability limits were selected using fuzzy inference for the formability knowledge. Park et al. [1998] have developed a computer aided process design system for axisymmetric deep drawing products, Pro-Deep, using G&TR strategy. The system was written in AutoLISP on the AutoCAD system. Knowledge based approach was used to develop the system. Kang et al. [2002] have applied computer aided process planning system for non-axisymmetric deep drawing products. They have used a modified entity-list to create 3-D part modeling and accumulated production rules for non-axisymmetric products. Their system was written in AutoLISP on the AutoCAD software (Release 14) environment.

The attempts made to develop computer aided process planning systems [Eshel et al., 1986; Sitaram et al., 1991; Tisza 1995; Esche et al., 1996; Sing et al., 1997; Park et al., 1998; Kang et al., 2002] are predicted the formability limits from the data tables. From the literature it is evident that, there is a need to predict formability limits by considering various affecting variables as the selection of limiting values from the data tables or handbooks may not consider all these variables.

1.5 Scope and Objective of the Present Work

Critical review of the published literature revels that there have been few attempts to develop an aid to the process designer to decide about the process sequence. However, attempts made by Sitaraman et al. [1991], Tisza [1995], Sing et al. [1997], Park et al. [1998] and Kang et al. [2002] are mainly based on expert system related to the limiting drawing ratio, sequencing etc. besides complicated way of object modeling. Development of an expert system regarding the formability limits of commonly deep drawn materials, for the range of process parameters used in the deep drawing process is very difficult. Formability limits of deep drawn materials requires the complete knowledge of the influence of the variables such as material property variations, friction conditions, punch/die and work-piece geometry on the process mechanics. Literature survey also reveals that attempts have been made to establish the relationship between normal anisotropy, strain hardening exponent, die arc radius and deep drawability for the first stage. Recently, Sonis et al. [2003] presented a process analysis model to determine the LDR for the first draw as well as for redraws considering the effects of normal anisotropy, coefficient of friction, strain hardening and die arc radius. They have neglected bending effects along die, punch profiles and there is no provision for wrinkling of the sheet while considering blank holding force. Jhonson and Millor [1972] concluded that maximum punch load is unaffected by the punch profile radius. In the present work bending along the punch profile is neglected as it occurs very early in drawing and that may not effects significantly on maximum drawing force. Bending and unbending along die arc radius are continuous till the end of drawing. Therefore bending along the die profile will considerably effects the maximum drawing force and affect the LDR. Particularly in redrawing, bending and unbending occurs at both blank holder profile and die profile, therefore, these effects are more significant than in the first draw.

In the present work the model presented by Sonis et al. [2003] is modified by adding bending effects along the die profile and by selecting blank holding force to avoid wrinkling. With these modifications, sheet thickness is introduced as an additional process variable in the calculation of LDR for the multi-stage deep drawing operations. The objective of the present work is to develop a computer aided product and process design system which uses the geometric primitives to model the object and an analytical model to estimate limiting drawing ratio for first as well as subsequent draws in conjunction with the available design guidelines in the form of design rules to produce the sequence of operations for the required geometry. The other objectives are

- Development of expert system in the form of design rules.
- Development of databases for material properties, friction coefficient.
- Generation of all possible alternate process sequences considering annealing between stages.

1.6 Organization of the Thesis

Brief discussion on the deep drawing process is presented in this chapter. Scope and objective of the present work is also defined in this chapter. The organization of the thesis report is as follows:

Chapter 2 presents the formulation based on the slab method, to estimate the limiting drawing ratio for the first draw as well for redraw.

Chapter 3 deals with the development of computer aided product and process design system for axisymmetric deep drawing. In this chapter various modules of the process designing system are discussed.

Chapter 4 compares the predictions of the model developed in the present work with the available experimental results for first draw, while for redraw the predictions are compared with available drawing ratios in metal handbook. Also, a parametric study is presented in this chapter.

Chapter 5 presents the case studies to demonstrate the capabilities of the system developed.

Chapter 6 concludes the report with scope for the future work.

Appendix describes the product and process design rules used in the present system.

Chapter 2

Model for Estimation of Limiting Drawing Ratio

2.1 Introduction

The drawability of the sheet metal is defined by the limiting drawing ratio (LDR), which is the ratio of the maximum diameter of blank that can be drawn successfully without tearing of cup, to the punch diameter. From the literature review presented in Chapter 1, it is evident that the LDR depends strongly on the normal anisotropy value ($\bar{R}$), strain hardening exponent (n) and die as well as punch geometry. A high normal anisotropy ($\bar{R}$) indicates the better drawability (higher limiting drawing ratio), and indicates high resistance to thinning. Thus, in order to estimate the limiting drawing ratio for each pass, an analytical model has been developed. In the present work, limiting drawing ratio is estimated for the cylindrical cup with a flat-bottomed punch using an integral technique based on the load maximum principle for localization of plastic flow. Leu[1999] also proposed an analytical model based on the same principle for the first draw only. In his model, limiting drawing ratio was estimated for a given cup radius. Also, the effect of thickness (bending and unbending effects) on the limiting drawing ratio was not considered in his work. In the present work, thickness of the sheet is taken into account by considering bending effects at the die profile. In addition, required blank holding force is selected as a function of sheet thickness and blank radius to avoid wrinkling. Mathematical models for predicting limiting drawing ratios in first as well as redraws are presented in section 2.2.

2.2 Mathematical Models for Prediction of LDR

Assumptions

- The material properties are assumed to be rotationally symmetric, so that there is a planar isotropy and normal anisotropy. The value of normal anisotropy is given by

$$\bar{R} = \frac{R_{0^o} + 2R_{45^o} + R_{90^o}}{4} \tag{2.1}$$

where R_{0^o}, R_{45^o} and R_{90^o} are the values of anisotropy at $0^o, 45^o, 90^o$ to the rolling direction.

- Material is assumed to be rigid-plastic.
- Deformation in the flange region is assumed to be plane strain i.e., the thickness remains constant. Although thinning occurs near the base and thickening occurs near the top of the cup but these changes are not considered in the present work as they are not very significant [Hosford, 1983].
- Material is assumed to be yielding according to Hill's anisotropic plasticity theory.
- The strain hardening characteristics of sheet metal is assumed to follow the form

$$\bar{\sigma} = K(\bar{\epsilon})^n \tag{2.2}$$

where $\bar{\sigma}$ is the generalized stress, $\bar{\epsilon}$ is the generalized strain, n is the strain hardening exponent and K is the material constant.

Hill's Anisotropic Yield Criteria

Using the Hill's anisotropic yield criteria [Hill, 1950], relationships of stresses and incremental strains are given by

$$\bar{\sigma} = \frac{1}{\sqrt{1+\bar{R}}}\left[(\sigma_\theta - \sigma_z)^2 + (\sigma_r - \sigma_z)^2 + \bar{R}(\sigma_r - \sigma_\theta)^2\right]^{\frac{1}{2}} \tag{2.3}$$

$$d\bar{\epsilon} = \frac{\sqrt{1+\bar{R}}}{1+2\bar{R}}\left[(d\epsilon_\theta - \bar{R}d\epsilon_z)^2 + (d\epsilon_r - \bar{R}d\epsilon_z)^2 + \bar{R}(d\epsilon_r - d\epsilon_\theta)^2\right]^{\frac{1}{2}} \tag{2.4}$$

$$\frac{d\epsilon_r}{\bar{R}(\sigma_r - \sigma_\theta) + (\sigma_r - \sigma_z)} = \frac{d\epsilon_\theta}{\bar{R}(\sigma_\theta - \sigma_r) + (\sigma_\theta - \sigma_z)} = \frac{d\epsilon_z}{(\sigma_z - \sigma_\theta) + (\sigma_z - \sigma_r)} = \frac{d\bar{\epsilon}}{(1+\bar{R})\bar{\sigma}} \tag{2.5}$$

where σ_r, σ_θ and σ_z are stresses in r, θ and z directions and $d\epsilon_r$, $d\epsilon_\theta$ and $d\epsilon_z$ are strain increments in the directions r, θ and z.

2.3 First Draw Analysis

Figure 2.1 shows the schematic diagram for a cup-drawing operation in which a circular blank of original radius R_0 and thickness t_0 is deep drawn by the flat-bottomed punch through a die opening of radius r_{cd}.

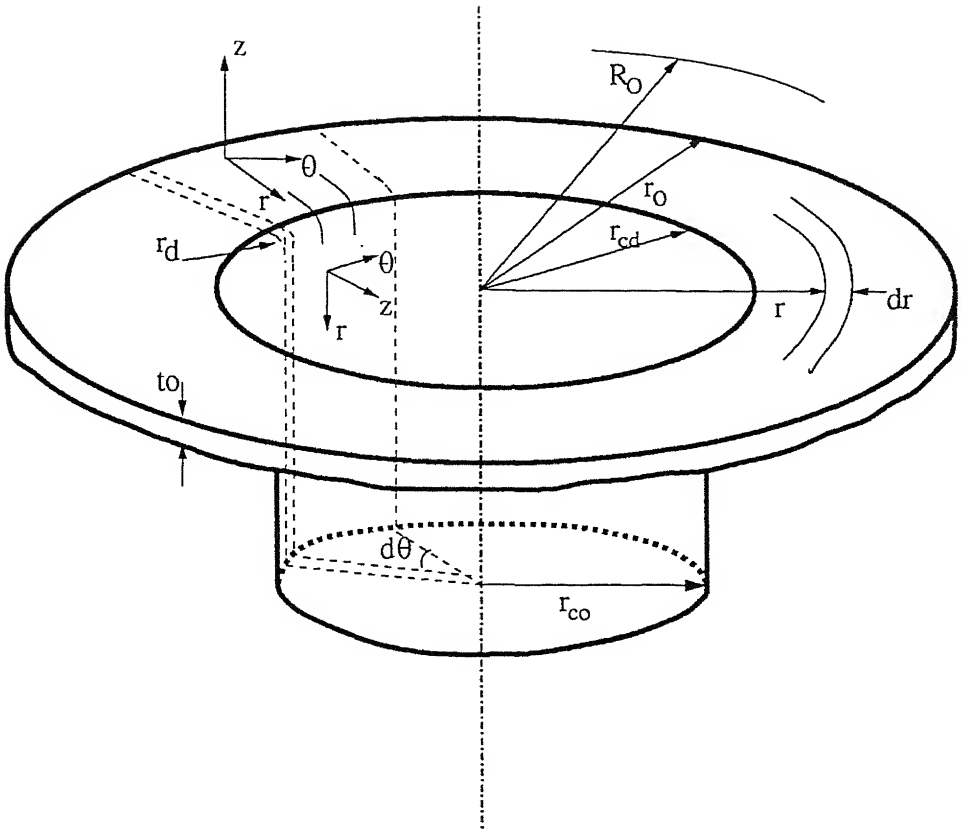

Figure 2.1: Schematic representation of cup drawing, showing the co-ordinate system and dimensional notations.

Critical Condition in Cup Wall

In deep drawing process, load gets transmitted through the cup wall. The maximum diametrical reduction is usually limited by the maximum allowable drawing force in the cup wall at the punch nose radius (r_p). The critical drawing load P_c is obtained using a criterion based on the tensile instability in the cup wall. The critical drawing force (P_c) at a certain stage of the punch stroke is given by

$$P_c = 2\pi r_{co} t \sigma_r \tag{2.6}$$

where t is the instantaneous thickness of the cup wall and is given by

$$t = t_0 e^{\epsilon_z} \tag{2.7}$$

Since the wall circumference is constrained by the punch from shrinking therefore one can obtain

$$d\epsilon_\theta = 0$$

Based on the plane strain deformation condition and volume constancy, one can get

$$d\epsilon_z = -d\epsilon_r$$

Substituting above relation in Eq. 2.4, one can obtain

$$d\epsilon_z = \frac{\sqrt{1+2\bar{R}}}{1+\bar{R}} d\bar{\epsilon}$$

and it can be written as

$$\epsilon_z = \frac{\sqrt{1+2\bar{R}}}{1+\bar{R}} \bar{\epsilon} \tag{2.8}$$

Since the cup wall is only under radial tensile stress σ_r, stress perpendicular to cup wall can be neglected and is given by

$$\sigma_z = 0$$

Using Eqs. 2.3 and 2.5, the radial tensile stress σ_r can be obtained as

$$\sigma_r = \frac{K(1+\bar{R})}{\sqrt{1+2\bar{R}}} \bar{\epsilon}^n \tag{2.9}$$

Critical drawing load (P_c) at the LDR can be obtained by maximizing the drawing force at the beginning of the punch nose radius in the cup wall with respect to the effective strain, i.e.

$$\frac{\partial P_c}{\partial \bar{\epsilon}} = 0 \tag{2.10}$$

Substituting Eq. 2.6 in the above equation gives

$$\frac{\partial (2\pi r_{co} t \sigma_r)}{\partial \bar{\epsilon}} = 0$$

Using Eqs. 2.9 and 2.7 one can get

$$\frac{\partial}{\partial \bar{\epsilon}} \left[2\pi r_{co} t \frac{K(1+\bar{R})}{\sqrt{1+2\bar{R}}} \bar{\epsilon}^n \times t_0 e^{\frac{\sqrt{1+2\bar{R}}}{1+\bar{R}} \bar{\epsilon}} \right] = 0$$

Above equation can be reduced to

$$\bar{\epsilon} = \frac{(1+\bar{R})}{\sqrt{1+2\bar{R}}} n \tag{2.11}$$

From Eqs. 2.6, 2.9 and 2.11, P_c at the onset of plastic instability can be written as

$$P_c = 2\pi r_{co} t_0 \left(\frac{1+\bar{R}}{\sqrt{1+2\bar{R}}} \right)^{1+n} (n^n e^{-n} K) \tag{2.12}$$

and the critical drawing stress at the onset of plastic instability can be obtained as

$$\sigma_{critical} = \left(\frac{1+\bar{R}}{\sqrt{1+2\bar{R}}}\right)^{1+n} (n^n e^{-n} K) \tag{2.13}$$

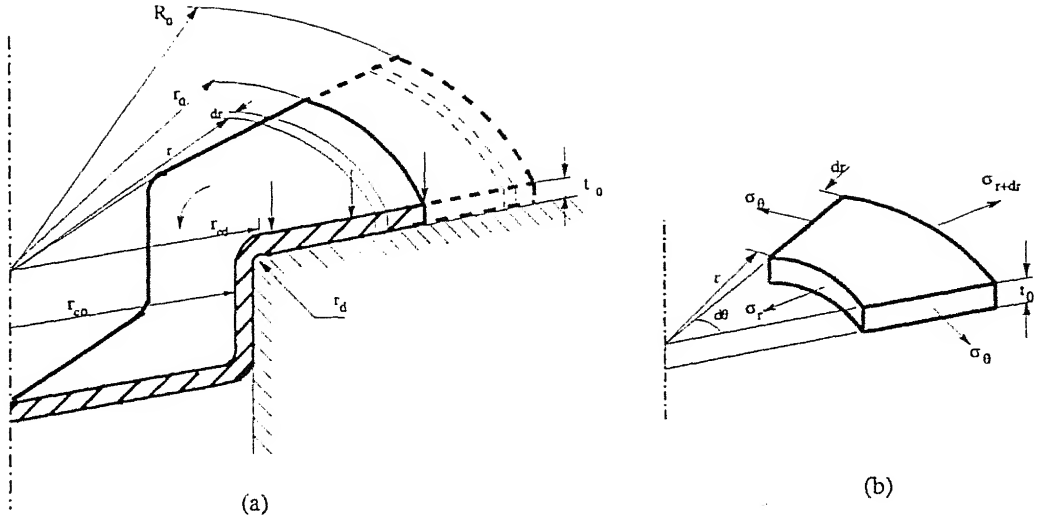

Figure 2.2: Radial stresses in the flange element

Pure Radial Drawing in the Flange

The stresses acting on an element in the flange region at the current radius r are shown in Fig. 2.2 b and the equation of radial equilibrium can be written as

$$r d\sigma_r - \sigma_r dr - \sigma_\theta dr = 0$$

Above equation can be written as

$$\frac{d\sigma_r}{dr} = -\frac{(\sigma_r - \sigma_\theta)}{r} \tag{2.14}$$

Under the plane strain deformation condition of the flange, i.e. $d\epsilon_z = 0$, the relationship of stresses σ_r and σ_θ can be obtained from Eq. 2.5 as

$$\sigma_z = \frac{(\sigma_r + \sigma_\theta)}{2}$$

Substituting the above equation in Eq. 2.3, one can get

$$(\sigma_r - \sigma_\theta) = \bar{\sigma}\left[\frac{2(1+\bar{R})}{2\bar{R}+1}\right]^{1/2} \tag{2.15}$$

Now, the effective strain $\bar{\epsilon}$ in the flange region is evaluated from the condition that the plane strain deformation take place in the flange region and is given by.

$$\bar{\epsilon} = \sqrt{\frac{2(1+\bar{R})}{2\bar{R}+1}}(-\epsilon_\theta)$$

where the hoop strain in the flange region, $-\epsilon_\theta = ln(\frac{R}{r})$ R being the initial radius of the annular ring which reaches radius r after the cup has been partially drawn. Substituting the above

equation in Eq. 2.2, one can get

$$\bar{\sigma} = K \left[\sqrt{\frac{2(1+\bar{R})}{2\bar{R}+1}} (ln(\frac{R}{r})) \right]^n \tag{2.16}$$

From Eqs. 2.14, 2.15 and 2.16 one can obtain

$$d\sigma_r = -K \left[\sqrt{\frac{2(1+\bar{R})}{2\bar{R}+1}} (ln(\frac{R}{r})) \right]^n \times \sqrt{\frac{2(1+\bar{R})}{2\bar{R}+1}} \frac{dr}{r}$$

Integrating the above equation from r_{cd} to r_0 for the maximum radius of R_0, the radial drawing stress at the position r_{cd} in the flange can be obtained as

$$\int_{r_{cd}}^{r_0} d\sigma_r = -K \left[\sqrt{\frac{2(1+\bar{R})}{2\bar{R}+1}} \right]^{1+n} \int_{r_0}^{r_{cd}} ln(\frac{R}{r})^n \frac{dr}{r}$$

the above equation can be written as

$$\sigma_r = K \left[\sqrt{\frac{2(1+\bar{R})}{2\bar{R}+1}} \right]^{1+n} \int_{r_0}^{r_{cd}} ln(\frac{R}{r})^n \frac{dr}{r} \tag{2.17}$$

Solution to the integral term in the above equation is given by

$$\int_{r_{cd}}^{r_0} (ln\frac{R}{r})^n \frac{dr}{r} = (1+n) ln\frac{r_0}{r_{cd}} - 2n \left[ln\frac{R_0+r_0}{R_2+r_{cd}} + \frac{r_0}{R_0+r_0} - \frac{r_{cd}}{R_2+r_{cd}} \right] \tag{2.18}$$

The derivation of $\int_{r_{cd}}^{r_0} (ln\frac{R}{r})^n \frac{dr}{r}$ is presented in Appendix A

Friction along Tool-Work Interfaces

The stress due to friction at tool-work interface can be quantified by assuming the blank holding force acting at the periphery of the blank (r_0). The resulting frictional stress (σ_f) increases the resulting radial stress (σ_r) in the flange region. Required blank holding pressure to avoid wrinkling depends on the sheet material, the relative sheet thickness ($\frac{t_0}{D_0}$) and the drawing ratio (DR). Siebel and Beisswanger have come up with an empirical relation (reported by Lange, [1985]) for the required blank holder pressure to avoid wrinkling and is given by

$$p_{BH} = 2.5\sigma_u \left[(DR-1)^2 + \frac{0.005 D_0}{t_0} \right] 10^{-3} \; MPa \tag{2.19}$$

where σ_u is the ultimate tensile strength of the material. Assuming the friction coefficient (μ) on blank-blank holder interface and die-blank interface are remains constant, the friction stress due to the blank holding pressure can be obtained as

$$\sigma_f = 2\,\mu \frac{\pi\,(R_0^2 - r_{cd}^2)\,p_{BH}}{2\pi r_0 t_0} \tag{2.20}$$

Siebel and Beisswanger have suggested that the punch travel at maximum drawing load is almost independent of the workpiece material and the drawing ratio and occurs at one-third of punch stroke (i.e.,when $r_0 \simeq 0.77R_0$) as reported by Lange, [1985]. The total radial drawing stress at the beginning of the die profile (r_{cd}) can be obtained by

$$\sigma_{r_{cd}} = \sigma_f + K \left[\sqrt{\frac{2(1+\bar{R})}{2\bar{R}+1}} \right]^{1+n} \int_{r_{cd}}^{r_0} \left(ln(\frac{R}{r}) \right)^n \frac{dr}{r} \tag{2.21}$$

Considering friction along the die profile, the radial drawing stress at the exit of the die arc (Fig. 2.3 a) can be obtained by

$$\sigma_{r_{co}} = e^{\mu\alpha}\, \sigma_{r_{cd}} \left(\frac{r_{cd}}{r_{co}} \right) = e^{\mu\alpha} \left[\sigma_f + K \left[\sqrt{\frac{2(1+\bar{R})}{2\bar{R}+1}} \right]^{1+n} \int_{r_{cd}}^{r_0} \left(ln(\frac{R}{r}) \right)^n \frac{dr}{r} \right] \left(\frac{r_{cd}}{r_{co}} \right) \tag{2.22}$$

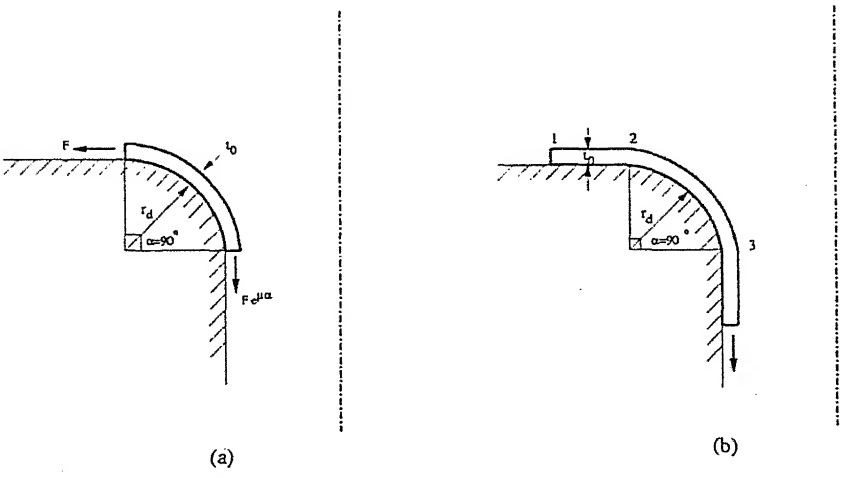

Figure 2.3: Drawing along die arc radius

Bending and Unbending at the Die Profile

In the region of the die arc radius the sheet metal undergoes two-fold bending. The central fiber is bent to a radius $r_d + \frac{t_0}{2}$ (Fig. 2.3 b) at the die entrance and is unbent again at the exit. The bending stress at the die exit can be obtained as [Lange, 1985]

$$\sigma_b = \frac{\bar{\sigma} t_0}{2r_d + t_0} \tag{2.23}$$

where $\bar{\sigma}$ is the mean value of flow stress at the die arc region and it can be evaluated by the average value of $\bar{\sigma}$ in the region of die arc radius between points 2 and 3 (ϵ_2, ϵ_3) as shown in Fig. 2.3 b. In order to determine the strains at points 2 and 3 the initial location of these points

in the undeformed blank must be ascertained. The strain at point 2 when the load is a maximum (at $r_0 \simeq 0.77R_0$) is given by

$$\epsilon_2 = ln(\frac{r_{2i}}{r_{cd}}) \tag{2.24}$$

where r_{2i} is the unknown initial radius on the blank and it can be calculated from the volume constancy and is given by

$$r_{2i} = \sqrt{R_0^2 + r_{cd}^2 - r_0^2} \tag{2.25}$$

The strain at point 3 can be obtained by adding the strain due to bending to the strain due to radial drawing and is given by

$$\epsilon_3 = ln(\frac{r_{3i}}{r_{cd}}) + ln(1 + \frac{t_0}{2r_d + t_0}) \tag{2.26}$$

where r_{3i} is the unknown initial radius on the blank and it can be calculated from the volume constancy one can get

$$r_{3i} = \sqrt{R_0^2 + r_{cd}^2 - r_0^2 - 8\,\pi(r_{cd} - \frac{2\,r_d}{\pi})r_d} \tag{2.27}$$

Mean strain at the die profile can be calculated by

$$\bar{\epsilon} = \frac{\epsilon_2 + \epsilon_3}{2} \tag{2.28}$$

The flow stress at the die profile is given by

$$\bar{\sigma} = K\bar{\epsilon}^n \tag{2.29}$$

Adding the bending stress obtained in Eq.2.23 to the Eq.2.22 one can get the total drawing stress in the wall at the die arc exit and is given by

$$\sigma_{total} = \sigma_b + e^{\mu\alpha}\left[\sigma_f + K\left[\sqrt{\frac{2(1+\bar{R})}{2\bar{R}+1}}\right]^{1+n}\int_{r_{cd}}^{r_0}\left(ln(\frac{R}{r})\right)^n\frac{dr}{r}\right]\left(\frac{r_{cd}}{r_{co}}\right) \tag{2.30}$$

The limiting drawing ratio is determined from the condition that the critical stress $\sigma_{critical}$ (Eq. 2.13) to cause plastic instability in the cup wall, is equal to the total drawing stress σ_{total} at the die exit (Eq. 2.30), due to continuity of stress. The expression for LDR_0 can be written as

$$\begin{aligned} f(LDR_0) = {} & e^{-\mu\alpha}\left(-C_1\frac{r_{co}}{r_{cd}} + \sigma_b\right) + 2\,\mu\,\frac{\pi\,(R_0^2 - r_{cd}^2)\,p_{BH}}{2\pi r_0 t_0} \\ & + C_2\left[(1+n)ln\frac{r_0}{r_{cd}} - 2n\left(ln\frac{R_0 + r_0}{R_2 + r_{cd}} + \frac{r_0}{R_0 + r_0} - \frac{r_{cd}}{R_2 + r_{cd}}\right)\right] \end{aligned} \tag{2.31}$$

where,

$$C_1 = \left(\frac{1+\bar{R}}{\sqrt{1+2\bar{R}}}\right)^{1+n}(n^n e^{-n}K)\ ;\ C_2 = K\left(\sqrt{\frac{2(1+\bar{R})}{2\bar{R}+1}}\right)^{1+n}$$

$$r_{co} = \frac{R_0}{LDR_0} \quad ; \quad r_{cd} = r_{co} + r_d \quad ; \quad \frac{r_0}{r_{cd}} = \sqrt{LDR_0^2(\frac{r_{co}}{r_{cd}})^2 - (\frac{R_2}{r_{cd}})^2 + 1}$$

where the $\frac{R_2}{r_{cd}}$ can be evaluated by the volume constancy of plastic deformation in the die arc region. Equating the volume of metal before and during radial drawing (Fig. 2.2a), one can get

$$\pi(R_2^2 - R_1^2)t_0 = 2\pi(r_{cd} - \frac{2r_d}{\pi})(\pi r_d \frac{t_0}{2})$$

and it can be written as

$$\frac{R_2}{r_{cd}} = \left[\pi\left(\frac{r_d}{\frac{R_0}{LDR_0} + r_d} - \frac{2{r_d}^2}{\pi(\frac{R_0}{LDR_0} + r_d)^2}\right) + \left(\frac{1}{1 + \frac{LDR_0\, r_d}{R_0}}\right)^2 \left(\frac{R_1}{r_{co}}\right)^2\right]^{\frac{1}{2}} \tag{2.32}$$

$\frac{R_1}{r_{co}}$ can be determined from the condition that the effective strain in the flange never exceeds the critical strain in the cup wall. Effective strain in flange, $\bar{\epsilon}$ is given by

$$\bar{\epsilon} = \sqrt{\frac{2(1+\bar{R})}{1+2\bar{R}}} ln\left(\frac{R_1}{r_{co}}\right) \tag{2.33}$$

Substituting Eq. 2.12 in the above equation one can get

$$\frac{R_1}{r_{co}} = e^{\sqrt{\frac{(1+\bar{R})}{2}}n} \tag{2.34}$$

Substituting Eqs. 2.32, 2.34 in 2.31 results an equation in terms of LDR_0. Thus Eq. 2.31 derived above is a function of the LDR in terms of initial blank thickness t_0, normal anisotropy $\bar{R}$, strain hardening exponent n, coefficient of friction μ, die arc radius r_d, initial blank radius R_0 and yield strength σ_0. This non-linear equation in terms of LDR can be solved by using Bisection Method.

2.4 Redraw Analysis

Often it is not possible to obtain the desired reduction in the first draw. Redrawing once or several times may be necessary. The characteristics of redrawing can be described using the same variables as found in the first draw operation. A cup just prior to the start of metal flow in the redraw die illustrated in Fig. 2.4 a. Redrawing, like cupping (first draw) is also characterized by the limiting reduction. During the first draw, strain hardening at the top of the cup wall is maximum and it goes on decreasing as we move towards the bottom of cup. The extent of strain hardening is determined by the amount of reduction achieved. The strain hardening in the cup is given by the condition that $\bar{\epsilon}$ is never more than about 3% greater than the numerical value of hoop strain induced during pure radial drawing [Johnson and Mellor, 1972]. So the strain induced in the first pass is given by

$$\bar{\epsilon}^{\,0} = ln\left(\frac{R_0}{r_{co}}\right) = ln\,(LDR_0)$$

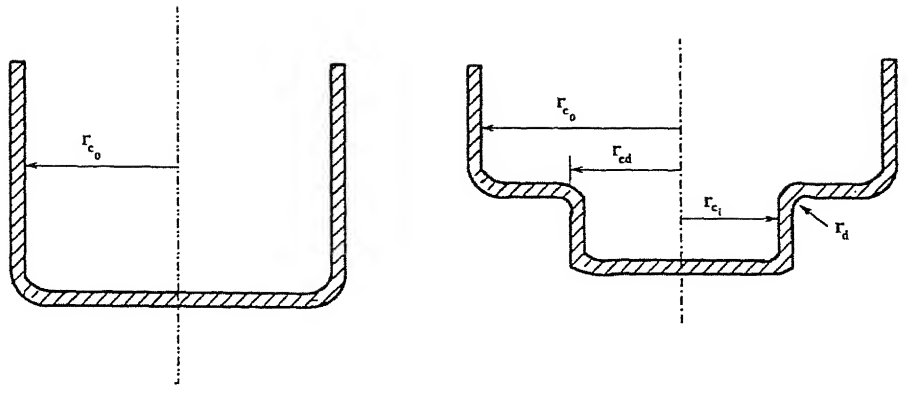

(a) First Draw Cup

(b) Partially Redrawn Cup

Figure 2.4: Redrawing of Cups

and for subsequent passes it is given by

$$\bar{\epsilon}^{(i-1)} = ln\left(\frac{r_{c_{i-1}}}{r_{c_i}}\right) = ln\,(LDR_i) \tag{2.35}$$

Where i denotes the number of draws and is given by $i = 1, 2, 3, ...N$.

Critical Condition in the Cup Wall

During a redraw operation, the punch which is smaller in diameter than the previous draw punch, contacts the bottom of the which was produced in the previous drawing operation. Unlike the cup wall and flange, the cup bottom has not seen any deformation in the prior draws, hence the yield strength can be presumed to be the same as that of initial material. Therefore, criterion for the plastic instability in the cup wall used in the first draw can be applied here. Maximizing the drawing force P with respect to the effective strain $\bar{\epsilon}$. Critical drawing load P_c at the onset of necking can be given as

$$P_c = 2\pi r_{c_i} t_0 \left(\frac{1+\bar{R}}{\sqrt{1+2\bar{R}}}\right)^{1+n} (n^n e^{-n} K) \tag{2.36}$$

and the critical drawing stress can be obtained as

$$\sigma_{critical} = \left(\frac{1+\bar{R}}{\sqrt{1+2\bar{R}}}\right)^{1+n} (n^n e^{-n} K) \tag{2.37}$$

Bending along Blank Holder Profile

The stress due to bending and unbending of the drawn cup at the blank holder profile (Fig. 2.5) is given by

$$\sigma_{b1} = \frac{\bar{\sigma}_1\, t_0}{2\, r_b + t_0} \tag{2.38}$$

where r_b is the blank holder arc radius and $\bar{\sigma}_1$ be the mean flow stress along the blank holder profile and it can be evaluated from the mean effective strain in that region is given by

$$\bar{\sigma}_1 = K\left[ln(LDR_{i-1}) + ln\left(\sqrt{1+\frac{t_0}{2r_b+t_0}}\right)\right]^n \tag{2.39}$$

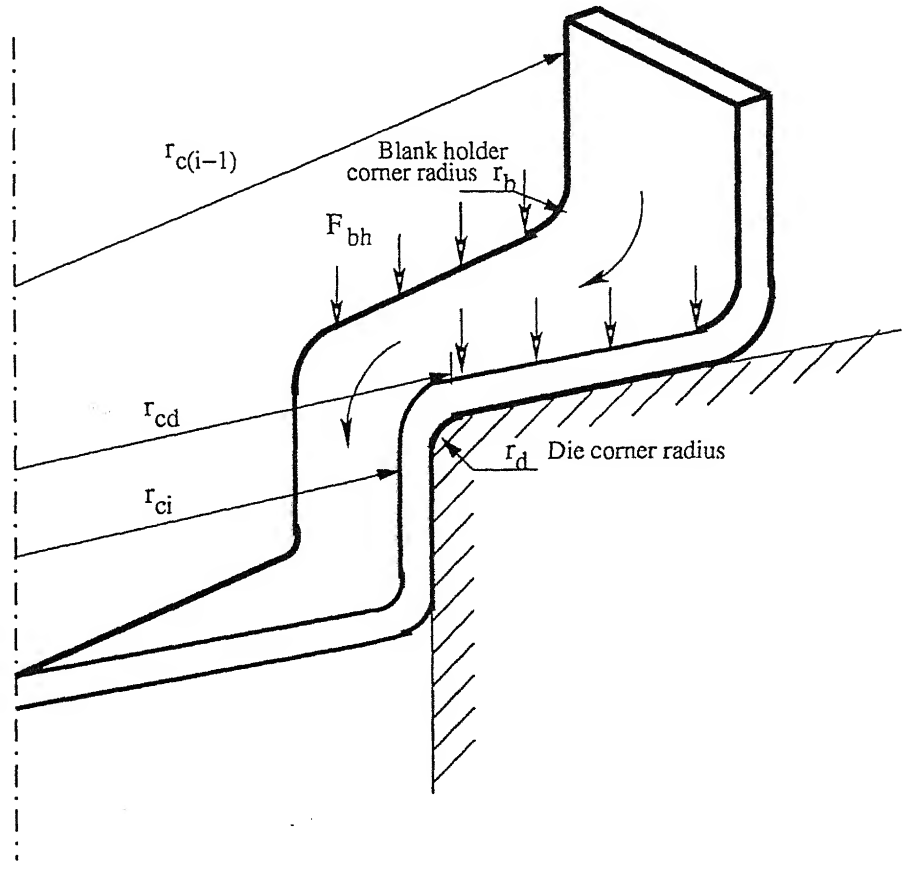

Figure 2.5: Section of a partial drawn cup

Pure Radial Drawing in the Flange Region

The annular portion of the sheet metal workpiece (see Fig. 2.5) between the blank holder and die is subjected to a pure radial drawing. The radial equilibrium equation of an element of the flange under the blank holder is given by

$$\frac{d\sigma_r}{dr} = -\frac{(\sigma_r - \sigma_\theta)}{r} \tag{2.40}$$

Assuming the plane strain condition $d\epsilon_z = 0$, one can get

$$(\sigma_r - \sigma_\theta) = \bar{\sigma}\sqrt{\frac{2(1+\bar{R})}{2\bar{R}+1}} \tag{2.41}$$

The effective strain $\bar{\epsilon}$ in the flange region is given by

$$\bar{\epsilon} = \sqrt{\frac{2(1+\bar{R})}{1+2\bar{R}}} ln(\frac{R}{r}) \tag{2.42}$$

The effective strain $\bar{\epsilon}$ after adding the strain induced in the cup wall due to the previous draws and bending along blank holder profile is given by

$$\bar{\epsilon} = ln\left(LDR_{(i-1)}\right) + ln\left(1 + \frac{t_0}{2r_b + t_0}\right) + \sqrt{\frac{2(1+\bar{R})}{1+2\bar{R}}} ln(\frac{R}{r}) \tag{2.43}$$

and the effective stress in the flange can be obtained as

$$\bar{\sigma} = K\left[ln\left(LDR_{(i-1)}\right) + ln\left(1 + \frac{t_0}{2r_b + t_0}\right) + \sqrt{\frac{2(1+\bar{R})}{1+2\bar{R}}} ln(\frac{R}{r})\right]^n \tag{2.44}$$

Redrawing can be considered as a steady state process as the material is drawn inward with the continuous supply from cup wall formed during the earlier draw [Hosford, 1983]. Integrating the above equation from r_{cd} to the maximum radius $r_{c_{i-1}}$ formed during earlier draw,

$$\int_{r_{cd}}^{r_{c_{i-1}}} d\sigma_r = \int_{r_{cd}}^{r_{c_{i-1}}} -K\left[ln(LDR_{i-1}) + ln\left(1 + \frac{t_0}{2r_b + t_0}\right) + \sqrt{\frac{2(1+\bar{R})}{1+2\bar{R}}} ln(\frac{R}{r})\right]^n \sqrt{\frac{2(1+\bar{R})}{1+2\bar{R}}} \frac{dr}{r}$$

Expanding using Binomial theorem and neglecting higher order terms, one can get

$$\sigma_r = K\sqrt{\frac{2(1+\bar{R})}{1+2\bar{R}}}\ [\epsilon_p]^n \int_{r_{cd}}^{r_{c(i-1)}} \left[1 + \frac{n\sqrt{\frac{2(1+\bar{R})}{1+2R}}}{\epsilon_{prev}} ln\frac{R}{r}\right] \frac{dr}{r}$$

where $\epsilon_p = ln\left(LDR_{(i-1)}\right) + ln\left(1 + \frac{t_0}{2r_b+t_0}\right)$. On simplification it reduces to

$$\sigma_r = K\sqrt{\frac{2(1+\bar{R})}{1+2\bar{R}}}\,[\epsilon_p]^n \left[ln(\frac{r_{c_{i-1}}}{r_{cd}}) + \frac{n\sqrt{\frac{2(1+\bar{R})}{1+2\bar{R}}}}{\epsilon_p} \int_{r_{cd}}^{r_{c_{i-1}}} ln\frac{R}{r}\frac{dr}{r}\right] \tag{2.45}$$

Expansion to the integration term $\int_{r_{cd}}^{r_{c_{i-1}}} ln(\frac{R}{r})\,\frac{dr}{r}$ is given by

$$\int_{r_{cd}}^{r_{c_{i-1}}} ln\frac{R}{r}\,\frac{dr}{r} = 2\Big[ln\frac{r_{c_{i-1}}}{r_{cd}} - \frac{1}{R_{i+1}^2 - r_{cd}^2}\Big[r_{c_{i-1}}\sqrt{R_{i+1}^2 - r_{cd}^2 + r_{c_{i-1}}^2} - r_{cd}\,R_{i+1} - (r_{c_{i-1}}^2 - r_{cd}^2)$$

$$+(R_{i+1}^2 - r_{cd}^2)\Big[ln\frac{r_{c_{i-1}} + \sqrt{R_{i+1}^2 - r_{cd}^2 + r_{c_{i-1}}^2}}{r_{cd} + R_{i+1}}\Big]\Big]\Big] \tag{2.46}$$

where R_{i+1} is the intermediate radius on the base of the cup. The derivation of $\int_{r_{cd}}^{r_{c_{i-1}}} ln(\frac{R}{r})\,\frac{dr}{r}$ is shown in Appendix A (II).

Friction along Tool-Work Interface

The radial friction stress induced in the flange region due to blank holding force without wrinkling consideration and is approximated [Leu, 1999] as

$$\sigma_f \simeq 2\mu(1.1\sigma_0)\frac{r_{c_{(i-1)}}}{r_{cd}} \tag{2.47}$$

Selection of blank holding force will be such that wrinkling should not occur. From the literature, wrinkling of sheet will be occur when the relative thickness $(\frac{t_0}{d_{c_{(i-1)}}})$ is less than 0.005. In the present model, for the values of $(\frac{t_0}{d_{c_{(i-1)}}})$ less than 0.005, required blank holding force is selected from the literature presented in chapter 3. Frictional stresses in Eq. 2.47 are modified accordingly with the chosen blank holding force. From Eqs. 2.38, 2.45 and 2.47, total drawing stress at the beginning of the die arc radius r_{cd} can be obtained as

$$\sigma_{r_{cd}} = \sigma_{b1} + \sigma_f + \sigma_r \tag{2.48}$$

Considering friction along the die profile, the radial drawing stress at the exit of the die profile can be obtained similar to the first draw (Fig. 2.2 b) and is given by

$$\sigma_{r_{c_i}} = e^{\mu\alpha}\,\sigma_{r_{cd}}\left(\frac{r_{cd}}{r_{c_i}}\right) \tag{2.49}$$

Bending along Die Arc Radius

Considering the bending and unbending of sheet along die arc radius, the resulting stress can be evaluated as

$$\sigma_{b2} = \frac{\bar{\sigma}_2\, t_0}{2\, r_d + t_0} \tag{2.50}$$

where r_d is the die arc radius and $\bar{\sigma}_2$ be the mean flow stress along the blank holder profile and it can be calculated similarly as in the case of first draw. The final expression can be written as

$$\bar{\sigma}_2 = K\left[ln(LDR_{i-1}) + ln\left(1 + \frac{t_0}{2r_b + t_0}\right) + ln(LDR_i) + ln\left(\sqrt{1 + \frac{t_0}{2r_d + t_0}}\right)\right]^n \tag{2.51}$$

The total drawing stress at the exit of die arc radius is evaluated from Eqs. 2.49 and 2.50 and is given by

$$\sigma_{total} = \sigma_{r_{c_i}} + \sigma_{b2} \tag{2.52}$$

The limiting drawing ratio is determined from the condition that the total drawing stress given by Eq. 2.37 in the cup wall is equal to the total drawing stress given by Eq. 2.52 due to continuity of stress. Equating these two, one can get

$$f(LDR_i) = \left[-C_1\frac{r_{c_i}}{r_{cd}} + \frac{\bar{\sigma}_2\, t_0}{2\, r_d + t_0}\right]e^{-\mu\alpha} + C_3\frac{r_{c_{(i-1)}}}{r_{cd}} + 2\mu(1.1\sigma_0)\frac{r_{c_{(i-1)}}}{r_{cd}}\left(1 - \frac{0.005\, d_{c_{(i-1)}}}{t_0}\right)$$

$$+C_4 ln\left(\frac{r_{c_{(i-1)}}}{r_{cd}}\right) + C_5\left[ln\left(\frac{r_{c_{(i-1)}}}{r_{cd}}\right) - \frac{1}{R^2_{(i+1)} - r^2_{cd}}\left[r_{c_{(i-1)}}\sqrt{R^2_{(i+1)} - r^2_{cd} + r^2_{c_{(i-1)}}}\right.\right.$$

$$-r_{cd}R_{(i+1)} - (r^2_{c_{(i-1)}} - r^2_{cd})\Big]\Big] - C_5 ln\left[\frac{r_{c_{(i-1)}} + \sqrt{R^2_{(i+1)} - r^2_{cd} + r^2_{c_{(i-1)}}}}{r_{cd} + R_{(i+1)}}\right] \quad (2.53)$$

where

$$C_3 = 2\mu(1.1\sigma_y) \;\; ; \;\; C_4 = K\sqrt{\frac{2(1+\bar{R})}{1+2\bar{R}}}\left[ln(LDR_{(i-1)})\right]^n \left[ln(LDR_{(i-1)})\right]^{n-1}$$

$$C_5 = 2Kn\frac{2(1+\bar{R})}{1+2\bar{R}} \;\; ; \;\; r_{c_i} = \frac{r_{c_{(i-1)}}}{LDR_i} \;\; ; \;\; r_{cd} = r_{c_i} + r_d$$

Constant C_1 remain the same as in the first draw analysis. $\frac{R_{i+1}}{r_{cd}}$ can be obtained by considering the volume constancy of plastic deformation in the die arc region as in the first draw analysis.

$$\frac{R_{i+1}}{r_{cd}} = \left[\pi\left(\frac{r_d}{\frac{r_{c_{i-1}}}{LDR_i} + r_d} - \frac{2r_d^2}{\pi(\frac{r_{c_{i-1}}}{LDR_i} + r_d)^2}\right) + \left(\frac{1}{1 + \frac{LDR_i\, r_d}{r_{c_{i-1}}}}\right)^2 \left(\frac{R_i}{r_{c_i}}\right)^2\right]^{\frac{1}{2}} \quad (2.54)$$

where, $\frac{R_i}{r_{c_i}} = e^{\sqrt{\frac{(1+\bar{R})}{2}}n}$; R_i and R_{i+1} are the intermediate radii of annular rings on the bottom of cup formed during the previous draw, which draws inward into the die to the radii r_{c_i} and r_{cd} respectively. Substituting Eq. 2.54 in Eq. 2.53 gives a general equation for redraw in terms of LDR_i, where $i = 1, 2, 3, ...N$ Solution of this non-linear equation is obtained by bisection method. While using the Eq. 2.53 for multiple passes, strain hardening caused during each pass should be taken into account for the subsequent passes.

Chapter 3

Product and Process Design System

3.1 Introduction

Almost all the attempts [Eshel et al., 1986; Sitaraman et al., 1991; Tisza et al., 1995; Eshe et al., 1996; Sing et al., 1997; Park et al., 1998 and Kang et al., 2002] made to develop computer aided process planning systems for deep drawing have used the formability limits (LDR) collected from the data tables or hand books. All these systems are based on Generate and test-and-rectify (G&TR) strategy [Eshel, 1986]. This strategy *generates* the initial sequence of deep drawing operation, *tests* workability and reliability of the deep drawing process outline and *rectifys* the process if a formability violation is predicted. The proposed product and process design system for deep drawing is a combination of analytical and empirical models. Analytical model is developed for finding formability limits considering affect of various variables instead of taking from the handbooks or data tables. Empirical rules are implemented and used in the form of design rules for the process sequencing. The aim of the proposed system is to generate process plan for a given final deep drawn product. The present system also generates possible alternate process plans considering annealing between stages. This facilitates the process designer to choose a particular process plan according to his requirements. Process plans for variety of axisymmetric flat bottomed deep drawn products like straight cups, stepped cups, flanged cups, cups with tapered elements and for certain types of conical cups can be obtained from the present system. The block diagram of the present system is shown in Fig. 3.1. The proposed system consists of following modules.

- Object Modeling and Interfacing: A feature based parametric design procedure is used to model the object. Interfacing module facilitates interaction with the other modules.
- Database : Database of the system basically contains the material properties of commonly used deep drawn materials and tribological data of lubricants used in the deep drawing.
- Analysis Module : The analysis model developed by Sonis et al. [2003] is modified to include sheet thickness as a variable by considering bending and straightening effects along die profile and the same is used for the prediction of LDR.

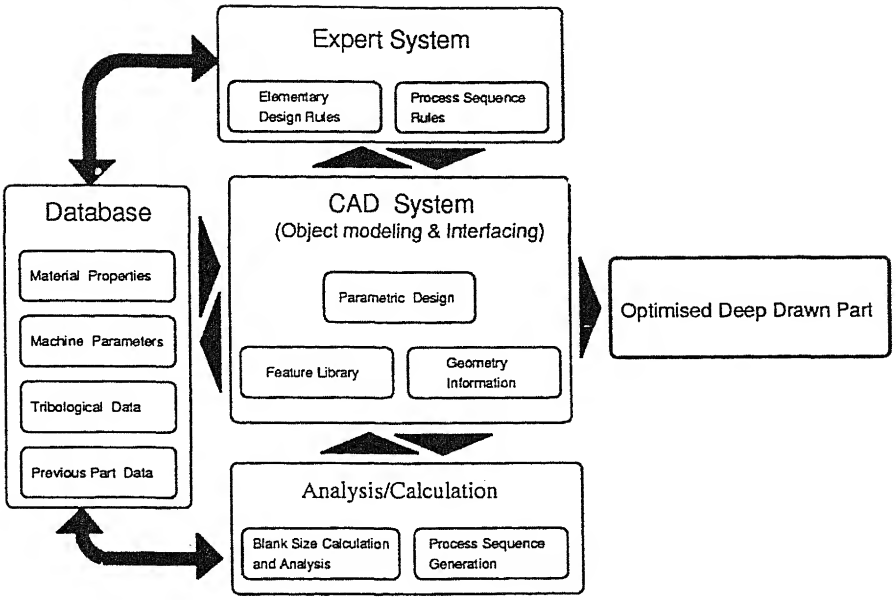

Figure 3.1: Block Diagram of Integrated Product and Process Design System

- Expert System : This module consists of elementary design rules for process design as well as for process sequence.
- Process Sequence Module: This module is developed for the automatic generation of the process sequence from the blank to the required final cup.
- Feasible Sequence Module: This module generates alternative process plans considering annealing and strength requirements.

3.2 Object Modeling and Interfacing

A feature based design module is developed to automate the input of geometric information to the process design system. In the present work, parametric design of features is used. The final object geometry for which a process sequence needs to be generated is the input to the system in the form of concatenation of line elements/features. The input geometry can be created by selecting the different elements/features such as horizontal, vertical, incline, concave arc, convex arc etc, from the feature library shown in Fig. 3.2. In the present case these features are recognized in the code using the symbols as follows.

h - horizontal element

v - vertical element

i - tapered element

r - counter clockwise quarter arc element

c - clockwise quarter arc element

a - counter clockwise angular arc element

x - clockwise angular arc element

Element geometry	Conventional name
	Horizontal
	Vertical
	Tapered
	Concave
	Conave – reduced

Figure 3.2: Element library

Interfacing module handles the data transfer between the various modules of the system.

3.2.1 Blank Size Calculation

To calculate the initial blank size for the required final cup geometry, material thickness is assumed to be constant. This implies that the surface area also remains constant. The surface area of the final part is in fact nearly identical to the initial surface area of the blank regardless the number of drawing operations. In order to account for the non-uniform flow of material, which leads to earing, a trim allowance must be incorporated when determining the blank shape. The required blank area obtained by analysis is multiplied by 1.15, which takes into account of any possible directionality and clearance for trimming.

To determine the blank size it is necessary to divide the entire axisymmetric part into various individual axisymmetric elements and calculate the surface area of each element. The surface area of axisymmetric shapes can be determined by using Pappus's second theorem [Miller, 1994]. Pappus's Second Theorem states that the area of any surface of revolution is the product of the path of the center of gravity of a curve along the axis of rotation, times the length of that curve. Figure. 3.4 shows some possible elements of an axisymmetric cup. Figure. 3.3 shows the path of the center of gravity and length of element of some elements. The path of the center of gravity P_1 and length L_1 of element 1 around the axis of rotation is given by:

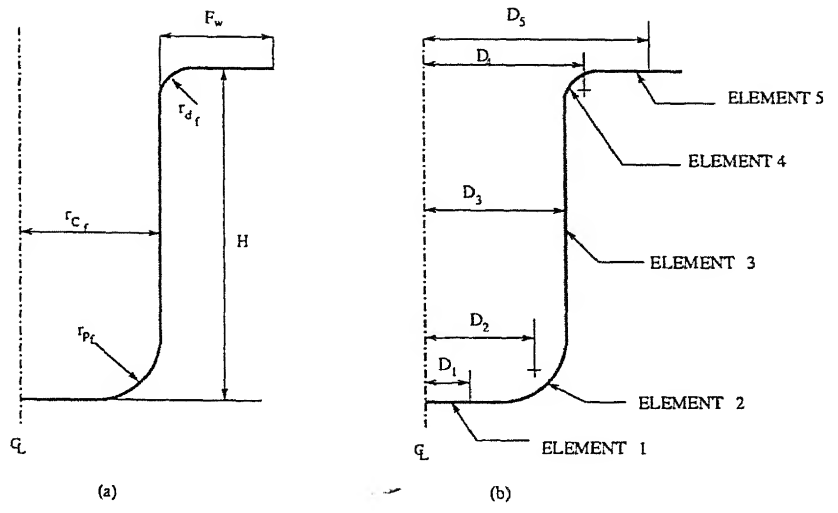

(a) Cup Dimensions (b) Distance to Elements

Figure 3.3: Cross section of an axisymmetric cup

For element 1:

$$P_1 = 2\pi D_1 = 2\pi \frac{r_{c_f} - r_{b_f}}{2}, \quad L_1 = r_{c_f} - r_{b_f}$$

For element 2:

$$P_2 = 2\pi D_2 = 2\pi (r_{c_f} - r_{b_f} + \frac{2r_{b_f}}{\pi}), \quad L_2 = \frac{r_{b_f}\pi}{2}$$

For element 3:

$$P_3 = 2\pi D_3 = 2\pi r_{c_f}, \quad L_3 = H - r_{d_f} - r_{b_f}$$

For element 4:

$$P_4 = 2\pi D_4 = 2\pi (r_{c_f} + r_{d_f} - \frac{2r_{d_f}}{\pi}), \quad L_4 = \frac{r_{d_f}\pi}{2}$$

For element 5:

$$P_5 = 2\pi D_5 = 2\pi (r_{c_f} + r_{d_f} + \frac{F_w - r_{d_f}}{2}), \quad L_5 = F_w - r_{d_f}$$

Sum the product of paths of the center of gravity and element lengths results in the surface area (SA) of the cup under consideration and is given by

$$SA = P_1 L_1 + P_2 L_2 + P_3 L_3 + P_4 L_4 + P_5 L_5$$

To account for any possible directionality in the material properties, the calculated surface area is multiplied by 1.15 in order to obtain the required blank area with proper clearance for trimming. Thus the initial blank diameter is given by

$$D_0 = \sqrt{\frac{4SA(1.15)}{\pi}}. \tag{3.1}$$

Element	Dimensions	$\bar{X}$	$\bar{Y}$	Length
Line	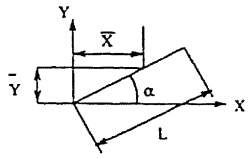	$\frac{L}{2}\cos\alpha$	$\frac{L}{2}\sin\alpha$	L
Quarter Circular Arc	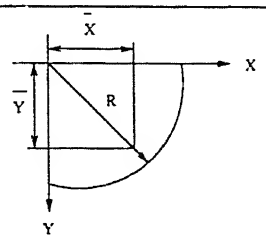	$\frac{2R}{\pi}$	$\frac{2R}{\pi}$	$\frac{\pi}{2}R$
Circular Arc	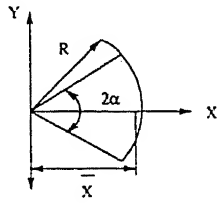	$\frac{R\sin\alpha}{\alpha}$	—	$2\alpha R$

Figure 3.4: Table of possible elements

3.3 Database

According to Martin(1975),"A database may be defined as a collection of interrelated data stored together without harmful or unnecessary redundancy to serve one or more applications in an optimal fashion; the data are stored so that they are independent of programs which use the data; a common and controlled approach is used in adding new data and in modifying and retrieving existing data within the database." The database of present system basically contains the material data for commonly used deep drawn materials and tribological data for the lubricants used in the process.

3.3.1 Material Database

The material database module contains information related to material in a relational form. The stress-strain relation of sheet metal is assumed to follow the form $\bar{\sigma_e} = K(\bar{\epsilon})^n$. However, the user can expand the material database to include new materials. The user can select any of the materials from the list presented in the Table 3.1. The code is flexible to enter the material properties manually for a material, which is not in the material database.

Alloy	Yield Strength (MPa)	Ultimate Strength (MPa)	Constant K (MPa)	Normal Anisotropy ($\bar{R}$)	Strain Hardening Exponent (n)	Critical Drawing Ratio
AA 3003	41	110.3	157.1	0.8	0.235	6.0
SAE 1006	200	310	617	1.4	0.310	6.0
CA-DDQ	155	330	610	2.1	0.263	6.0
BA-DDQ	157	338	612	1.76	0.248	6.0
DQ killed	172	300	610	1.6	0.220	6.0
Stainless Steel	250	570	1450	1.0	0.400	5.0

Table 3.1: Alloy types: AA 3003 aluminum alloy, others are steel alloys, DDQ-deep drawing quality; CA-continuous annealing; BA-batch annealing

3.3.2 Tribological Database

In general, lubricants used in the deep drawing operation are of two types namely, oil based and water based. The final selection of lubrication largely depends upon the severity of the forming operation. Table 3.2 suggests lubricants for a given work piece material. Improper lubrication will cause failure by increased friction, which causes large tensile forces in the cup wall leading to failure. Lubrication also affects the life of tooling (dies). In the deep drawing there is a sliding

Alloy	μ	Suggested lubricant
Corbon Steel	0.05 - 0.1	MO; SP-EM
Stainless Steel	0.05 - 0.1	EP- MO; EP-MO-EM; PC
Al Alloys	0.05 - 0.1	FA-M; FO

Table 3.2: Typical lubricants used in deep drawing: Hyphenation indicates that several components are used in the lubricant. EM - emulsion (the listed lubricants are emulsified and 1-20% dispersed in water); EP - extreme pressure compounds (containing S, Cl and / or P); FA - fatty acids, alcohols amines and esters; MO - mineral oil; PC - polymer coating

contact between the die surface and the work metal. The value of coefficient of friction (μ) lies between 0.05 to 0.10 [Schuler,1998].

3.4 Analysis Module

In deep drawing the formability limits from the initial blank to final size can be measured in terms of limiting drawing ratios (LDR's). The model presented by Sonis et al. [2003] is

modified to include sheet thickness as a variable which has significant effect on LDR values. In the present model bending, unbending effects are introduced in the calculation of LDR for the multi-stage deep drawing operation. A condition for prevention of wrinkling is incorporated to select the blank holding force. The present analysis model also predicts LDR values after performing annealing operation between stages by assuming all the previous strain gets nullified after annealing. Analysis model used in the present system is presented in chapter 2.

3.5 Expert System

An Expert system can be defined as "a computing system capable of representing and reasoning about some knowledge rich domain, which usually requires a human expert, with a view toward solving problems and/or giving advice." Typically, such a system contains a knowledge base containing accumulated experience and a set of rules for applying the knowledge base to each particular situation that is described to the program. In the present system, the guidelines available in the literature are collected and implemented in the form of design rules. These rules are presented in the Appendix B.

3.6 Process Sequencing Module

A process sequence module is developed for the automatic generation of the process sequence from the blank to the required final cup. This module consists of two sub-modules namely geometric sequence module and a rectification module.

3.6.1 Geometric Sequence Module

This module automatically generates the process sequence in the backward direction starting from the component geometry based only on the geometrical features of the cup. This module identifies the current deformation zone and generates previous deformation zone by considering the shape of previous deformed zone is a straight and vertical non-flanged cup. This procedure is repeated until the previous shape is the flat circular blank. This process is called generate strategy in the G&TR system. Geometric sequencing is the first step in any process sequencing system for deep drawing. The rules for geometric sequencing are presented in Appendix B.

3.6.2 Rectification Module

The process sequence generated using the geometrical design module may not be feasible, as the formability of the material is not taken into consideration. Adding new intermediate stages to the geometric sequence where the process analysis module predicts formability violation modifies process sequence. Present system automatically select the die and punch geometries according to the geometrical details of the cup at each drawing stage without violating fundamental design

rules presented in Appendix B. Analysis module of the present system is used to generate the rectified process sequence, considering formability and the geometric sequence instead of testing the formability violation using the decision tables for a given material. Important rules for the rectification of geometric sequence are presented in Appendix B.

3.7 Feasible Sequences

This module generates alternative process sequences by performing annealing between stages. Annealing is required whenever the total reduction reaches a critical value. This value is different for different materials. The present system generates all possible sequences irrespective of the critical drawing ratio to minimize the number of stages. The optimum process sequence can be selected by considering minimum number of stages and strength requirements of the final cup. The selected process sequence may not be economical, as the cost of tooling and cost of annealing are not considered in the present work.

Chapter 4

Validation and Studies on LDR

4.1 Introduction

To test the validity of the analysis model presented in Chapter 2, its prediction are compared with the available experimental results [Thorp, 1973; El-Sebaie and Mellor, 1972; Leu, 1999] for the first draw. The predicted values of limiting drawing ratios for the subsequent passes are compared with the suggested drawing ratios for SAE-1006 material by Lange, [1985]. Comprehensive parametric study is carried out to study the influence of process variables such as sheet thickness, die arc radius, coefficient of friction, normal anisotropy, strain hardening exponent, etc. on limiting drawing ratio for first draw as well as for redraws.

4.2 validation

First Draw

Table 4.2 shows the comparison between the predictions of present model with the experimental results of Thorp [1973] (reported by Leu [1999]) and it can be seen that the experimental results and predictions of the present model are in good agreement.

Table 4.2 shows the comparison between the predictions of the present model with the experimental results of El-Sebaie and Mellor [1972]. They carried out experiments by forming the cylindrical cups from the circular blanks of nominal blank thickness of 0.71 mm. Punch head used had a stem diameter of 38 mm and a profile radius of 4 mm. The diameter of the die opening was 39.945 mm giving a radial clearance of 37% of nominal blank thickness. The blanks were lubricated on both sides using Droyt-Sol 4 M. A series of blanks were produced increasing in steps of 1 mm on the diameter. In the final stages of the tests to determine the limiting drawing ratio the increment of 1 mm was reduced to 0.4 mm. The conditions used by El-Sebaie and Mellor [1972] are used to estimate the limiting drawing ratio using the present model. For the lubricant Droyt-Sol 4 M, coefficient of friction (μ) is taken as 0.10 as reported by Leu[1999]. It can be seen that the results obtained are in good agreement with the results of El-Sebaie and

Mellor [1972].

Material type	t_0 (in)	r (in)	r_d (in)	$\sigma_u \times 10^2$ (lbf in)^2	σ_0 (lbf in)^2	$\bar{R}$	n	LDR (Present)	LDR [Thorp]
MS1	0.0356	1.04220	0.26780	426	29379.3	1.18	0.187	2.23	2.49
MS2	0.0347	1.04265	0.26735	488	37538.5	1.05	0.170	2.21	2.43
MS3	0.0312	1.04440	0.26560	436	29459.5	1.14	0.203	2.23	2.46
MS4	0.0288	1.04560	0.26440	545	43600.0	1.06	0.174	2.21	2.40
MS5	0.0288	1.04560	0.26440	534	42380.9	1.18	0.183	2.25	2.42
MS6	0.0390	1.04050	0.26950	473	40084.7	1.27	0.156	2.27	2.39
MS7	0.0394	1.04030	0.26970	465	35496.2	1.13	0.187	2.22	2.36

Table 4.1: Comparison of experimental and theoretical data of LDR for mild steel sheets. Experiments were carried out by Thorp [1973] as reported by Leu [1999]. Material: Mild steel, $\mu = 0.05$, Lubricant: Polythene film + Vaseline

Material type	t_0 (mm)	K (Kpmm^{-2})	σ_0 (Kpmm^{-2})	$\bar{R}$	n	LDR (Present)	LDR El-Sebaie,Millor
HH Al	0.70	13.37	10.36	0.49	0.041	2.23	2.10
Soft Al	0.70	12.02	2.93	0.61	0.227	2.15	2.05
Soft 70/30 brass	0.75	75.30	3.69	0.83	0.485	2.22	2.19

Table 4.2: Comparison of experimental and theoretical data of LDR for non-ferrous sheets. Lubricant : Droyt-Sol 4M, mineral oil. $\mu = 0.10$, cup radius = 19.623 mm, $r_d = 7.450$ mm. Experiments were carried out by El-Sebaie and Mellor [1972].

Table 4.3 shows the comparison of experimental LDR values presented by Leu [1999] with LDR values obtained using present model. Leu [1999] conducted experiments on blanks which were cut by WC-EDM technique to avoid irregularities in the rim. Lubricants, Zinc stearate $Z_n(O_{18}H_{35}O_2)$ and press oil S-295H (a higher-pressure hydraulic oil), were used at the contact interface. He carried experiments from sheet of diameter 100 mm with the diameter progressively increased by 5 mm until the sheet was fractured. The predicted values of the present analysis model are in good agreement with the experimental values.

Redraw

To establish the validity of the present model, its predictions are compared with the suggested drawing ratios given in Handbook of Metal Forming, Lange[1985] for SAE-1006 and are shown in Table 4.4. Lange[1985] reported drawing ratios for deep drawing of cylindrical components

Item	Cup radius r (mm)	Die corner radius, r_d (mm)	Coeff. of friction μ	LDR Experimental Leu [1999]	LDR Calculated Leu [1999]	LDR Calculated (Present)
Material: CA-DDQ steel, $\bar{\sigma} = 610\ \epsilon^{0.263}$, t_0=1.0 mm, σ_0=155 MPa and $\bar{R}$=2.1						
E1	30.75	8.5	0.1	2.23	2.45	2.35
E2	30.75	8.5	0.2	2.13	2.15	2.18
Material: BA-DDQ steel, $\bar{\sigma} = 612\ \epsilon^{0.248}$, t_0=1.0 mm, σ_0=157 MPa and $\bar{R}$=1.76						
E3	30.75	8.5	0.1	2.23	2.35	2.30
E4	30.75	8.5	0.2	2.13	2.07	2.12
Material: BA-DDQ steel, $\bar{\sigma} = 619\ \epsilon^{0.264}$, t_0=1.2 mm, σ_0=138 MPa and $\bar{R}$=1.8						
E5	30.65	8.6	0.1	2.22	2.39	2.29
E6	30.65	8.6	0.2	2.14	2.13	2.15
E7	30.78	8.6	0.1	2.24	2.38	2.29
E8	30.78	8.6	0.2	2.16	2.12	2.15
E9	30.86	8.6	0.1	2.17	2.38	2.29
E10	30.86	8.6	0.2	2.14	2.12	2.15
Material: BA-CQ2 steel, $\bar{\sigma} = 622\ \epsilon^{0.238}$, t_0=1.2 mm, σ_0=171 MPa and $\bar{R}$=1.54						
E11	30.86	5.4	0.2	2.06	1.91	2.00
E12	30.86	8.6	0.2	2.10	2.01	2.16
E13	30.86	10.6	0.2	2.11	2.07	2.17
E14	30.86	12.6	0.2	2.14	2.13	2.23
E15	30.86	14.6	0.2	2.17	2.19	2.28

Table 4.3: Comparison of experimental data of LDR presented by Leu[1999] with the calculated LDR values for various steel sheets: BA, batch annealing; CA, continuous annealing; CQ, commercial quality; DDQ, deep drawing quality

with flat bottom for the different relative sheet thickness ranges (1.5-2.0, 1.0-1.5, 0.6-1.0, 0.3-0.6, 0.15-0.3 and 0.08-0.15). The relative sheet thickness is given by $\frac{t_0}{D_0} \times 100$ The relative sheet thickness is used to select the blank holding force to avoid wrinkling (see chapter 3). For the relative sheet thickness less than 0.50, blank holder force is required to avoid wrinkling [Eary and Reed, 1974]. Present analysis has been carried out by considering the blank-holding force during deep drawing, therefore, comparisons are made for different relative sheet thickness values less than 0.50 as it needs blank holding force. The value of normal anisotropy for most of the deep drawing quality steels vary from 1.2 to 1.6 [ASM Handbook, 1992]. Here, for estimating the limiting drawing ratio using the present model, the value of normal anisotropy is taken as 1.4 for SAE-1006. The material properties of SAE-1006 steel are [ASM Handbook, 1992] given by

Generalized stress $(\bar{\sigma}) =$ $617(\bar{\epsilon})^{0.310}$ MPa

Yield Strength $(\sigma_0) =$ 200 MPa

Normal Anisotropy$(\bar{R}) =$ 1.4

The thickness of the initial blank is chosen as 1.0 mm and the initial blank diameter is calculated to satisfy the chosen relative sheet thickness value. Since the data regarding the die geometry

and friction condition are not reported by Lange[1985], die arc radius for the first draw is chosen as $8.5t_0$ and for the subsequent draws it is taken as 0.8 times of previous draw die arc radius [Lange, 1985]. Blank holder corner radius is chosen as 8 mm in case of redraws and coefficient of friction (μ) is taken as 0.10 [Schuler, 1998]. From the table 4.4, it can be seen that the predictions

Number of draw	Relative sheet thickness ($\frac{t_0}{2R_0} \times 100$)					
	Lange [1985]			Present work		
	0.3-0.6	0.15-0.3	0.08-0.15	0.50	0.25	0.15
1	1.72-1.82	1.67-1.72	1.59-1.67	2.18	2.02	1.86
2	1.26-1.28	1.25-1.26	1.22-1.25	1.34	1.27	1.26
3	1.23-1.25	1.22-1.23	1.19-1.22	1.29	1.22	1.21
4	1.20-1.22	1.18-1.20	1.16-1.18	1.26	1.18	1.17
5	1.16-1.18	1.15-1.16	1.14-1.15	1.22	1.15	1.14

Table 4.4: Comparison of theoretical data of LDR for Redraws without intermediate annealing with drawing ratio suggested by Lange [1985].
Sheet metal thickness, $t_0 = 1.0$ mm. *Source:Handbook of Blanking Technology,Romanowski[1959].*

of the present model are reasonably good agreement with the limiting drawing ratios given by [Lange, 1985]. The discrepancy in the result may be due to the following reasons:

- different die geometry used.
- different friction conditions used.
- thickness of the sheet considered as 1.0 mm in the present work.

4.3 Studies on LDR

Comprehensive parametric study has been carried out to study the effect of various process parameters on the limiting drawing ratio for first and redraws.The material chosen for the study is CA-DDQ steel as it has better drawability characteristics. Figures 4.1, 4.2 and 4.3 show the variation of LDR in case of first draw with die arc radius(r_d) for different values of normal anisotropy($\bar{R}$), strain hardening index(n) and friction coefficient(μ) with and without bending effects. It can be seen that in all the cases, bending effects are more significant at small die arc

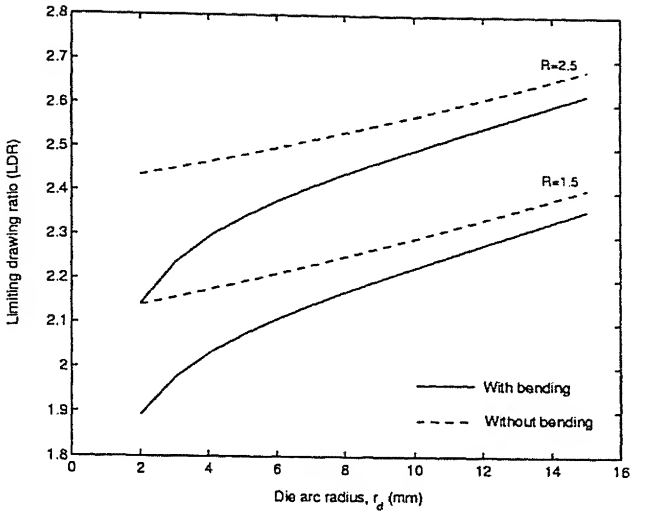

Figure 4.1: Variation of LDR with die arc radius for different values of normal anisotropy for first draw. ($\bar{\sigma} = 610\bar{\epsilon}^{0.263}$ MPa, $\sigma_0 = 155$ MPa, $\mu = 0.1$, $R_0 = 100$ mm,$r_d = 8.5$ mm, $t_0 = 1.0$ mm)

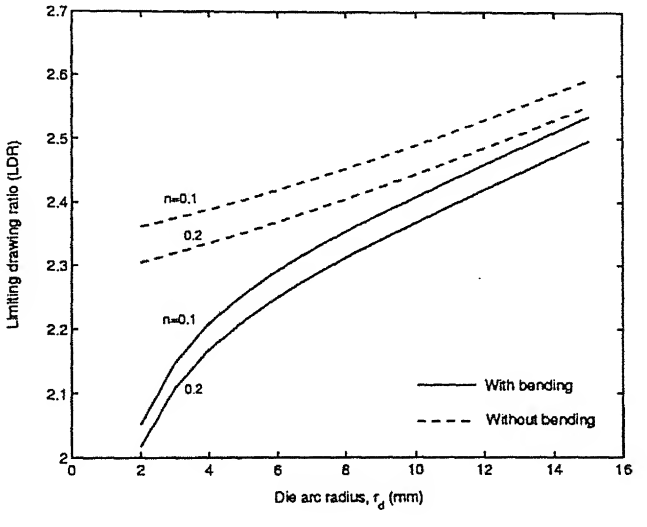

Figure 4.2: Variation of LDR with die arc radius for different values of strain hardening index for first draw. ($\bar{\sigma} = 610\bar{\epsilon}^{0.263}$ MPa, $\sigma_0 = 155$ MPa, $\mu = 0.1$, $R_0 = 100$ mm,$r_d = 8.5$ mm, $t_0 = 1.0$ mm)

radii. This can be attributed to the reduction in LDR when small die arc radius is used. From the above figures, it is clear that die arc radius between 4 to 10 times sheet thickness is always a good practice. Figures 4.4, 4.5 and 4.6 show the variation of LDR with blank thickness for different values of normal anisotropy($\bar{R}$), strain hardening index(n) and friction coefficient(μ) with and without bending effects. It can be seen that initially the LDR increases with increase in thickness and starts decreasing slowly with further increase in thickness. This is because of

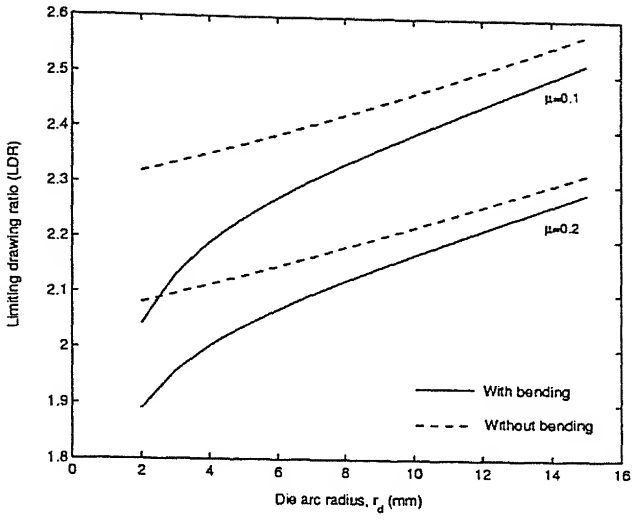

Figure 4.3: Variation of LDR with die arc radius for different values of friction coefficient for first draw. ($\bar{\sigma} = 610\bar{\epsilon}^{0.263}$ MPa, $\sigma_0 = 155$ MPa, $\mu = 0.1$, $R_0 = 100$ mm,$r_d = 8.5$ mm, $t_0 = 1.0$ mm)

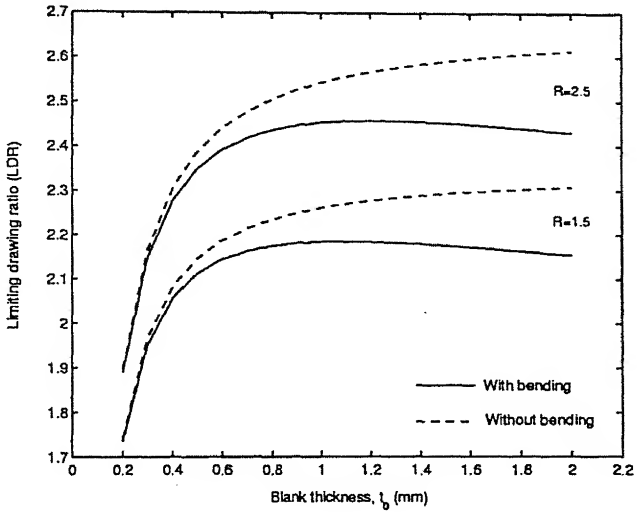

Figure 4.4: Variation of LDR with blank thickness for different values of normal anisotropy for first draw. ($\bar{\sigma} = 610\bar{\epsilon}^{0.263}$ MPa, $\sigma_0 = 155$ MPa, $\mu = 0.1$, $R_0 = 100$ mm,$r_d = 8.5$ mm, $t_0 = 1.0$ mm)

simultaneous effects of bending and frictional stresses. Bending stresses increases with increase in blank thickness at the same time frictional stresses decreases as less blank holding force is sufficient to prevent wrinkling in thicker sheets. At the small values of blank thickness, high blank holding force is required to prevent wrinkling. Hence for the thin sheets frictional stresses dominate over bending stresses and vice versa.

Figure 4.7 shows the variation of LDR with the relative sheet thickness ($\frac{t_0}{D_0} \times 100$) by varying blank radius for two sheet thicknesses with and without bending effects. It can be seen that

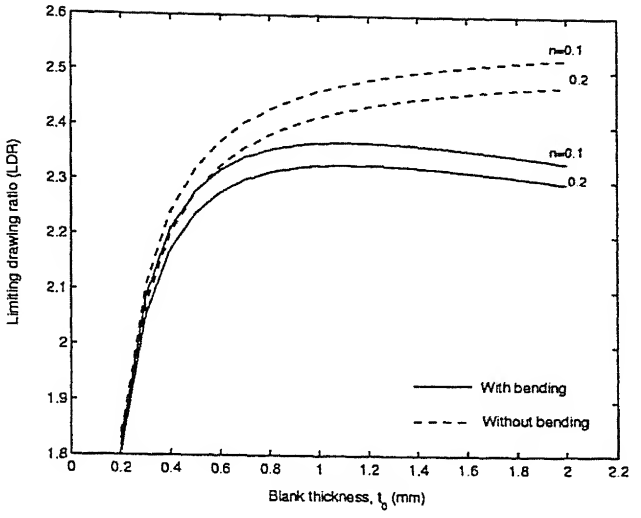

Figure 4.5: Variation of LDR with blank thickness for different values of strain hardening index for first draw. ($\bar{\sigma} = 610\bar{\epsilon}^{0.263}$ MPa, $\sigma_0 = 155$ MPa, $\mu = 0.1$, $R_0 = 100$ mm,$r_d = 8.5$ mm, $t_0 = 1.0$ mm)

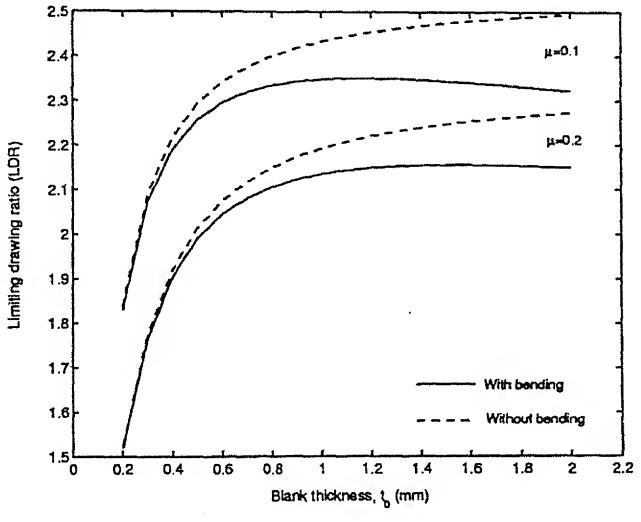

Figure 4.6: Variation of LDR with blank thickness for different values of friction coefficient for first draw. ($\bar{\sigma} = 610\bar{\epsilon}^{0.263}$ MPa, $\sigma_0 = 155$ MPa, $\mu = 0.1$, $R_0 = 100$ mm,$r_d = 8.5$ mm, $t_0 = 1.0$ mm)

LDR increases with increase in $\frac{t_0}{D_0}$ ratio. This is because of reduction in frictional stresses due to decrease in blank radius. Bending stresses dominate over frictional stresses for thicker sheets. This can be clearly seen from the figure for thickness values 1 mm and 2 mm as LDR values decreases for the sheet thickness 2 mm.

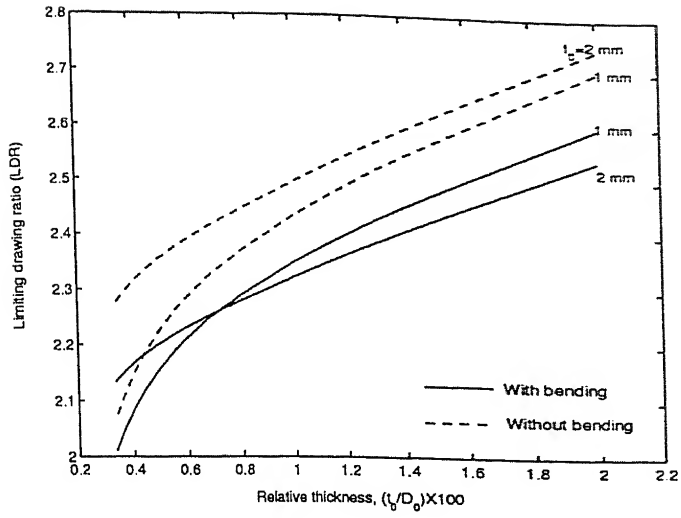

Figure 4.7: Variation of LDR with the ratio of blank thickness to blank diameter for different values of sheet thickness for first draw. ($\bar{\sigma} = 610\bar{\epsilon}^{0.263}$ MPa, $\sigma_0 = 155$ MPa, $\mu = 0.1$, $R_0 = 100$ mm,$r_d = 8.5$ mm)

Redraw

The maximum strain induced in the cup depends upon the extent of reduction achieved in the previous draws. This strain induced during the previous draws have been taken into account while carrying out the parametric study for redraw. Fig. 4.8 shows the effect of previous strain induced in the first draw on the LDR in the second redraw. It is clear that less the induced previous strain more LDR can be achieved in the second draw.

Figure 4.9 shows the variation of limiting drawing ratio with the die arc radius with and without bending effects. It can be seen that the effect of bending and unbending are more significant than in the case of first draw as bending occurs at both blank holder profile and die profile in the redraw. For the sheet thickness of 1 mm at 2 mm die arc radius, approximately 12% change in LDR is observed due to bending effects in case of first draw and 16% change is observed in second draw.

Figures 4.10,4.11 and 4.12 shows the variation of limiting drawing ratio with die arc radius for different values of normal anisotropy($\bar{R}$), strain hardening index(n) and friction coefficient(μ) with bending effects. In all the cases LDR values increases with increase in die arc radius as observed in the case of first draw.

Figure 4.13 shows the variation of first draw LDR and second draw LDR with the blank thickness. In case of redraw the LDR increases with increase in thickness up to certain value and starts decreasing with further increase in thickness. This can be explained from Fig. 4.14. For the values of $\frac{t_0}{d_0}$ less than 0.005 frictional stresses are dominating due to high blank holding force required to avoid wrinkling. Increase in thickness (increase in $\frac{t_0}{d_0}$) causes increase in bending stresses faster than decrease in frictional stress and hence LDR will decrease.

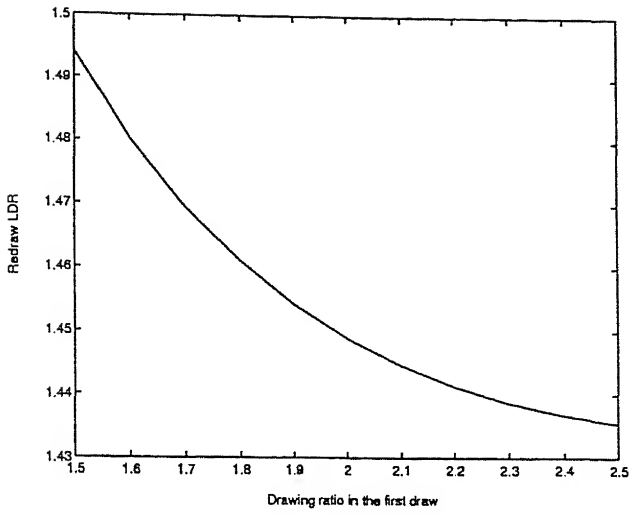

Figure 4.8: Variation of redraw LDR with drawing ratio used in first draw. ($\bar{\sigma} = 610\bar{\epsilon}^{0.263}$ MPa, $\sigma_0 = 155$ MPa, $\bar{R} = 2.1$, $\mu = 0.1$, $R_0 = 200$ mm, $r_d = 8$ mm, $r_d = 8$ mm,$t_0 = 1.0$ mm)

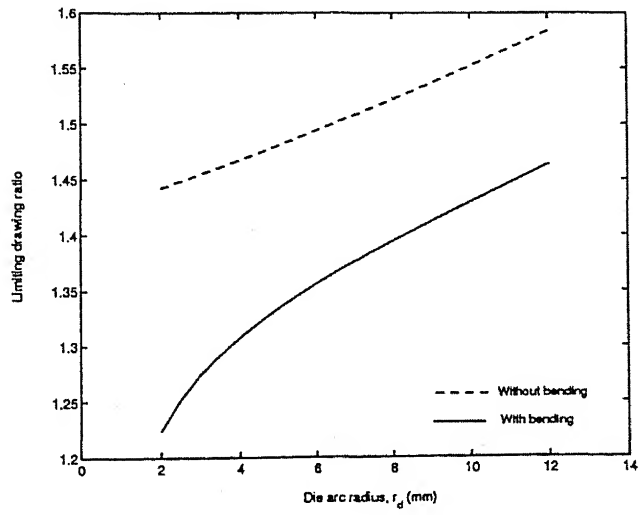

Figure 4.9: Variation of LDR with die arc radius for redraw. ($\bar{\sigma} = 610\bar{\epsilon}^{0.263}$ MPa, $\sigma_0 = 155$ MPa, $\bar{R} = 2.1$, $\mu = 0.1$, $R_0 = 200$ mm, $r_b = 8$ mm, $r_d = 8$ mm,$t_0 = 1.0$ mm)

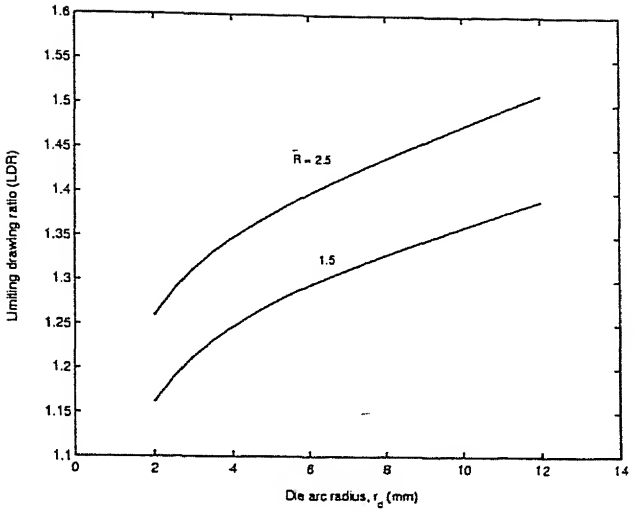

Figure 4.10: Variation of LDR with die arc radius for different values of normal anisotropy for redraw. ($\bar{\sigma} = 610\bar{\epsilon}^{0.263}$ MPa, $\sigma_0 = 155$ MPa, $\mu = 0.1$, $R_0 = 200$ mm, $r_b = 8$ mm, $r_d = 8$ mm,$t_0 = 1.0$ mm)

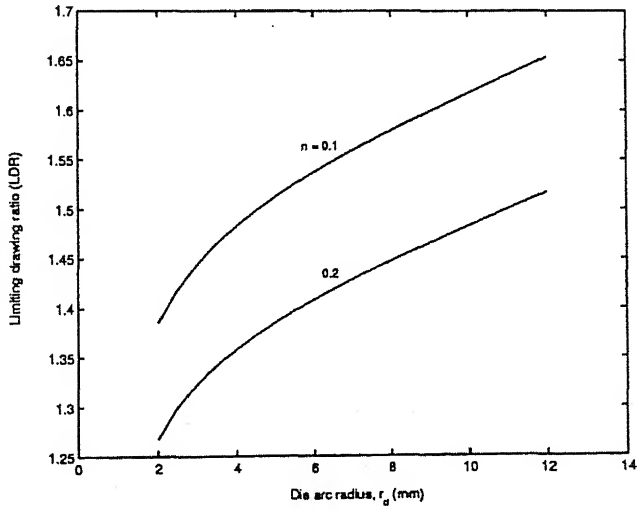

Figure 4.11: Variation of LDR with die arc radius for different values of strain hardening index for redraw. ($\bar{\sigma} = 610\bar{\epsilon}^{0.263}$ MPa, $\sigma_0 = 155$ MPa, $\bar{R} = 2.1$, $\mu = 0.1$, $R_0 = 200$ mm, $r_b = 8$ mm,$r_d = 8$ mm, $t_0 = 1.0$ mm)

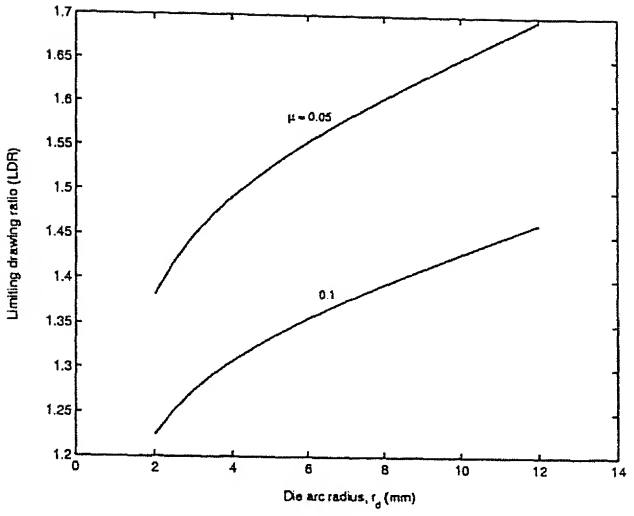

Figure 4.12: Variation of LDR with die arc radius for different values of fiction coefficient for redraw. ($\bar{\sigma} = 610\bar{\epsilon}^{0.263}$ MPa, $\sigma_0 = 155$ MPa, $\bar{R} = 2.1$, $R_0 = 200$ mm, $r_b = 8$ mm, $r_d = 8$ mm, $t_0 = 1.0$ mm)

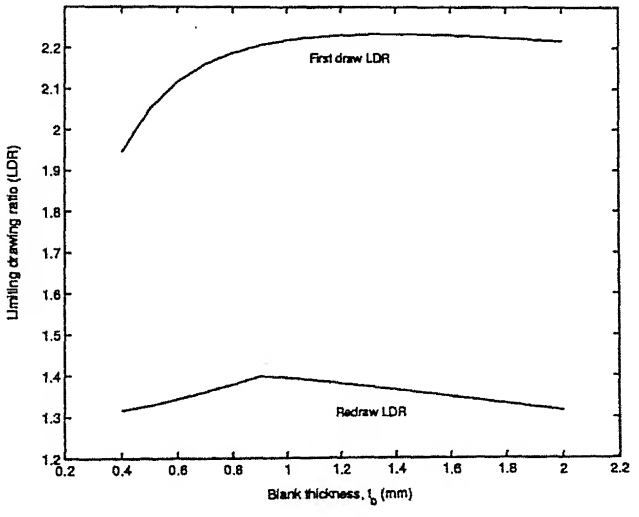

Figure 4.13: Variation of LDR with the blank thickness for the first draw as well as redraw. ($\bar{\sigma} = 610\bar{\epsilon}^{0.263}$ MPa, $\sigma_0 = 155$ MPa, $\bar{R} = 1.5$, $R_0 = 100$ mm, $r_b = 8$ mm, $r_d = 6.8$ mm, $t_0 = 1.0$ mm)

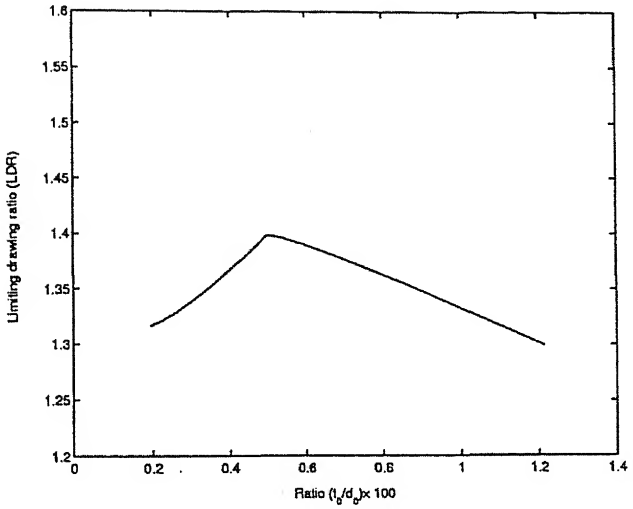

Figure 4.14: Variation of LDR with the relative thickness $\frac{t_0}{2r_{i-1}} \times 100$ for redraw. ($\bar{\sigma} = 610\bar{\epsilon}^{0.263}$ MPa, $\sigma_0 = 155$ MPa, $\bar{R} = 1.5$, $R_0 = 100$ mm, $r_b = 8$ mm, $r_d = 6.8$ mm, $t_0 = 1.0$ mm)

Chapter 5

Case Studies for Process Sequencing

5.1 Introduction

The developed product and process design system for axisymmetric deep drawing is tested with process sequences available in the literature [Jones, 1951; Eshel et al., 1986; Sitaraman et al., 1991; ASM hand book,1992; Park et al.,1998] and are presented in section 5.2. The capabilities of the present system are demonstrated through several case studies and are presented in section 5.3. Formability as well as geometric information related to each stage is presented in the tabular form along with the process sequence presented in graphical form. The notations used in this section for the features are as follows

h - horizontal element

v - vertical element

i - tapered element

r - counter clockwise quarter arc element

c - clockwise quarter arc element

a - counter clockwise angular arc element

x - clockwise angular arc element

5.2 Validation

5.2.1 Case 1

The process sequence for a deep drawn component (motor housing) presented by Park et al. [1998] is chosen here for the comparison. They have used cold-rolled steel having blank thickness of 1.2 mm for producing motor housing. But, they have not given the material properties of cold-rolled steel used in their work. SAE-1006 steel is used to compare the predictions of the present process design system with the predictions of Park et al. [1998] and whose properties are given in chapter 3. The friction coefficient is assumed to be 0.1 which is not mentioned by the Park et al. [1998]. Fig. 5.1 shows the process sequence used in industrial practice for producing the

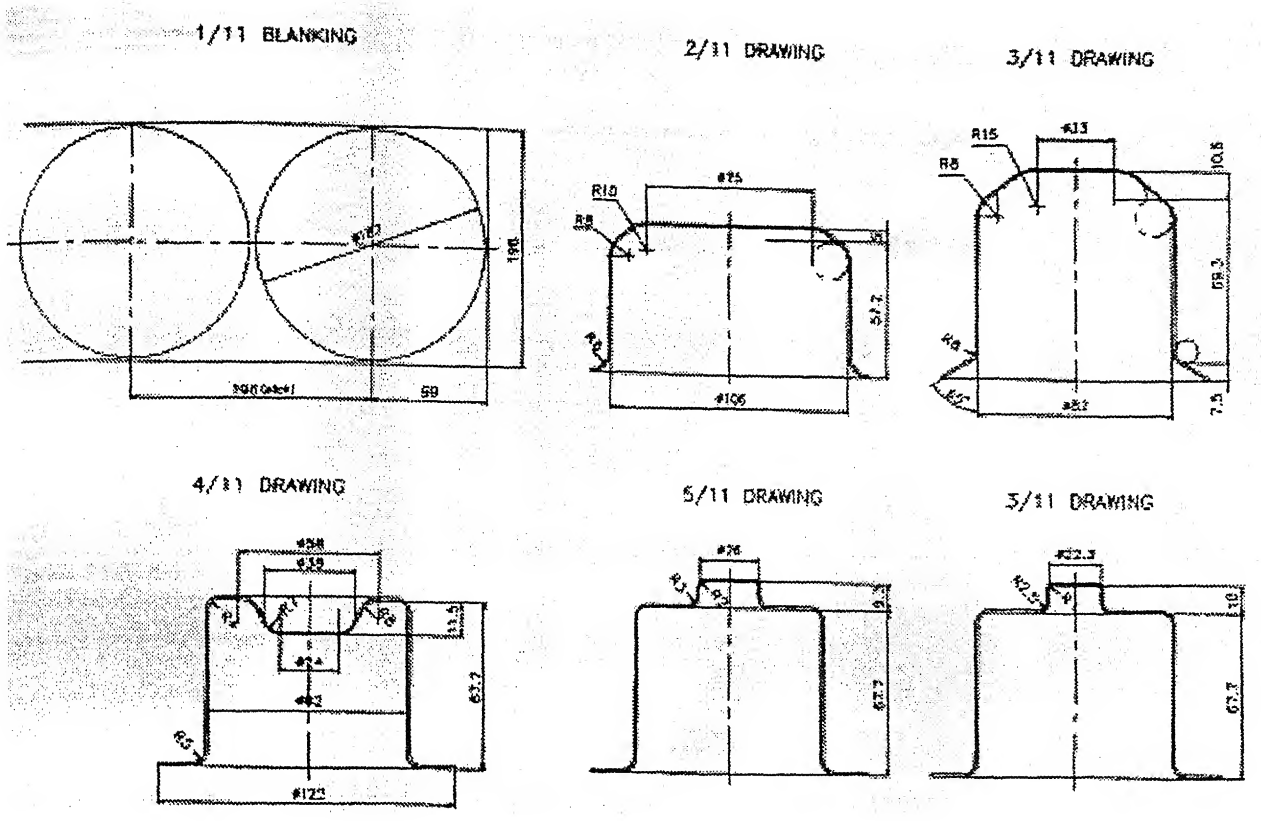

Figure 5.1: Process sequence of the motor-housing: industrial practice [Park et al., 1998]

motor housing presented by Park et al. [1998]. Figure. 5.9 shows the process sequence generated by Park et al. [1998] using the process planning system developed by them. Initially Park et al. [1998] obtained the process sequence having 8 passes using the LDR values from the data tables, they modified the sequence to 6 passes using corrected drawing ratios. Fig. 5.3 shows the process sequence generated by the present process design system. Optimal die and punch profile radii are used in the present process design system and same are used in LDR calculations. In the final stage the product is sized to the required values. The sequence generated by the present system having 5 drawing passes and a finishing pass. Tables 5.1 and 5.2 show the formability information and the geometrical information respectively. The sequence generated by the present system is in good agreement with the sequence presented by Park et al. [1998]. The discrepancy is attributed to differences in material properties, different friction conditions, tool geometry and blank holding force used in both the systems.

5.2.2 Case 2

Eshel et al. [1986] presented the use of their AGFPO (Automatic Generation of Forming Process Outlines) system for generating process sequence for a deep drawn component shown in Fig. 5.4, the same is used here to compare the predictive capabilities of the present system. The material

Process	1	2	3	4	5
Draw Ratio	0.47	0.90	0.53	0.74	0.82
Clearance(mm)	1.72	1.64	1.56	1.44	1.26
P.Force(ton)	11.26	9.25	6.73	4.15	2.75
B.H Force(ton)	2.59	2.13	1.55	0.96	0.63

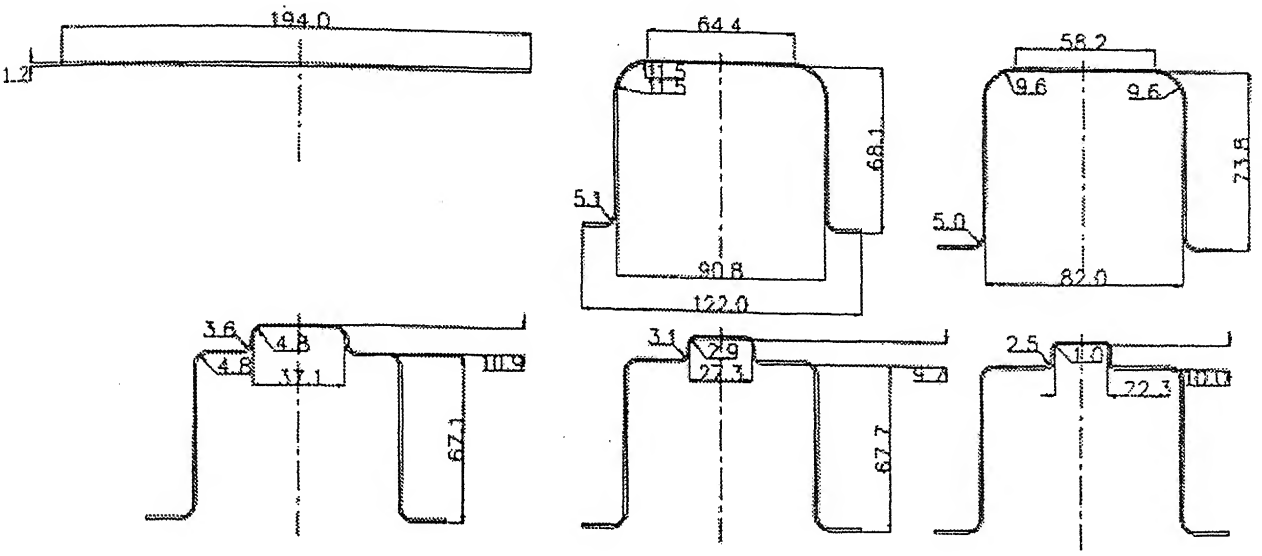

Figure 5.2: Process sequence of the motor-housing [Park et al., 1998]

Stage	Die Arc Radius (mm)	Punch Arc Radius (mm)	DR_i	DR_{total}	Cup Radius (mm)	Max. Punch Force (Tons)
1	5.00	7.00	2.02	2.02	50.85	18.18
2	5.00	7.00	1.10	2.21	46.40	16.59
3	9.60	11.60	1.50	3.31	30.98	11.08
4	7.68	9.68	1.45	4.81	21.30	7.62
5	4.80	4.80	1.44	6.93	14.80	5.29

Table 5.1: Formability information for the process sequence shown in Fig. 5.3

used in their work is austenitic stainless steel of thickness of 1/16 in. (1.5875 mm), but they have not reported the material properties. In the present system the properties of austenitic stainless steel are taken as presented in chapter 3 and friction coefficient is assumed to be 0.1. Figure 5.5 shows the process sequence generated by the present system and it can be seen that it is in good agreement with the process sequence generated by AGFPO (Fig. 5.4) developed by Eshel et al. [1986]. Table 5.3 and Fig. 5.6 show the formability and geometrical information for the sequence generated by the present system. The discrepancy attributed to differences in tool geometry, material properties and friction conditions used in the both the systems.

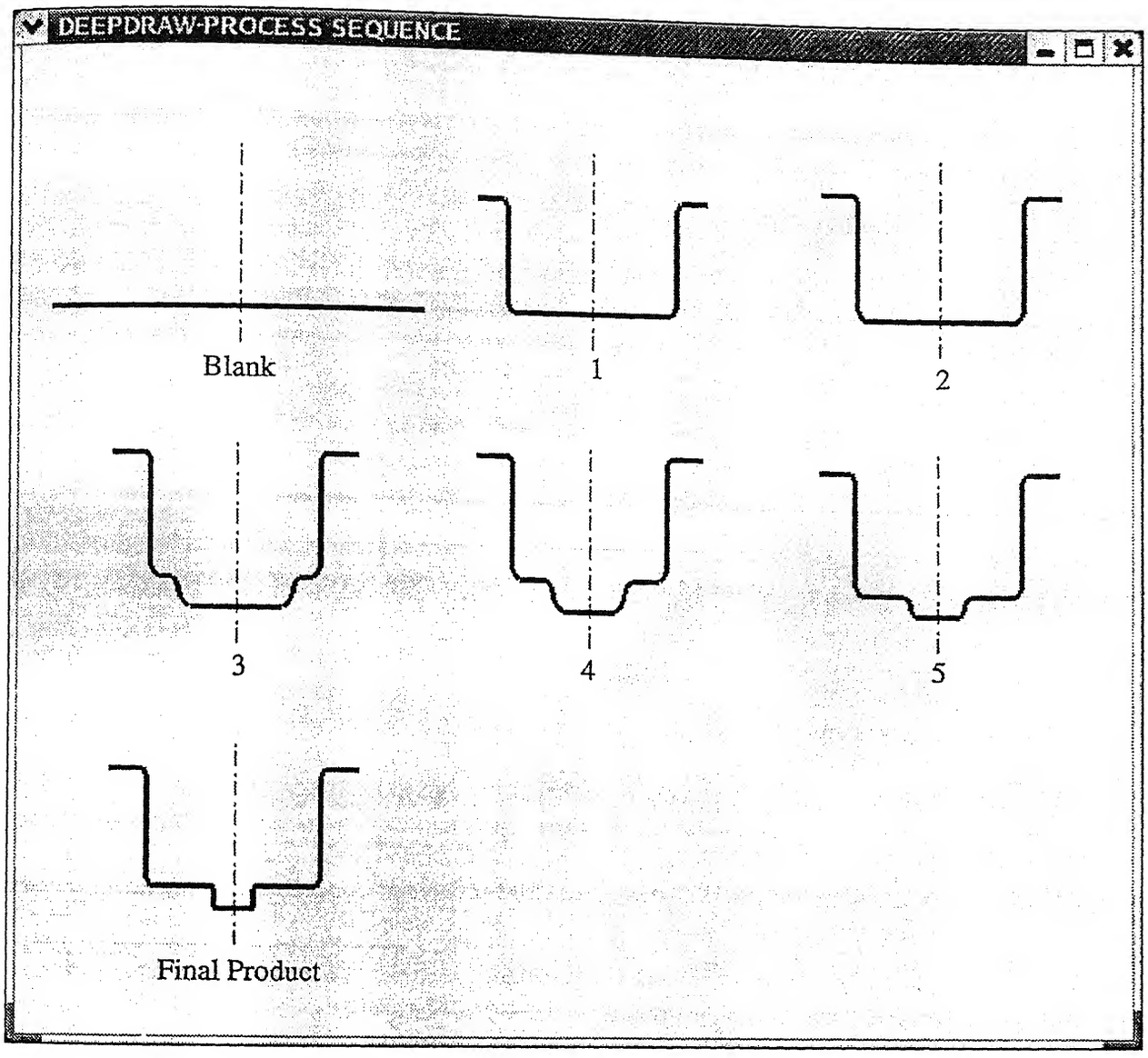

Figure 5.3: Process sequence generated by the present system for the motor-housing reported in Fig. 5.1

5.2.3 case 3

Figure 5.7 shows the process sequence followed in industrial practice for a deep drawn component produced by cold-rolled sheet of 1.65 mm thickness [Jones, 1951]. The process sequences generated by Sitaraman at al. [1991] and Park et al. [1998] using data tables to select formability limits for the component shown in Fig. 5.7 are shown in Fig. 5.8 and 5.9 respectively. To compare the predictions of the present system, SAE-1006 material is chosen and friction coefficient is taken as 0.1. Figure 5.10 shows the process sequence generated by the present system and table 5.4 and 5.5 present the formability and geometrical information respectively for the generated sequence. Sequence generated by the present system (Fig. 5.10) having less number of stages

Stage	h	r	v	c	h	r	v	c	h
0	102.54								
1	43.85	7.00	51.76	5.00	11.65				
2	39.40	7.00	58.97	5.00	15.00				
3	26.18	4.80	0.00	4.80	3.62	7.00	56.85	5.00	15.00
4	16.50	4.80	0.00	4.80	13.30	7.00	56.85	5.00	15.00
5	10.00	4.80	1.16	4.80	19.80	7.00	56.85	5.00	15.00
SIZING	10.00	1.00	9.00	2.50	30.00	4.00	55.00	5.00	15.00

Table 5.2: Geometric information for the process sequence shown in Fig. 5.3

Stage	Die Arc Radius (mm)	Punch Arc Radius (mm)	DR_i	DR_{total}	Cup Radius (mm)	Max. Punch Force (Tons)
1	6.35	12.70	1.81	1.81	72.27	60.29
2	12.64	14.64	1.37	2.48	52.73	43.99
3	6.35	6.35	1.17	2.89	45.25	37.75
4	12.64	14.64	1.43	4.15	31.54	26.31
5	6.35	8.35	1.07	4.46	29.35	24.48

Table 5.3: Formability information for the sequence shown in Fig. 5.5

Stage	Die Arc Radius (mm)	Punch Arc Radius (mm)	DR_i	DR_{total}	Cup Radius (mm)	Max. Punch Force (Tons)
1	13.04	15.04	2.34	2.34	35.82	17.39
2	6.52	12.43	1.14	2.66	31.54	15.32
3	6.52	6.52	1.36	3.61	23.19	11.26

Table 5.4: Formability information for the sequence shown in Fig. 5.10

compared to other sequences(Figs. 5.7, 5.8 and 5.9). The discrepancy attributed to differences in tool geometry, material properties and friction conditions used in the both the systems.

5.2.4 case 4

Process sequence generated by the present system for a conical cup is compared with the process sequence presented in the ASM material handbook, [1992] using aluminium alloy of thickness

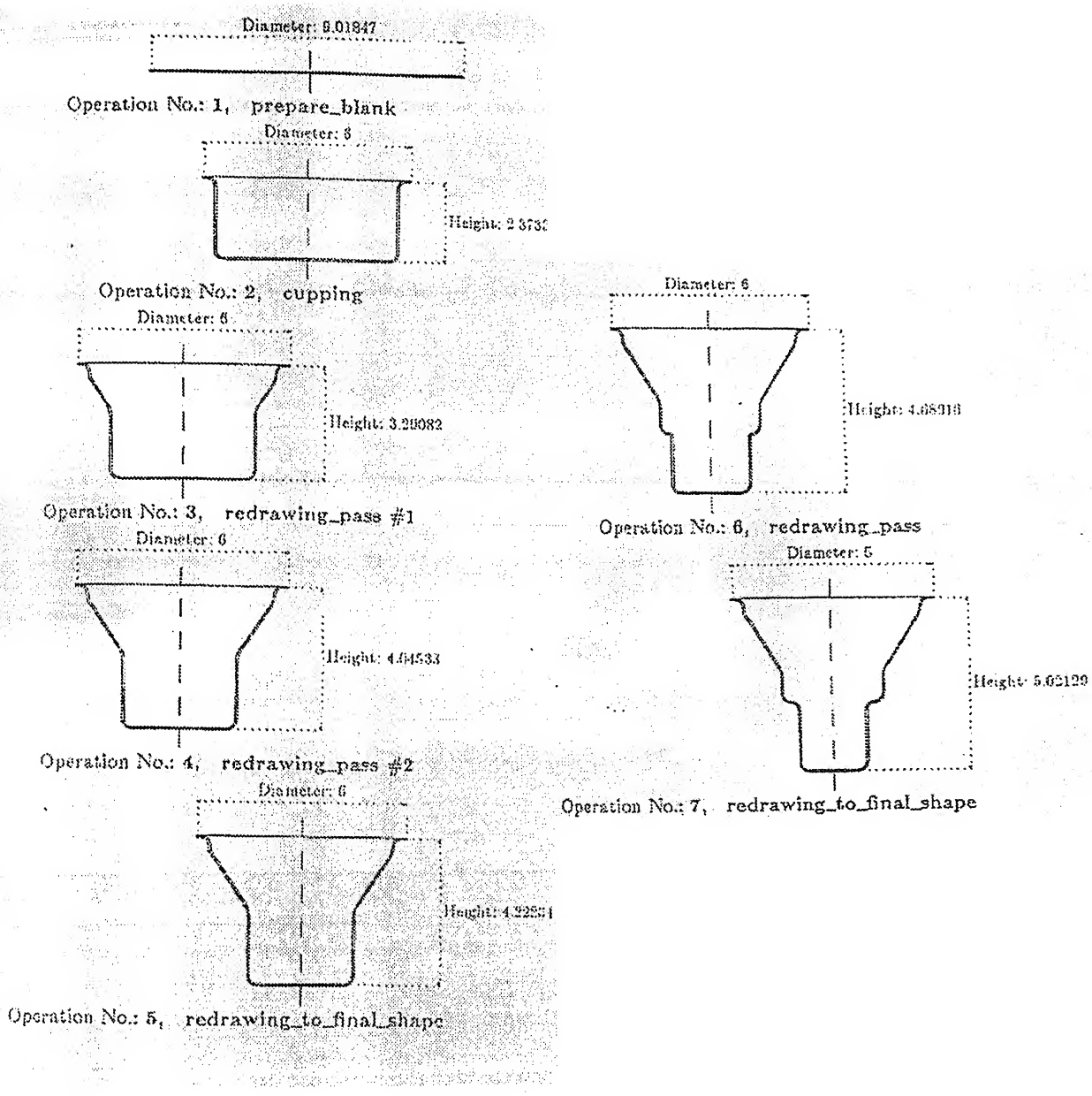

Figure 5.4: Process sequence generated by AGFPO [Eshel et al., 1986].

Stage	h	r	v	x	i	a	v	x	i
0	83.76								
1	20.78	15.04	51.49	13.04	11.89				
2	25.02	6.52	56.65	6.52	21.00				
3	16.67	6.52	37.83	6.52	2.11	6.52	23.37	6.52	21.00
SIZING	16.67	3.00	51.00	3.00	10.50	3.00	30.20	3.00	9.00

Table 5.5: Geometric information for the sequence shown in Fig. 5.10

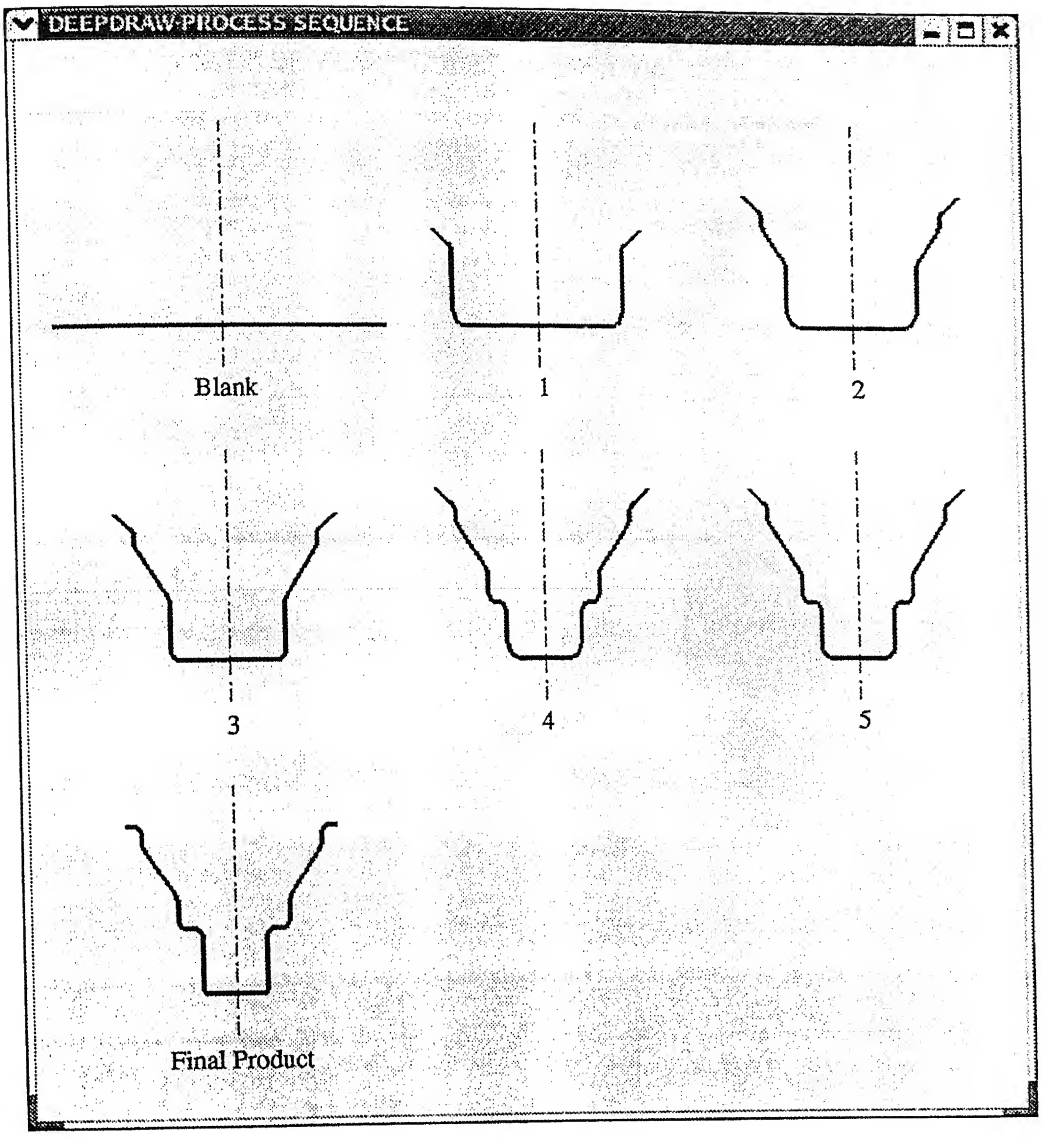

Figure 5.5: Process sequence generated by present system

Stage	h	r	v	c	h	r	v	x	i	a	v	x	i
Sequence no.1													
0	130.93												
1	59.57	12.70	47.63	6.35	18.51								
2	38.09	14.64	32.60	12.64	28.40	12.70	4.76	6.35	18.51				
3	38.90	6.35	39.42	6.35	44.00	12.70	4.76	6.35	18.51				
4	20.06	11.48	23.29	9.48	0.00	6.35	14.91	6.35	44.00	12.70	4.76	6.35	18.51
5	21.00	8.35	29.46	6.35	3.20	6.35	14.91	6.35	44.00	12.70	4.76	6.35	18.51
SIZING	21.00	4.76	40.00	6.35	5.00	6.35	12.70	12.70	44.00	12.70	5.00	6.35	4.00

Figure 5.6: Geometric information for the sequence shown in Fig. 5.5

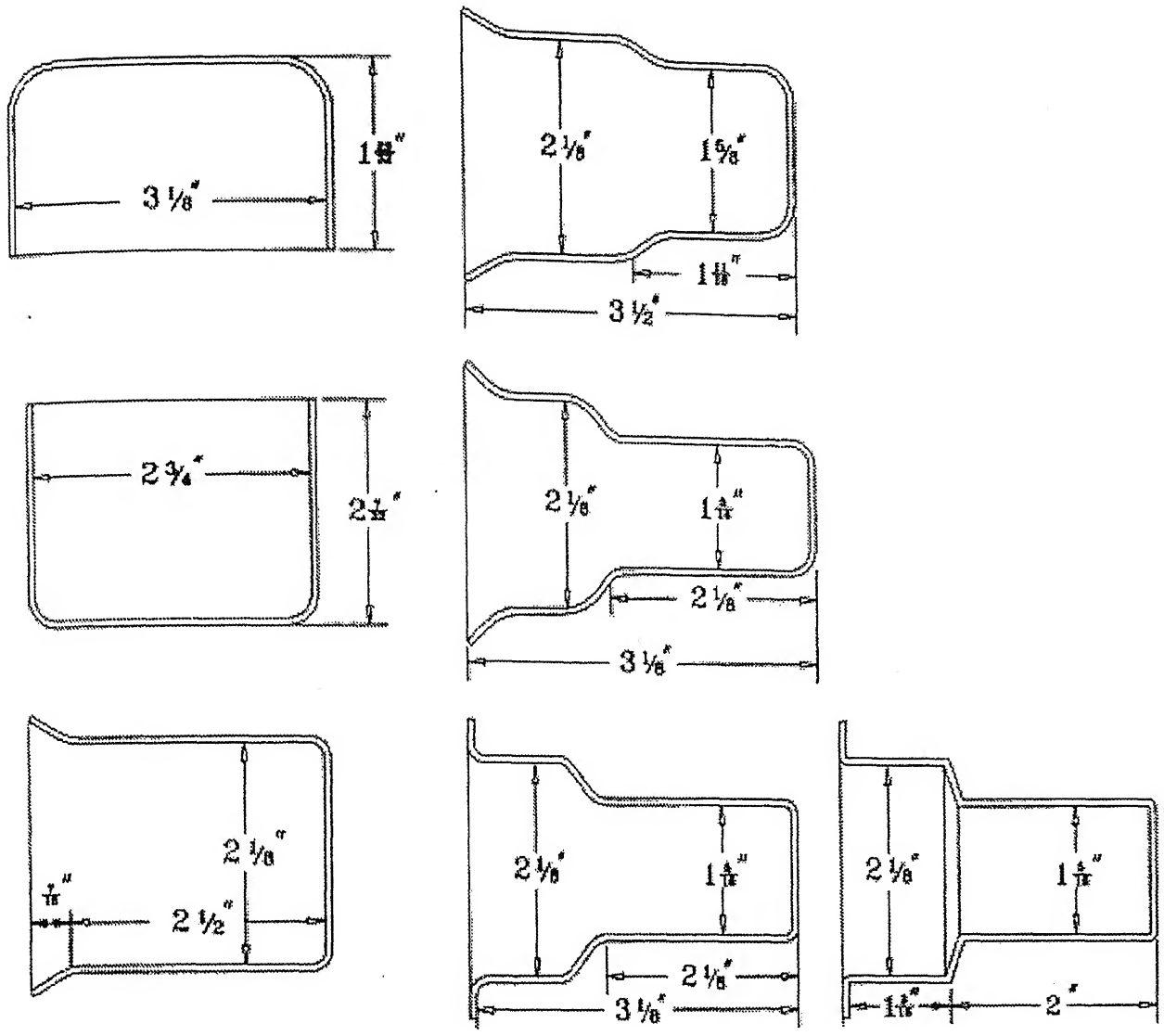

Figure 5.7: Process sequence used in industrial practice [Jones, 1951].

1.63 mm. As the properties of the material is not mentioned, AA-3003 material is chosen in the present work and the friction coefficient is assumed to be 0.05. Figure 5.11 shows the process sequence reported in ASM material handbook, [1992] and Fig. 5.12 shows the process sequence generated by the present system. Tables 5.6 and 5.7 show formability and geometrical information of the sequence generated by the present system (Fig. 5.12) respectively. The process sequence generated by the present system is in good agreement with sequence reported by ASM material handbook, [1992].

5.2.5 Case 5

In this case process sequence for an automobile differential gear case presented by Jones, [1951] is considered to compare with the process sequence generated by the present system. SAE-1006

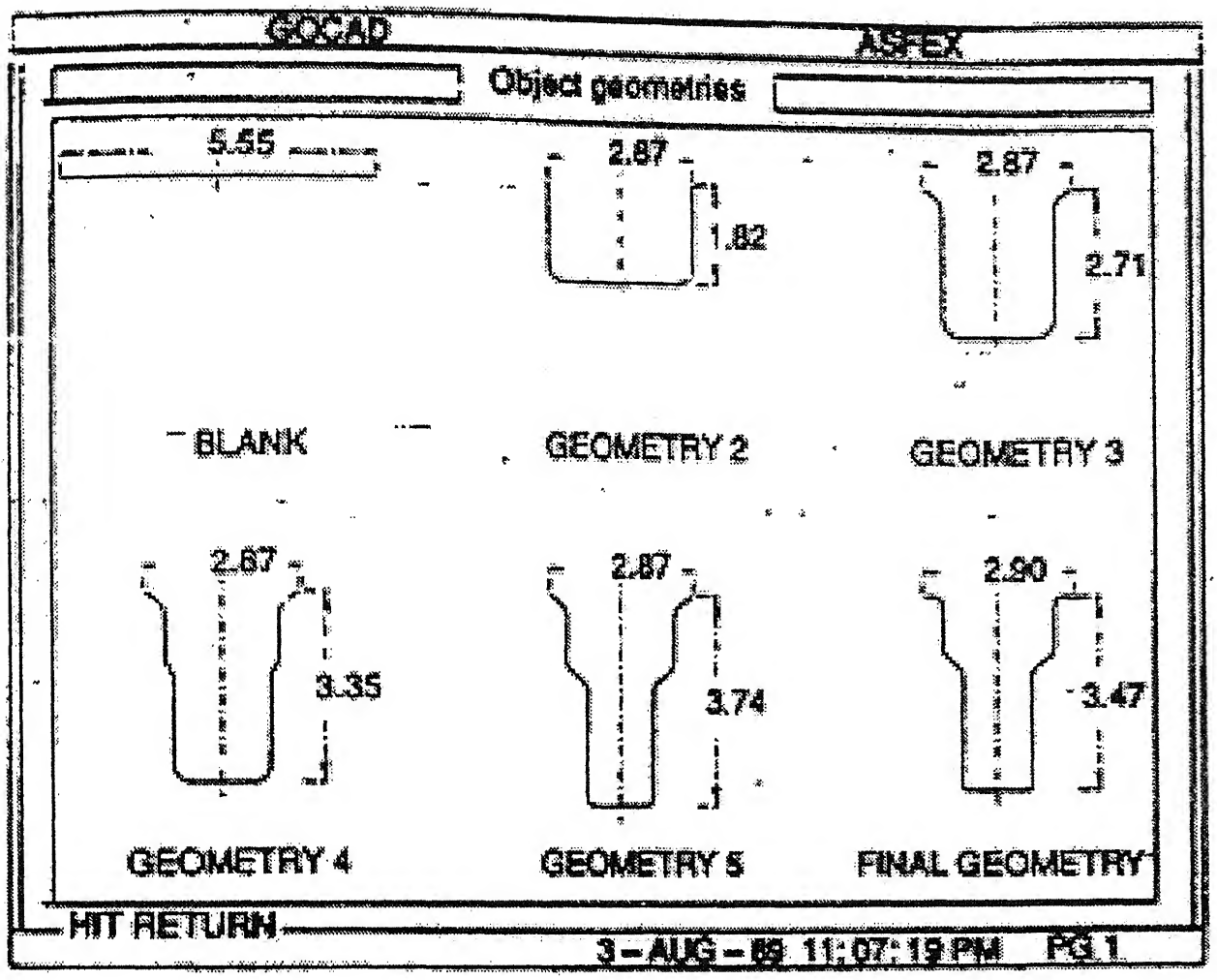

Figure 5.8: Process sequence presented by Sitaraman et al. [1991].

Stage	Die Arc Radius (mm)	Punch Arc Radius (mm)	DR_i	DR_{total}	Cup Radius (mm)	Max. Punch Force (Tons)
1	13.04	15.04	2.04	2.04	76.68	8.11
2	6.52	12.43	1.05	2.15	72.80	7.70
3	8.15	11.41	1.43	3.35	50.91	5.38
4	8.15	11.41	1.11	3.70	46.00	4.86

Table 5.6: Formability information for the sequence shown in Fig. 5.12

Process	1	2	3	4	5
Draw Ratio	0.49	0.80	0.73	0.80	1.00
Clearance(mm)	2.42	2.31	2.20	2.03	1.77
P.Force(ton)	8.83	9.94	6.37	5.23	3.74
B.H Force(ton)	1.24	1.39	0.89	0.73	0.52

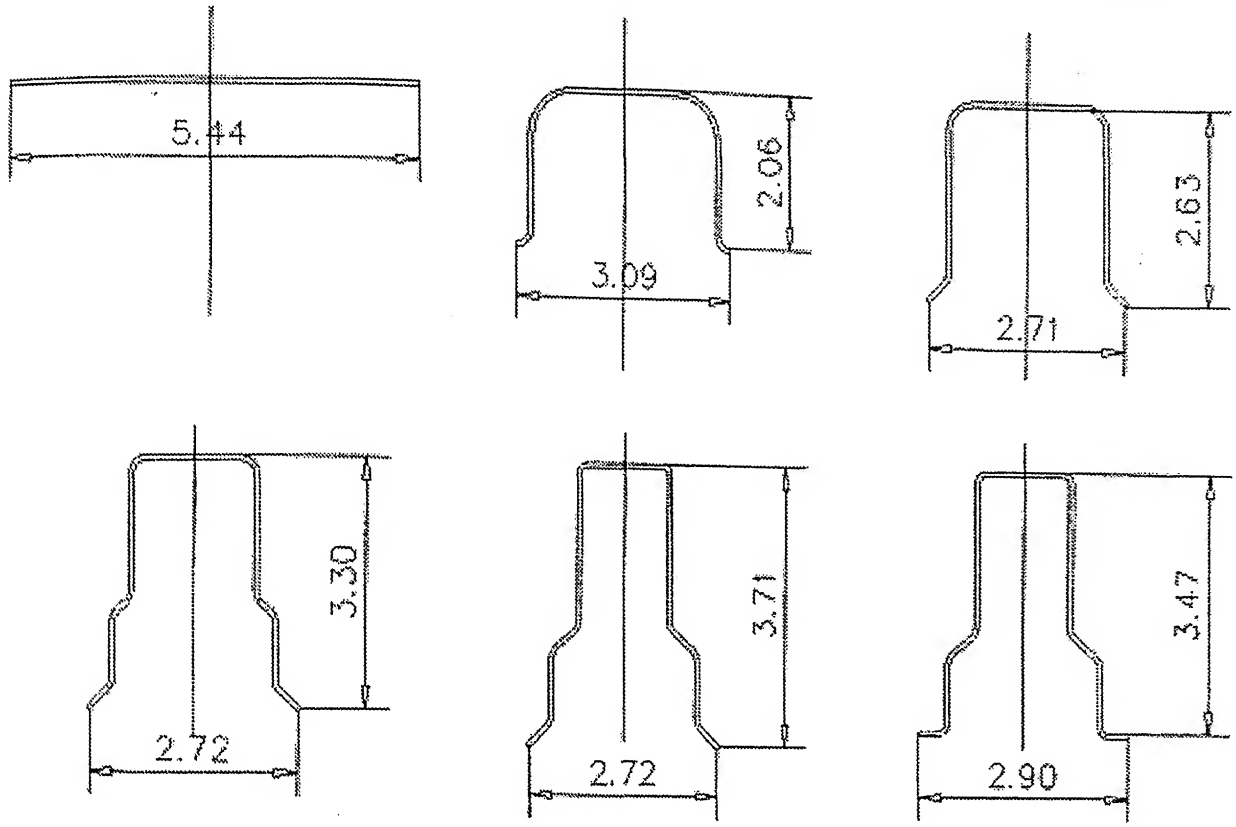

Figure 5.9: Process sequence presented by Park et al. [1998].

Stage	h	a	v	x	i	a	v	x	i
0	156.66								
1	61.64	15.04	113.30	0.00	0.00				
2	61.39	11.41	99.30	6.52	20.00				
3	39.50	11.41	48.91	8.15	22.87	11.41	53.00	6.52	20.00
4	34.59	11.41	53.00	8.15	29.82	11.41	53.00	6.52	20.00
	h	a	i	x	h				
SIZING	41.00	5.00	155.00	5.00	20.00				

Table 5.7: Geometric information for the sequence shown in Fig. 5.12

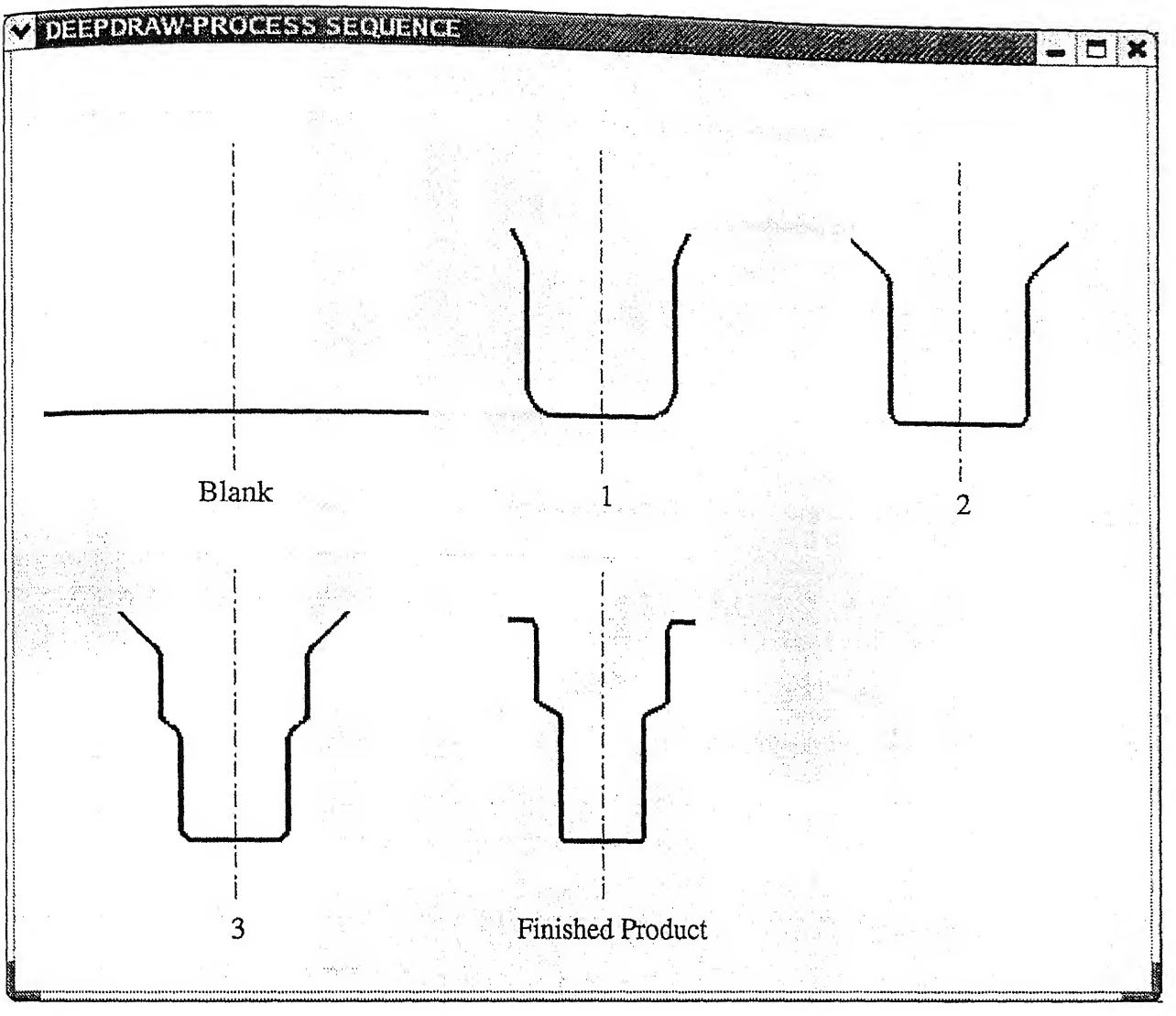

Figure 5.10: Process sequence generated by the present system.

material is used in the present work to generate the process sequence. The sheet thickness is given as 5/32 in.(3.96) mm and the friction coefficient is assumed to be 0.1. Figure 5.13 shows the process sequence reported by Jones, [1951]. Figure 5.14 shows the process sequence generated by the present system. Finished part is obtained in the present system in five passes where as industrial practice uses 8 passes. This discrepancy attributed to the different materials used in present work and in actual practice. Tables 5.8 and 5.9 shows the formability information and geometrical information for the process sequence generated by the present system (Fig. 5.14).

5.3 Case Studies

The process sequences reported in this section are generated by using the rules presented in Appendix B along with the process analysis model presented in chapter 2. The geometric stages in

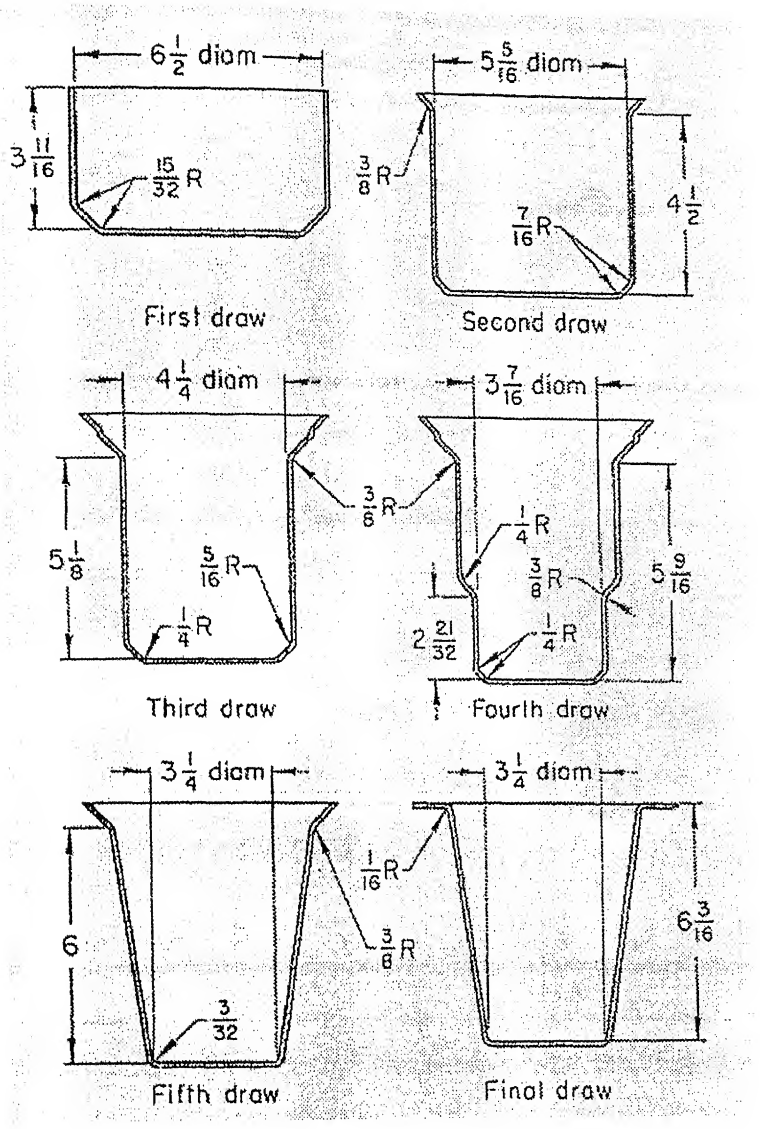

Figure 5.11: Process sequence used in industry [ASM handbook, 1992].

Stage	Die Arc Radius (mm)	Punch Arc Radius (mm)	DR_i	DR_{total}	Cup Radius (mm)	Max. Punch Force (Tons)
1	16.00	18.00	2.20	2.20	57.28	68.27
2	16.00	18.00	1.04	2.29	54.93	65.46
3	16.00	16.00	1.51	5.01	36.35	43.32
4	16.00	16.00	1.14	5.69	32.00	38.14

Table 5.8: Formability information for the process sequence shown in Fig. 5.14

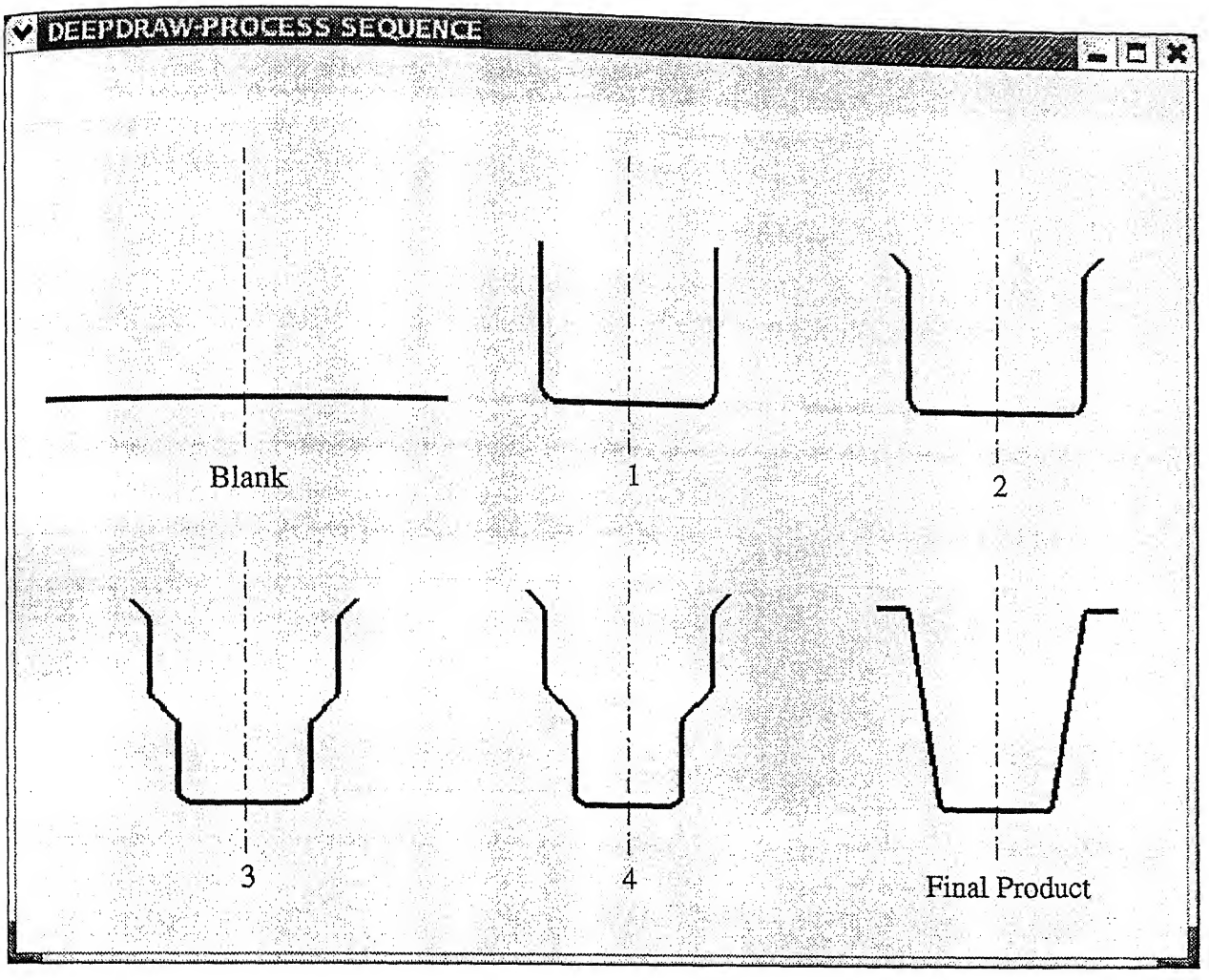

Figure 5.12: Process sequence generated by the present system.

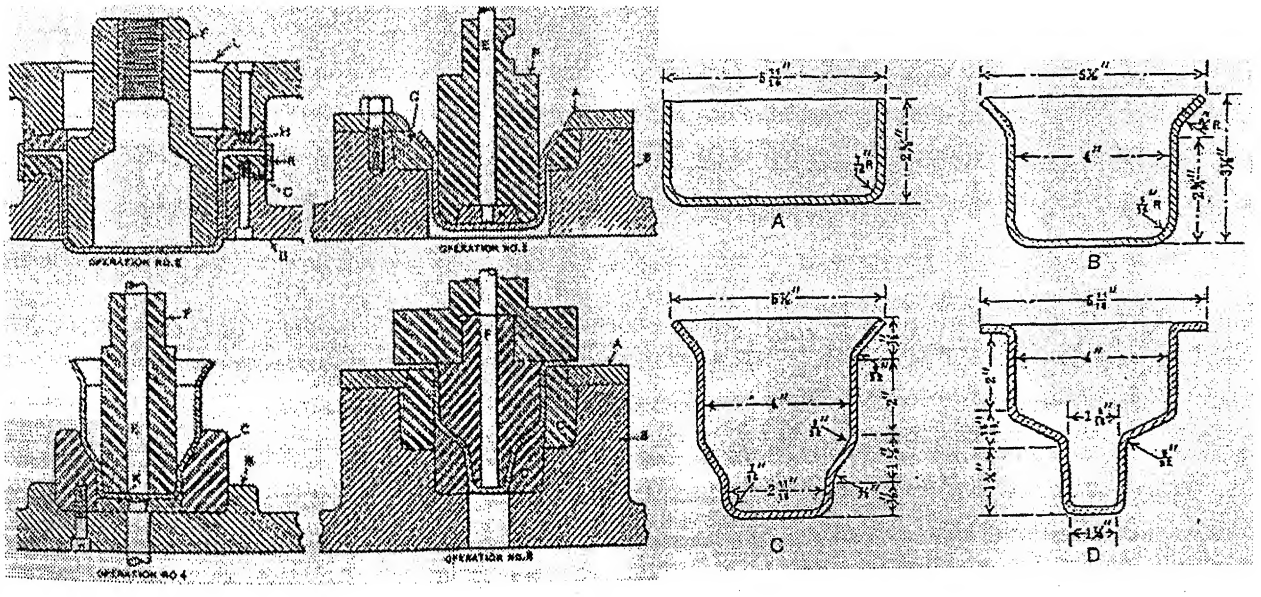

Figure 5.13: Process sequence for differential gear case: industrial practice [Jones, 1951].

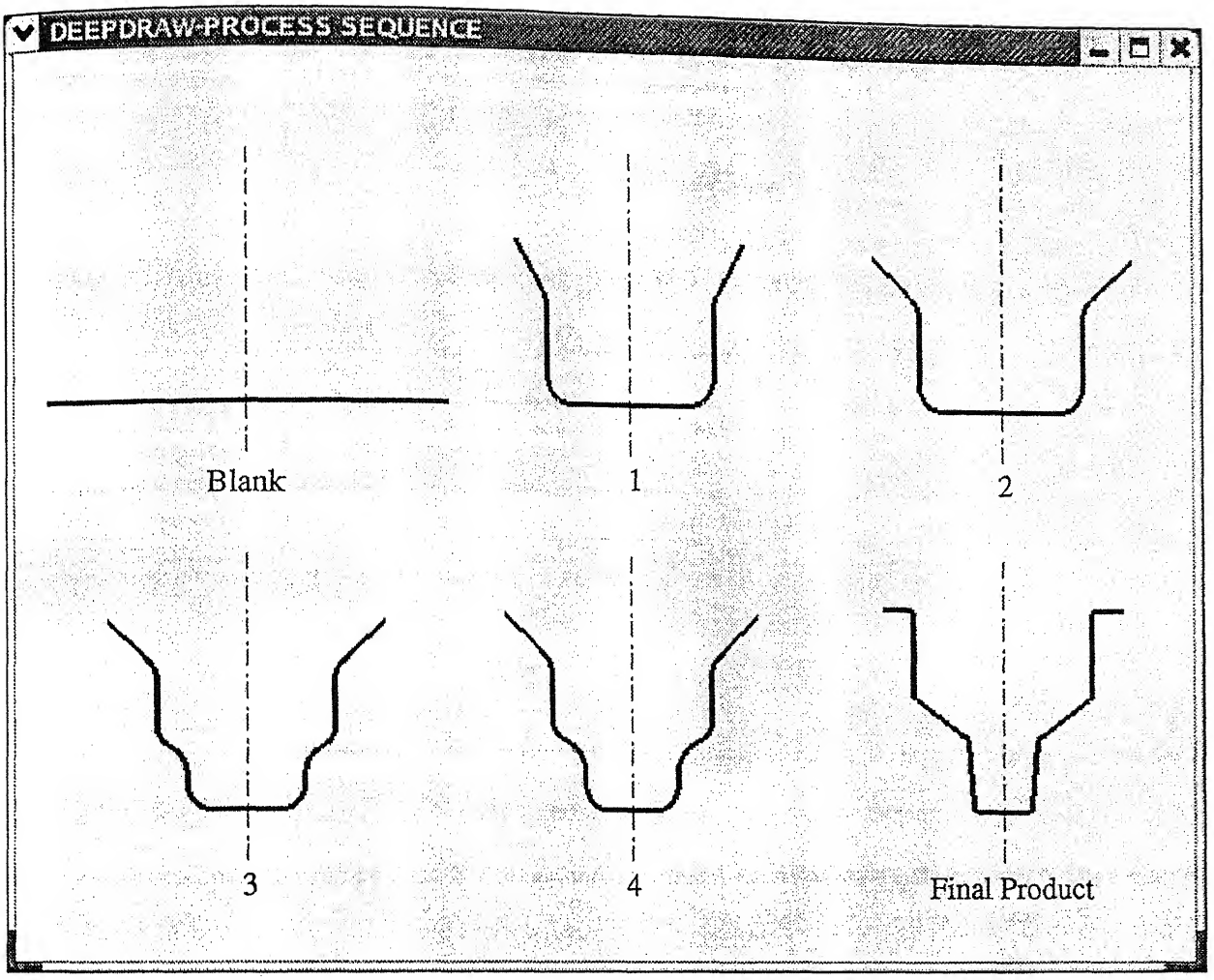

Figure 5.14: Process sequence for differential gear case generated by present system.

Stage	h	r	v	x	i	a	v	x	i
0	126.01								
1	39.28	18.00	44.10	16.00	39.28				
2	38.93	16.00	44.10	16.00	34.10				
3	20.35	16.00	7.17	16.00	6.04	16.00	27.34	16.00	34.10
4	16.00	16.00	9.32	16.00	11.35	16.00	27.34	16.00	34.10
SIZING	16.00	4.00	42.00	4.00	40.00	4.00	50.00	4.00	15.00

Table 5.9: Geometric information for the process sequence shown in Fig. 5.14

Stage	Die Arc Radius (mm)	Punch Arc Radius (mm)	DR_i	DR_{total}	Cup Radius (mm)	Max. Punch Force (Tons)
sequence 1: Without annealing						
1	8.00	10.00	1.94	1.94	116.03	34.57
2	6.40	8.40	1.26	2.44	92.19	27.47
3	5.12	7.12	1.25	3.06	73.69	21.95
4	4.00	6.10	1.23	3.75	60.00	17.88
sequence 2: Annealing after stage no.1						
1	8.00	10.00	1.94	1.94	116.03	34.57
2	7.20	9.20	1.84	1.84	63.14	18.81
3	5.76	5.00	1.05	1.93	60.00	17.88
sequence 3: Annealing after stage no.2						
1	8.00	10.00	1.94	1.94	116.03	34.57
2	7.20	9.20	1.27	2.47	91.30	27.20
3	5.76	5.00	1.52	1.52	60.00	17.88

Table 5.10: Formability information for the process sequences shown in Fig. 5.15

a sequence are graphically represented with solid lines and the intermediate stages are represented with dotted lines.

5.3.1 Straight Cup without Flange

Figure 5.15 shows the possible sequences with and without annealing between stages. Tables 5.10 and 5.11 show the formability and geometrical information respectively for the above sequences. It can be seen from the Fig. 5.15, sequence 1 having four stages to produce final component without performing annealing between stages and sequences 2, 3 have three stages in each case by performing annealing after stage 1 and stage 2 respectively in the sequence 1. From the formability information (table 5.10), sequences 2 and 3 have less tooling cost than sequence 1. The total power needed to produce the final cup is least in sequence 2 and the strength of the final cup is more than sequence 3. The selection of a particular sequence depends on cost of tooling, cost for heat-treatment and strength requirement of the final cup. Cost comparisons are not considered in the present work. Hence sequence 2 will be optimal sequence with respect to tooling cost and power requirements.

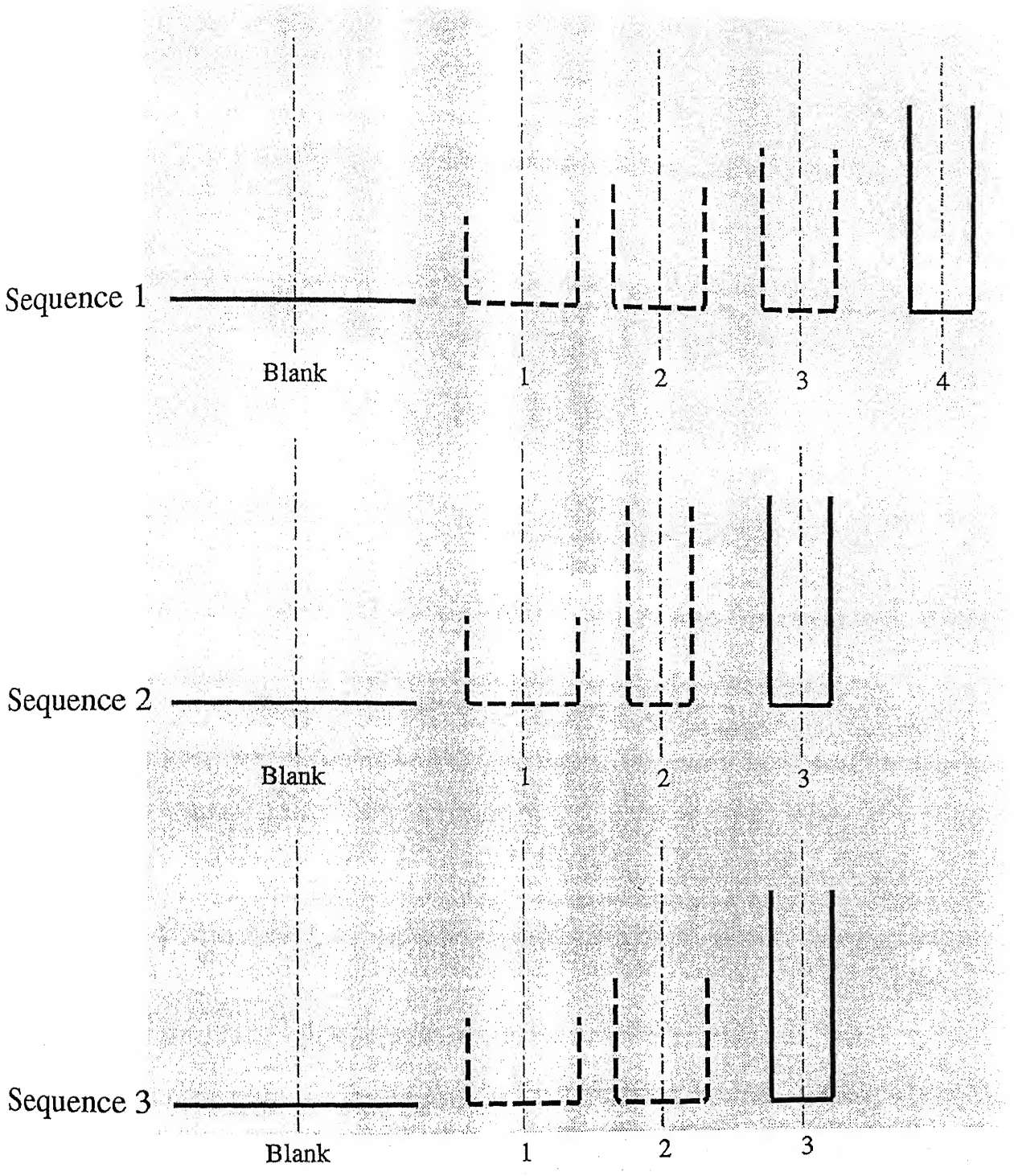

Figure 5.15: Process sequence for non-flanged straight cup. (CA-DDQ steel, t_0=1 mm, μ=0.1)

Stage	h	r	v
Sequence no.1			
0	225.25		
1	106.03	10.00	154.98
2	83.79	8.40	224.36
3	66.57	7.12	303.41
4	55.00	5.00	390.00
Sequence no.2			
0	225.25		
1	106.03	10.00	154.98
2	53.94	9.20	365.07
3	55.00	5.00	390.00
Sequence no.3			
0	225.25		
1	106.03	10.00	154.98
2	82.10	9.20	227.01
3	55.00	5.00	390.00

Table 5.11: Geometric information for the process sequences shown in Fig. 5.15

Stage	Die Arc Radius (mm)	Punch Arc Radius (mm)	DR_i	DR_{total}	Cup Radius (mm)	Max. Punch Force (Tons)
1	8.00	10.00	2.09	2.09	115.99	36.56
2	5.00	8.40	1.29	2.69	90.00	28.37

Table 5.12: Formability information for the process sequences shown in Fig. 5.16

5.3.2 Straight Cup with Narrow Flange

Figure 5.16 shows the process sequence for a narrow-flanged straight cup generated by the present system. Tables 5.12, 5.13 show the formability and the geometrical information respectively for the above sequence. It can be seen from the Fig. 5.16, the narrow flange is generated gradually with a decrease in flange angle and is flattened in the last stage.

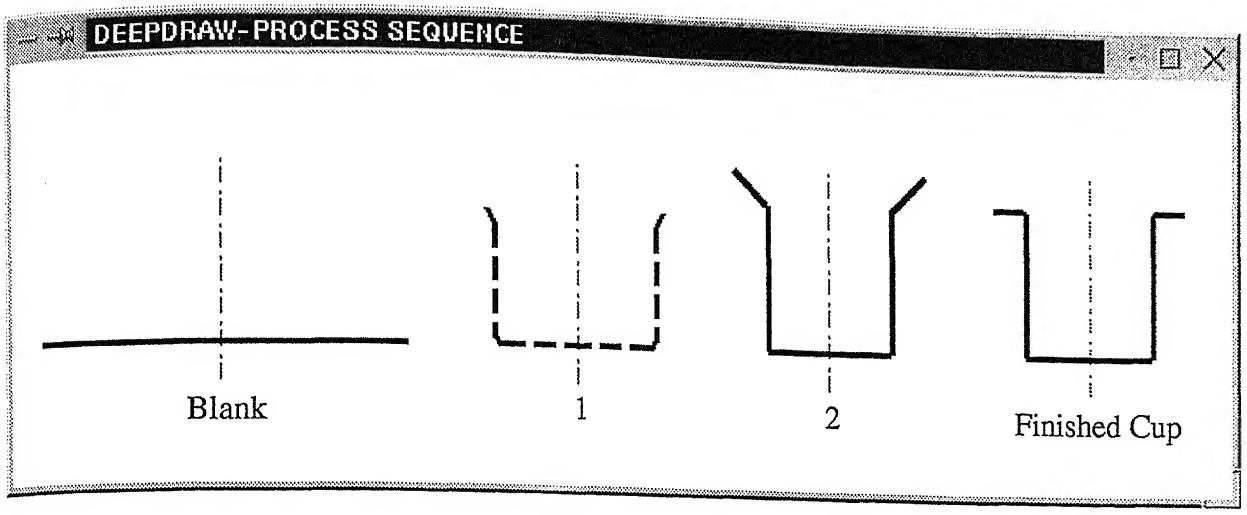

Figure 5.16: Process sequence for narrow flanged cup. (CA-DDQ steel, t_0=1 mm, μ=0.1)

Stage	h	r	v	x	i
Sequence no.1					
0	242.45				
1	105.99	10.00	149.59	8.00	33.27
2	84.00	6.00	190.00	5.00	64.67
SIZING	84.00	6.00	190.00	5.00	35.00

Table 5.13: Geometric information for the process sequences shown in Fig. 5.16

5.3.3 Straight Cup with Wide Flange

Figure 5.17 shows the possible sequences generated by the present system for a cup with wide flange. It can be seen that, the flange is formed to the outer diameter of the final cup in the first stage itself. In the subsequent stages the flange is widened gradually by reducing the cup diameter. Tables 5.14 and 5.15 show the formability information and the geometrical information respectively. It can be seen from the Fig. 5.17, sequence 1 having four stages to produce final cup without annealing and sequences 2, 3 have three stages each case by performing annealing after stage 1 and stage 2 respectively in the sequence 1. Hence sequence 2 will be optimal sequence with respect to tooling cost and power requirements.

5.3.4 Stepped Cup without Flange

Figure 5.18 shows the sequences generated by the present system for a stepped cup without flange. Tables 5.16 and 5.17 show the formability and the geometrical information respectively for the above process sequences. It can be seen from the Fig. 5.18, sequence 1 has six stages to

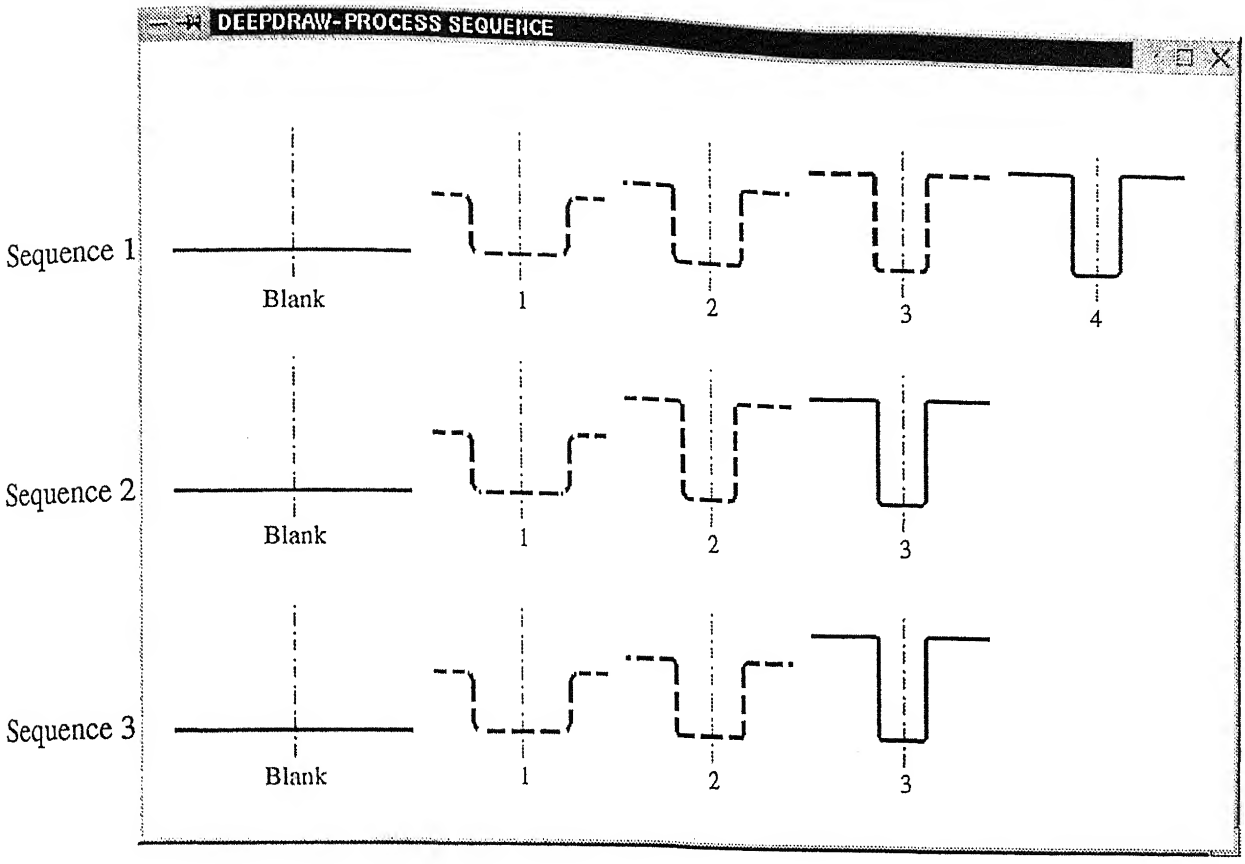

Figure 5.17: Process sequences for wide flanged cup. (CA-DDQ steel, t_0=1 mm, μ=0.1)

produce final cup without annealing, sequences 2 has four stages by performing annealing after first geometric stage (after stage 1) in sequence 1 and sequence 3 has five stages by performing annealing after second geometric stage (after stage 3) in sequence 1. Hence sequence 2 will be optimal sequence with respect to tooling cost and power requirements.

5.3.5 Stepped Cup with Narrow Flange

Figure 5.19 shows the sequences generated by the present system. Table 5.18 and Fig. 5.20 show the formability and the geometrical information respectively for the above sequences. It can be seen from the Fig. 5.19, sequence 1 has seven stages to produce final cup without annealing and sequences 2, 3 have six stages in each case by performing annealing after first geometric stage (stage 2) and second geometric stage (stage 4) respectively in the sequence 1. Hence sequence 2 will be optimal sequence with respect to tooling cost and power requirements.

5.3.6 Stepped Cup with Wide Flange

Figure 5.21 shows the sequences generated by the present system for a stepped cup with wide flange. Table 5.19 and Fig. 5.22 show the formability and the geometrical information respectively

Stage	Die Arc Radius (mm)	Punch Arc Radius (mm)	DR_i	DR_{total}	Cup Radius (mm)	Max. Punch Force (Tons)
sequence 1: Without annealing						
1	15.00	17.00	2.27	2.27	80.82	25.48
2	8.40	10.40	1.43	3.24	56.61	17.84
3	5.00	10.00	1.34	4.35	42.18	13.30
4	5.00	10.00	1.05	4.59	40.00	12.61
sequence 2: Annealing after stage no.1						
1	15.00	17.00	2.27	2.27	80.82	25.48
2	7.20	10.00	1.84	1.84	43.86	13.83
3	5.76	10.00	1.10	2.02	40.00	12.61
sequence 3: Annealing after stage no.2						
1	15.00	17.00	2.27	2.27	80.82	25.48
2	7.20	9.20	1.40	3.19	57.60	18.16
3	5.76	10.00	1.44	1.44	40.00	12.61

Table 5.14: Formability information for the process sequences shown in Fig. 5.17

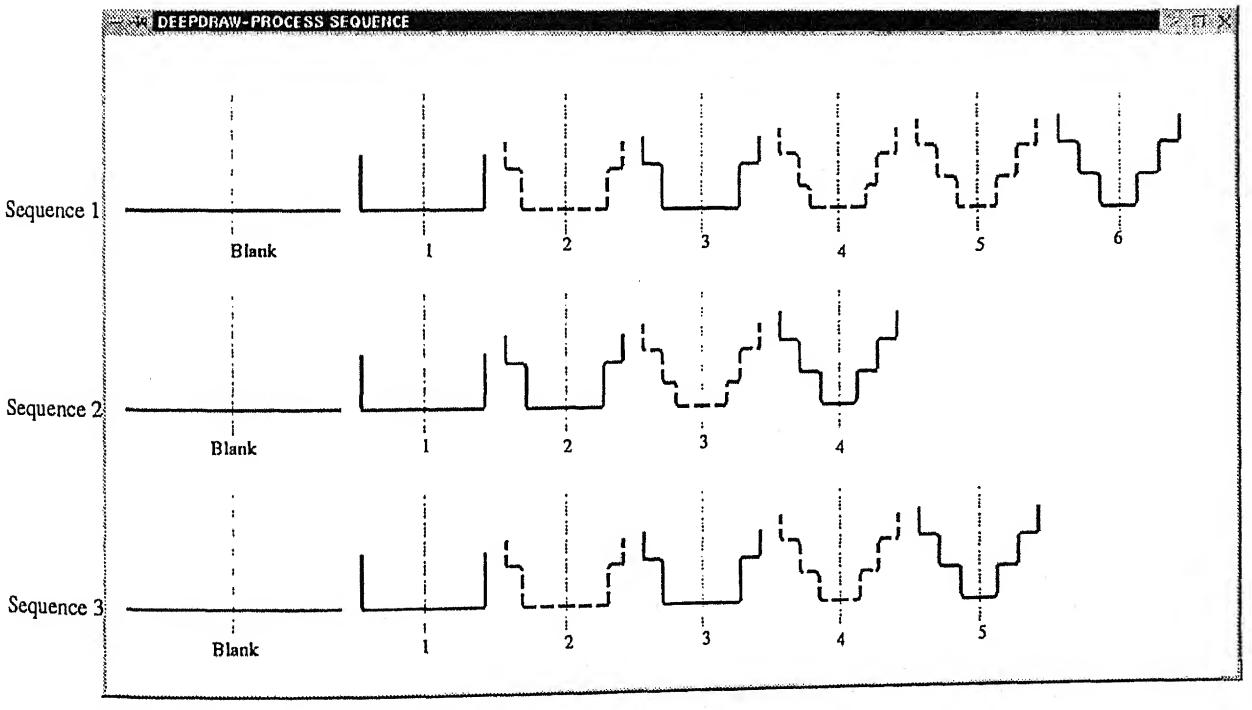

Figure 5.18: Process sequences for stepped cup without flange. (CA-DDQ steel, t_0=1 mm, μ=0.1)

Stage	h	r	v	c	h
Sequence no.1					
0	183.58				
1	63.82	17.00	60.19	15.00	49.18
2	46.21	10.40	100.01	10.50	77.89
3	32.18	10.00	140.43	7.35	95.47
4	30.00	10.00	150.00	5.00	100.00
Sequence no.2					
0	183.58				
1	63.82	17.00	60.19	15.00	49.18
2	33.86	10.00	132.76	10.50	90.64
3	30.00	10.00	150.00	5.00	100.00
Sequence no.3					
0	183.58				
1	63.82	17.00	60.19	15.00	49.18
2	48.40	9.20	98.73	10.50	76.90
3	30.00	10.00	150.00	5.00	100.00

Table 5.15: Geometric information for the process sequences shown in Fig. 5.17

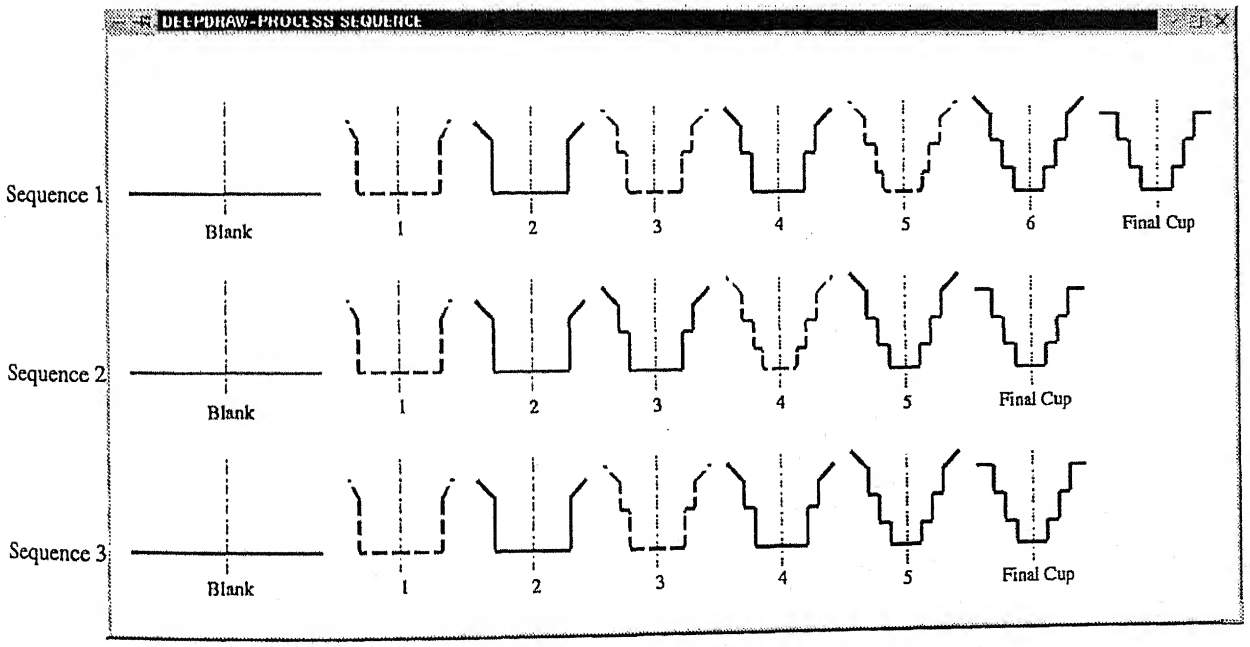

Figure 5.19: Process sequences for stepped cup with narrow flange. (CA-DDQ steel, t_0=1 mm, μ=0.1)

Stage	Die Arc Radius (mm)	Punch Arc Radius (mm)	DR_i	DR_{total}	Cup Radius (mm)	Max. Punch Force (Tons)
sequence 1: Without annealing						
1	4.00	6.00	1.64	1.64	133.00	41.93
2	8.00	9.00	1.34	2.20	98.91	31.18
3	8.00	9.00	1.11	2.45	89.00	28.06
4	10.00	10.00	1.39	3.41	63.80	20.11
5	10.00	10.00	1.45	4.95	43.98	13.86
6	10.00	10.00	1.10	5.44	40.00	12.61
sequence 2: Annealing after stage no.1						
1	4.00	6.00	1.64	1.64	133.00	41.93
2	8.00	9.00	1.49	1.49	89.00	28.06
3	10.00	10.00	1.54	2.31	57.61	18.16
4	10.00	10.00	1.44	3.32	40.00	12.61
sequence 3: Annealing after stage no.3						
1	4.00	6.00	1.64	1.64	133.00	41.93
2	8.00	9.00	1.34	2.20	98.91	31.18
3	8.00	9.00	1.11	2.45	89.00	28.06
4	10.00	10.00	1.91	1.91	46.48	14.65
5	10.00	10.00	1.16	2.22	40.00	12.61

Table 5.16: Formability information for the process sequences shown in Fig. 5.18

for the above sequences. It can be seen from the Fig. 5.21, sequence 1 has five stages to produce final cup without annealing and sequences 2, 3 have four stages in each case by performing annealing after first geometric stage (stage 1) and second geometric stage (stage 3) respectively in the sequence 1. Hence sequence 2 will be optimal sequence with respect to tooling cost and power requirements.

5.3.7 Cup having Tapered Elements with Narrow Flange

Figure 5.23 shows the process sequences generated by the present system. Table 5.20 and Fig. 5.24 show the formability and the geometrical information respectively for the above sequences. It can be seen from the Fig. 5.23, sequence 1 has six stages to produce final cup without annealing, sequences 2 has six stages by performing annealing after first geometric stage (after stage 1) in sequence 1 and sequence 3 has five stages by performing annealing after second geometric stage (after stage 3) in sequence 1. Hence sequence 3 will be optimal sequence with respect to tooling cost and power requirements.

Stage	h	r	v	c	h	r	v	c	h	r	v
Sequence no.1											
0	217.80										
1	127.00	6.00	108.43								
2	89.91	9.00	68.86	8.00	20.09	6.00	50.00				
3	80.00	9.00	77.61	8.00	30.00	6.00	50.00				
4	53.80	10.00	27.08	10.00	6.20	9.00	50.00	8.00	30.00	6.00	50.00
5	33.98	10.00	44.44	10.00	26.02	9.00	50.00	8.00	30.00	6.00	50.00
6	30.00	10.00	50.00	10.00	30.00	9.00	50.00	8.00	30.00	6.00	50.00
Sequence no.2											
0	217.80										
1	127.00	6.00	108.43								
2	80.00	9.00	77.61	8.00	30.00	6.00	50.00				
3	47.61	10.00	31.22	10.00	12.39	9.00	50.00	8.00	30.00	6.00	50.00
4	30.00	10.00	50.00	10.00	30.00	9.00	50.00	8.00	30.00	6.00	50.00
Sequence no.3											
0	217.80										
1	127.00	6.00	108.43								
2	89.91	9.00	68.86	8.00	20.09	6.00	50.00				
3	80.00	9.00	77.61	8.00	30.00	6.00	50.00				
4	36.48	10.00	41.44	10.00	23.52	9.00	50.00	8.00	30.00	6.00	50.00
5	30.00	10.00	50.00	10.00	30.00	9.00	50.00	8.00	30.00	6.00	50.00

Table 5.17: Geometric information for the process sequences shown in Fig. 5.18

5.3.8 Cup having Tapered Elements with Wide Flange

Figure 5.25 shows the process sequences generated by the present system. Table 5.21 and Fig. 5.26 show the formability and the geometrical information respectively for the generated process sequences. It can be seen from the Fig. 5.25, sequence 1 has four stages to produce final cup without annealing and sequences 2, 3 have three stages in each case by performing annealing after first geometric stage (stage 1) and second geometric stage (stage 3) respectively in the sequence 1. Hence sequence 2 will be optimal sequence with respect to tooling cost and power requirements.

5.3.9 Conical Cup with 30° Cone Angle

Figure 5.27 shows the process sequence generated by the present system for a conical cup having 30° cone angle. Table 5.22 and Fig. 5.28 show the formability and the geometrical information

Stage	Die Arc Radius (mm)	Punch Arc Radius (mm)	DR_i	DR_{total}	Cup Radius (mm)	Max. Punch Force (Tons)
sequence 1: Without annealing						
1	8.00	10.00	2.15	2.15	92.28	29.09
2	5.00	8.40	1.05	2.26	88.00	27.74
3	8.00	10.00	1.36	3.07	64.69	20.39
4	5.00	5.00	1.03	3.16	63.00	19.86
5	8.00	10.00	1.36	4.31	46.16	14.55
6	5.00	5.00	1.32	5.68	35.00	11.03
sequence 2: Annealing after stage no.2						
1	8.00	10.00	2.15	2.15	92.28	29.09
2	5.00	8.40	1.05	2.26	88.00	27.74
3	5.00	5.00	1.40	1.40	63.00	19.86
4	8.00	10.00	1.54	2.15	40.94	12.90
5	5.00	5.00	1.17	2.51	35.00	11.03
sequence 3: Annealing after stage no.4						
1	8.00	10.00	2.15	2.15	92.28	29.09
2	5.00	8.40	1.05	2.26	88.00	27.74
3	8.00	10.00	1.36	3.07	64.69	20.39
4	5.00	5.00	1.03	3.16	63.00	19.86
5	5.00	5.00	1.80	1.80	35.00	11.03

Table 5.18: Formability information for the process sequences shown in Fig. 5.19

respectively for the generated process sequences. The number of steps required to produce final conical cup depends on the cone angle. Lesser the cone angle, less number of steps are enough to produce the final cone.

5.3.10 Conical Cup having 20° Cone Angle with Wide Flange

Figure 5.29 shows the process sequence generated by the present system. Tables 5.23 and 5.24 show the formability and the geometrical information respectively for the above sequences.

Stage	h	r	v	c	h	r	v	c	h	r	v	x	i
Sequence no.1													
0	198.85												
1	82.28	10.00	108.07	8.00	44.35								
2	83.00	5.00	108.07	5.00	52.09								
3	54.69	10.00	68.75	8.00	10.31	5.00	50.00	5.00	52.09				
4	58.00	5.00	75.40	5.00	15.00	5.00	50.00	5.00	52.09				
5	36.16	10.00	24.43	8.00	3.84	5.00	50.00	5.00	15.00	5.00	50.00	5.00	52.09
6	30.00	5.00	40.00	5.00	18.00	5.00	50.00	5.00	15.00	5.00	50.00	5.00	52.09
SIZING	30.00	5.00	40.00	5.00	18.00	5.00	50.00	5.00	15.00	5.00	50.00	5.00	30.00
Sequence no.2													
0	198.85												
1	82.28	10.00	108.07	8.00	44.35								
2	83.00	5.00	108.07	5.00	52.09								
3	58.00	5.00	75.40	5.00	15.00	5.00	50.00	5.00	52.09				
4	30.94	10.00	28.86	8.00	9.06	5.00	50.00	5.00	15.00	5.00	50.00	5.00	52.09
5	30.00	5.00	40.00	5.00	18.00	5.00	50.00	5.00	15.00	5.00	50.00	5.00	52.09
SIZING	30.00	5.00	40.00	5.00	18.00	5.00	50.00	5.00	15.00	5.00	50.00	5.00	30.00
Sequence no.3													
0	198.85												
1	82.28	10.00	108.07	8.00	44.35								
2	83.00	5.00	108.07	5.00	52.09								
3	54.69	10.00	68.75	8.00	10.31	5.00	50.00	5.00	52.09				
4	58.00	5.00	75.40	5.00	15.00	5.00	50.00	5.00	52.09				
5	30.00	5.00	40.00	5.00	18.00	5.00	50.00	5.00	15.00	5.00	50.00	5.00	52.09
SIZING	30.00	5.00	40.00	5.00	18.00	5.00	50.00	5.00	15.00	5.00	50.00	5.00	30.00

Figure 5.20: Geometric information for the process sequences shown in Fig. 5.19

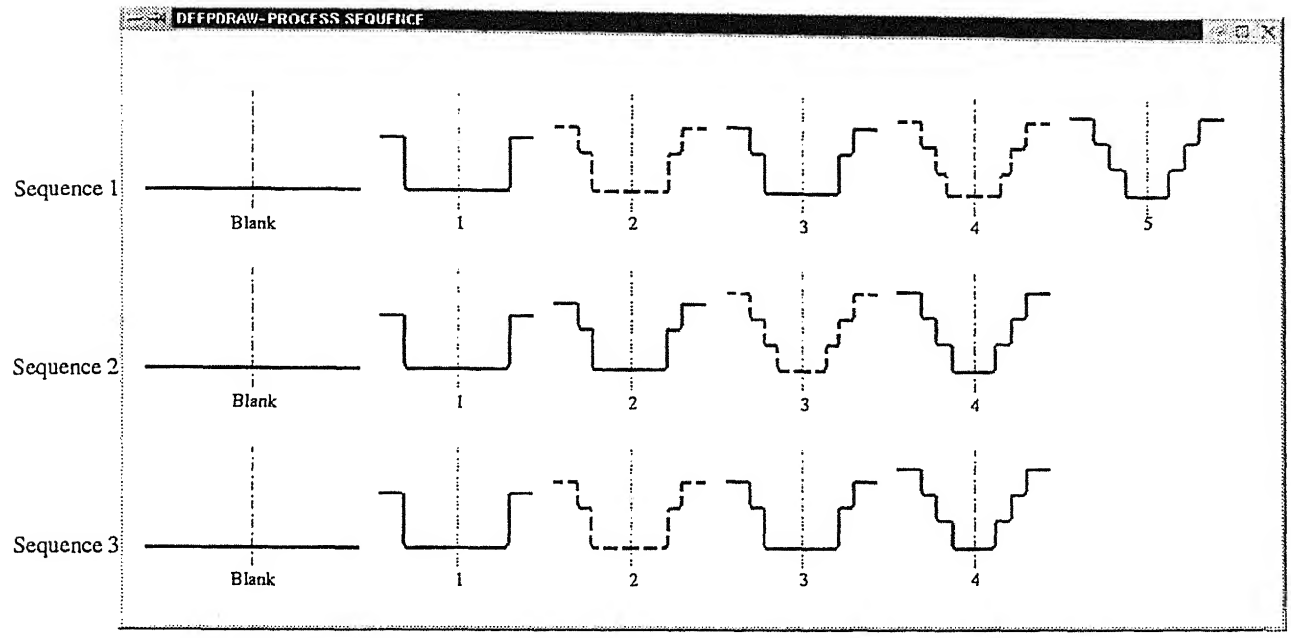

Figure 5.21: Process sequences for stepped cup with wide flange. (CA-DDQ steel, t_0=1 mm, μ=0.1)

Stage	Die Arc Radius (mm)	Punch Arc Radius (mm)	DR_i	DR_{total}	Cup Radius (mm)	Max. Punch Force (Tons)
sequence 1: Without annealing						
1	5.00	8.00	2.01	2.01	119.00	37.51
2	8.00	8.00	1.34	2.70	88.55	27.92
3	5.00	8.00	1.03	2.78	86.00	27.11
4	8.00	10.00	1.37	3.80	62.93	19.84
5	8.00	10.00	1.26	4.79	50.00	15.76
sequence 2: Annealing after stage no.1						
1	5.00	8.00	2.01	2.01	119.00	37.51
2	5.00	8.00	1.38	1.38	86.00	27.11
3	8.00	10.00	1.54	2.13	55.80	17.59
4	8.00	10.00	1.12	2.38	50.00	15.76
sequence 3: Annealing after stage no.3						
1	5.00	8.00	2.01	2.01	119.00	37.51
2	8.00	8.00	1.34	2.70	88.55	27.92
3	5.00	8.00	1.03	2.78	86.00	27.11
4	8.00	10.00	1.72	1.72	50.00	15.76

Table 5.19: Formability information for the process sequences shown in Fig. 5.21

Stage	h	r	v	c	h	r	v	c	h	r	v	c	h
Sequence no.1													
0	239.34												
1	111.00	8.00	106.07	5.00	50.00								
2	80.55	8.00	72.93	8.00	14.45	8.00	45.00	5.00	50.00				
3	78.00	8.00	77.11	5.00	20.00	8.00	45.00	5.00	50.00				
4	52.93	10.00	33.64	8.00	7.07	8.00	45.00	5.00	20.00	8.00	45.00	5.00	50.00
5	40.00	10.00	45.00	8.00	20.00	8.00	45.00	5.00	20.00	8.00	45.00	5.00	50.00
Sequence no.2													
0	239.34												
1	111.00	8.00	106.07	5.00	50.00								
2	78.00	8.00	77.11	5.00	20.00	8.00	45.00	5.00	50.00				
3	45.80	10.00	39.26	8.00	14.20	8.00	45.00	5.00	20.00	8.00	45.00	5.00	50.00
4	40.00	10.00	45.00	8.00	20.00	8.00	45.00	5.00	20.00	8.00	45.00	5.00	50.00
Sequence no.3													
0	239.34												
1	111.00	8.00	106.07	5.00	50.00								
2	80.55	8.00	72.93	8.00	14.45	8.00	45.00	5.00	50.00				
3	78.00	8.00	77.11	5.00	20.00	8.00	45.00	5.00	50.00				
4	40.00	10.00	45.00	8.00	20.00	8.00	45.00	5.00	20.00	8.00	45.00	5.00	50.00

Figure 5.22: Geometric information for the process sequences shown in Fig. 5.21

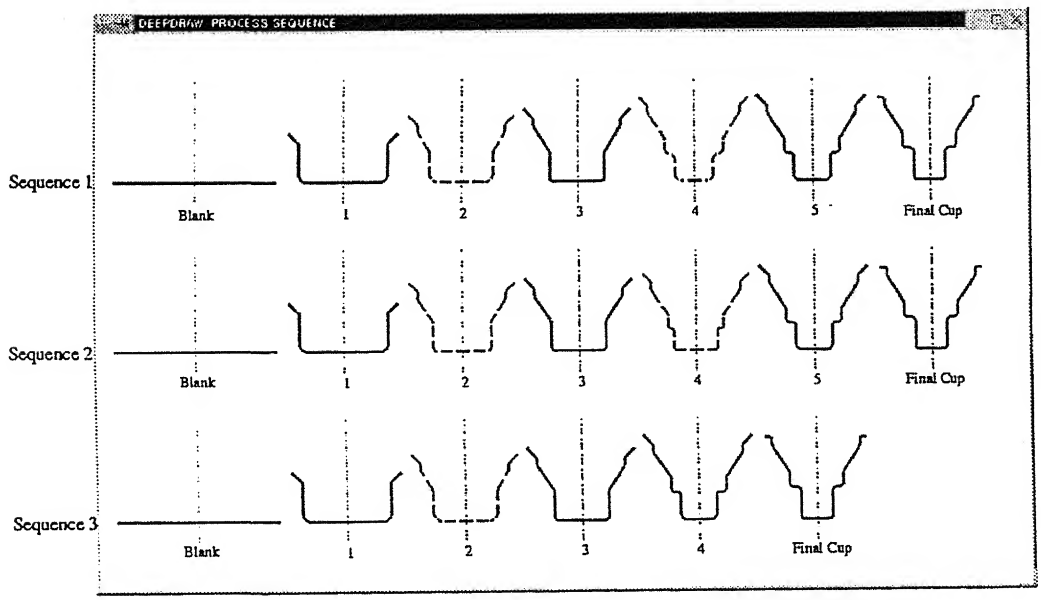

Figure 5.23: Process sequences for cup having tapered element with narrow flange. (Austenitic stainless steel, t_0=1.58 mm, μ=0.1)

Stage	Die Arc Radius (mm)	Punch Arc Radius (mm)	DR_i	DR_{total}	Cup Radius (mm)	Max. Punch Force (Tons)
sequence 1: Without annealing						
1	6.35	12.70	1.81	1.81	72.27	60.29
2	12.64	14.64	1.37	2.48	52.73	43.99
3	6.35	6.35	1.17	2.89	45.25	37.75
4	12.64	14.64	1.43	4.15	31.54	26.31
5	6.35	8.35	1.07	4.46	29.35	24.48
sequence 2: Annealing after stage no.1						
1	6.35	12.70	1.81	1.81	72.27	60.29
2	6.35	6.35	1.53	1.75	47.37	39.52
3	6.35	6.35	1.05	1.83	45.25	37.75
4	6.35	8.35	1.26	2.72	35.86	29.92
5	6.35	8.35	1.22	3.32	29.35	24.48
sequence 3: Annealing after stage no.3						
1	6.35	12.70	1.81	1.81	72.27	60.29
2	12.64	14.64	1.37	2.48	52.73	43.99
3	6.35	6.35	1.17	2.89	45.25	37.75
4	6.35	8.35	1.54	1.54	29.35	24.48

Table 5.20: Formability information for the process sequences shown in Fig. 5.23

Stage	h	r	v	c	h	r	v	x	i	a	v	x	i
Sequence no.1													
0	130.93												
1	59.57	12.70	47.63	6.35	18.51								
2	38.09	14.64	32.60	12.64	28.40	12.70	4.76	6.35	18.51				
3	38.90	6.35	39.42	6.35	44.00	12.70	4.76	6.35	18.51				
4	20.06	11.48	23.29	9.48	0.00	6.35	14.91	6.35	44.00	12.70	4.76	6.35	18.51
5	21.00	8.35	29.47	6.35	3.20	6.35	14.91	6.35	44.00	12.70	4.76	6.35	18.51
SIZING	21.00	4.76	40.00	6.35	5.00	6.35	12.70	12.70	44.00	12.70	5.00	6.35	4.00
Sequence no.2													
0	130.93												
1	59.57	12.70	47.63	6.35	18.51								
2	41.02	6.35	39.15	6.35	40.10	12.70	4.76	6.35	18.51				
3	38.90	6.35	39.42	6.35	44.00	12.70	4.76	6.35	18.51				
4	30.67	5.19	26.18	3.19	0.00	6.35	14.91	6.35	44.00	12.70	4.76	6.35	18.51
5	21.00	8.35	29.47	6.35	3.20	6.35	14.91	6.35	44.00	12.70	4.76	6.35	18.51
SIZING	21.00	4.76	40.00	6.35	5.00	6.35	12.70	12.70	44.00	12.70	5.00	6.35	4.00
Sequence no.3													
0	130.93												
1	59.57	12.70	47.63	6.35	18.51								
2	38.09	14.64	32.60	12.64	28.40	12.70	4.76	6.35	18.51				
3	38.90	6.35	39.42	6.35	44.00	12.70	4.76	6.35	18.51				
4	21.00	8.35	29.47	6.35	3.20	6.35	14.91	6.35	44.00	12.70	4.76	6.35	18.51
SIZING	21.00	4.76	40.00	6.35	5.00	6.35	12.70	12.70	44.00	12.70	5.00	6.35	4.00

Figure 5.24: Geometrical information for the process sequences shown in Fig. 5.23.

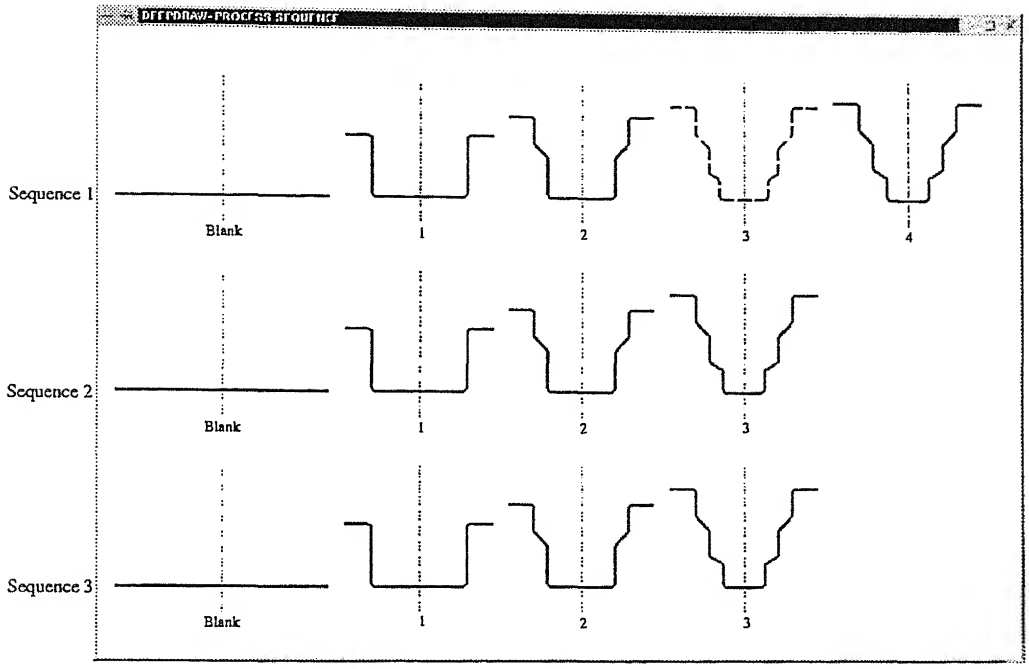

Figure 5.25: Process sequences for cup having tapered elements with Wide flange. (CA-DDQ steel, t_0=1 mm, μ=0.1)

Stage	Die Arc Radius (mm)	Punch Arc Radius (mm)	DR_i	DR_{total}	Cup Radius (mm)	Max. Punch Force (Tons)
sequence 1: Without annealing						
1	7.00	10.00	2.16	2.16	92.20	29.07
2	6.00	10.00	1.39	3.00	66.32	20.90
3	8.00	10.00	1.41	4.24	47.00	14.82
4	8.00	10.00	1.18	4.98	40.00	12.61
sequence 2: Annealing after stage no.1						
1	7.00	10.00	2.16	2.16	92.20	29.07
2	6.00	10.00	1.39	1.39	66.32	20.90
3	8.00	10.00	1.66	2.31	40.00	12.61
sequence 3: Annealing after stage no.2						
1	7.00	10.00	2.16	2.16	92.20	29.07
2	6.00	10.00	1.39	3.00	66.32	20.90
3	8.00	10.00	1.66	1.66	40.00	12.61

Table 5.21: Formability information for the process sequence shown in Fig. 5.25

Stage	h	r	v	x	i	a	v	x	i	a	v	c	h
Sequence no.1													
0	199.21												
1	82.20	10.00	100.44	7.00	40.00								
2	56.32	10.00	66.05	6.00	30.00	10.00	40.00	7.00	40.00				
3	37.00	10.00	25.12	8.00	11.92	10.00	40.00	6.00	30.00	10.00	40.00	7.00	40.00
4	30.00	10.00	30.00	8.00	20.00	10.00	40.00	6.00	30.00	10.00	40.00	7.00	40.00
Sequence no.2													
0	199.21												
1	82.20	10.00	100.44	7.00	40.00								
2	56.32	10.00	66.05	6.00	30.00	10.00	40.00	7.00	40.00				
3	30.00	10.00	30.00	8.00	20.00	10.00	40.00	6.00	30.00	10.00	40.00	7.00	40.00
Sequence no.3													
0	199.21												
1	82.20	10.00	100.44	7.00	40.00								
2	56.32	10.00	66.05	6.00	30.00	10.00	40.00	7.00	40.00				
3	30.00	10.00	30.00	8.00	20.00	10.00	40.00	6.00	30.00	10.00	40.00	7.00	40.00

Figure 5.26: Geometric information for the process sequence shown in Fig. 5.25

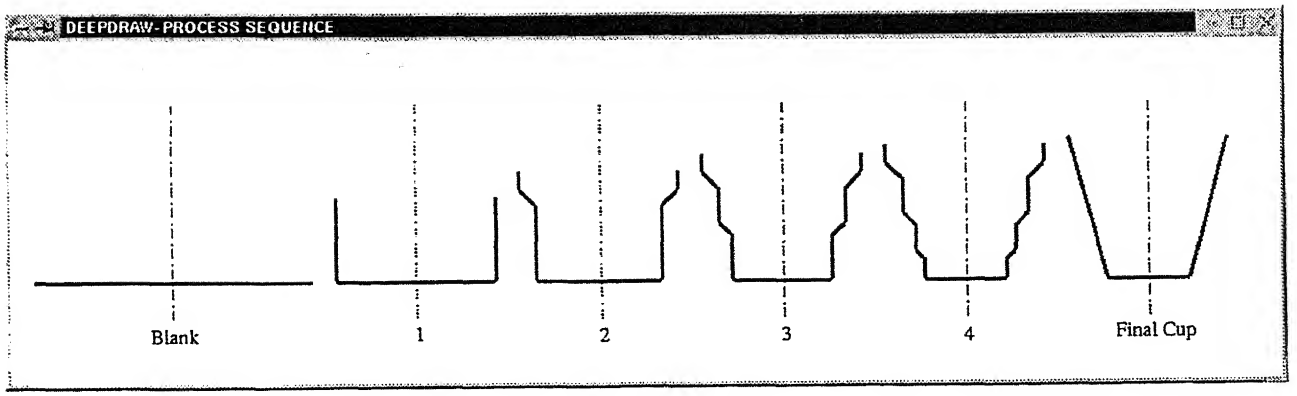

Figure 5.27: Process sequences for conical cup having cone angle 30°. (CA-DDQ steel, t_0=1 mm, μ=0.1)

Stage	Die Arc Radius (mm)	Punch Arc Radius (mm)	DR_i	DR_{total}	Cup Radius (mm)	Max. Punch Force (Tons)
1	5.00	7.00	1.76	1.76	162.40	51.19
2	5.00	7.00	1.25	2.21	129.44	40.80
3	5.00	7.00	1.25	2.76	103.41	32.60
4	5.00	7.00	1.22	3.36	85.00	26.79

Table 5.22: Formability information for the process sequence shown in Fig. 5.27

Stage	h	a	v	x	i	a	v	x	i	a	v	x	i	a	v
Sequence no.1															
0	285.70														
1	155.40	7.00	166.13												
2	122.44	7.00	146.05	5.00	41.65	7.00	34.17								
3	96.41	7.00	83.77	5.00	31.86	7.00	66.14	5.00	41.65	7.00	34.17				
4	78.00	7.00	34.17	5.00	21.08	7.00	45.32	5.00	31.86	7.00	66.14	5.00	41.65	7.00	34.17
	h	a	i												
SIZING	80.00	5.00	300.00												

Figure 5.28: Geometric information for the process sequence shown in Fig. 5.27

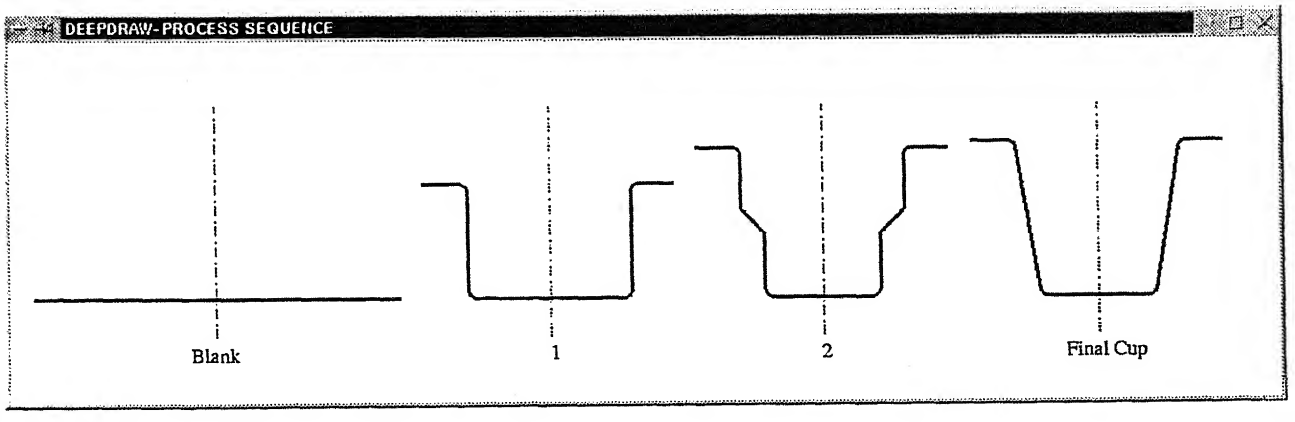

Figure 5.29: Process sequences for conical cup having cone angle 20^o with wide flange. (CA-DDQ steel, t_0=1 mm, μ=0.1)

Stage	Die Arc Radius (mm)	Punch Arc Radius (mm)	DR_i	DR_{total}	Cup Radius (mm)	Max. Punch Force (Tons)
1	5.00	7.00	2.21	2.21	57.26	18.05
2	5.00	7.00	1.43	3.17	40.00	12.61

Table 5.23: Formability information for the process sequence shown in Fig. 5.29

Stage	h	a	v	x	i	a	v	x	h
Sequence no.1									
0	126.62								
1	50.26	7.00	67.58	5.00	25.00				
2	33.00	7.00	34.63	5.00	19.45	7.00	34.63	5.00	25.00
	h	a	i	x	h				
SIZING	35.00	5.00	100.00	5.00	25.00				

Table 5.24: Geometric information for the process sequence shown in Fig. 5.29

Chapter 6

Conclusions and Scope for the Future Work

6.1 Conclusions

The following conclusions are drawn from the present work:

- Analysis model presented by Sonis et al. [2003] is modified by introducing sheet thickness as a variable by considering bending and straightening effects along the die profile. A provision to avoid wrinkling is considered while selecting the blank holding force. The limiting drawing ratios for the first as well as subsequent draws predicted by the analysis model are in good agreement with the LDR values available in the literature [Thorp, 1973; El-Sebaie and Mellor, 1972; Leu, 1991 and Lange, 1985].
- The guidelines and the practices followed in deep drawing process are collected from the handbooks, research papers and are implemented in the form of design rules.
- Process sequences generated by the present system are tested with the process sequences available in the literature [Jones, 1951; Eshel et al., 1986; Sitaraman et al., 1991; ASM hand book,1992; Park et al.,1998], they are in good agreement.
- Alternative sequences are generated by performing annealing between stages.
- An attempt is made to develop an intelligent aid to the process designer for manufacturing of axisymmetric deep drawn components.

6.2 Scope for the Future Work

Future work can be planned to consider the following aspects for the process design of deep drawing operation:

- In the present work, thickness variation (thinning and thickening) and effect of punch profile radius are not included in the analysis model. These effects can be include to get more accurate results.
- Planar anisotroty has to be incorporated to predict earing of sheet.
- The present work is developed for the flat-bottmmed deep drawn cups only. The process design systems can be extended for other axisymmetric shapes.
- Three dimensional modeling can be done for the geometric description.
- Cost analysis can be done for the selection of optimum process sequence.

References

1. Ahmetoglu, M., Broek, T.R., Kinzel, G., Altan, T., Control of Blank Holder Force to Eliminate Wrinkling and Fracture in Deep Drawing Rectangular Parts, *Annals of CIRP*, Vol. 44, No. 1, pp 247-250, 1995.

2. Altan, T, Oh, S.I., and Gegel, H., *Metal Forming: Fundamentals and Applications,* ASM Internatioanl, 1983.

3. Atkinson, M., *Sheet Metal Industries*, Vol. 44, pp 167-178, 1967.

4. Chiang, D.C., and Kobayashi, Shiro, The Effect of Anisotropy and Workhardening Characteristics on Stress and Strain Distribution in Deep Drawing, *Trans ASME, Journal for Engg. for Industry,* Nov. 1966.

5. Chung, S.Y. and Swift, H.W., Cup Drawing from a Flat Blank. Part I Experimental Investigation,*Proc. Instn Mech. Engrs.*, U.K. pp 199-211, 1951.

6. ASM Handbook, 1992.

7. Doege, E., Schulte, S. Design of Deep Drawn Components with Elementary Calculation Methods, *J. of Mat. Processing Tech.*, Vol.34, pp 439 -447, 1992.

8. *Die Design HandBook*, McGraw-Hill Book Co. Inc.,1955.

9. Eary, D.F., and Reed, E.A.,*Techniques of pressworking sheet metal*, Prentice Hall, Englewood Cliffs.

10. Emani, S. Axisymmetrical Plastic Flow of Anisotropic Sheet During Deep Drawing, *Sheet Metal Industries*, No. 4, April 1984.

11. El-Sebaie and Mellor, P.B., Plastic Instability Conditions in the Deep Drawing of a Circular Blank of Sheet Metal, *Int. J. of Mech. Science*, Vol. 14, pp 535-556, 1972.

12. Esche. S.K., Khamitkar, S., Kinzel, G.L., Altan T., Process and Die Design for Multi-step Forming of Round Parts from Sheet Metal, *J. of Mat. Processing Tech.*, Vol. 59, pp 24-33, 1996.

13. Esche, S.K., Ahmetoglu, M., Kinzel, G.L., Altan T., Numerical and Experimental Investigation of Redrawing of Sheet Metals, *J. of Mat. Processing Tech.*, Vol. 98, pp 17-24, 2000.

14. Eshel, G., Barash, M. and Johnson, W.,Rule Based Modeling for Planning Axisymmetrical Deep Drawing, *J. of Mech. Working Tech.*, Vol.14, pp 1-115, 1986.

15. Fogg, B., Theoretical Analysis for the Redrawing of the Cylindrical Cups Through Conical Dies Without Pressure Sleeves, *J. of Mech. Engrs Science*, Vol. 10, pp 141-152, 1968.

16. Groover, M.P., *Fundamentals of Modern Manufacturing*, John Wiley&sons, Inc, 1995.

17. Hill, R., *The Mathematical Theory of Plasticity*, Clarendon Press, Oxford (U.K.), 1950.

18. Hosford, W.F., and Caddell, R.M., *Metal Forming - Mechanics and Metallurgy*, Prentice Hall, Englewood Cliffs, 1983

19. Johnson, W., amd Mellor, P.B., *Engineering Plasticity*, Van Nostrand and Reinhold, 1972.

20. Jones, F.D., *Die Design and Die Making Practice*, Industrial Press, 1951.

21. Kang, S.S., Park, D.H., and Choi, B.K., *Int. J. of Mat. Processing. Tech.*, Vol. 124, pp 36-48, 2002.

22. Korhonen, A.S., Drawing Force in Deep Drawing of Cylindrical Cup with Flat Nosed Punch, *J. for Engg. for Ind.*, Vol 104, pp 29-37, 1982.

23. Lange, K., *HandBook of Metal Forming*, McGraw-Hill Book Co.,1985.

24. Leu, D.K., Prediction of the Limiting Drawing Ratio and the Maximum Drawing Load in Cup Drawing, *Int. J. of Mach. Tools Manuf.*, Vol. 37, No. 2, pp 201-213, 1997.

25. Leu, D.K., The Limiting Drawing Ratio for Plastic Instability of the Cup Drawing Process *Int. J. of Mat. Processing Tech.*, Vol. 86, No. 2, pp 168-176, 1999.

26. Min, D.K., Jeon, B.H., Kim, H.J., Kim, N., A Study on Process Improvements of Multi-Stage Deep Drawing by The Finite Element Method, *Int. J. of Mat. Processing Tech.*, Vol. 54, pp 230-238, 1995.

27. Oskada, K., Wang, C.C. and Mori, K. Controlled FEM Simulation for Determining History of Blank Holding Force in Deep Drawing, *Annals of CIRP*, Vol. 44, No. 1, pp 243-246, 1995.

28. Park, S.B., Choi, Y., Kim, B.M. and Choi, J.C., *J Mat. Processing Tech.*, Vol. 75, pp 17-26, 1998.

29. Parsa, M.H., Yamaguchi, K., Takakura, N., Imatani, S., Consideration of the Redrawing of Sheet Metals Based on Finite Element Simulation, *Int. J. of Mat. Processing Tech.*, Vol. 47, pp 87-101, 1994.

30. Reissner, J., and Meier, M., Instability of the Annular Ring as a Deep Drawn Flange Under Real Conditions, *Annals of CIRP*, Vol. 32, No.1, pp 187-190, 1983.

31. Reissner, J., and Ehrismann, R., Computer-Aided Deep Drawing of Two Part Cans, *Annals of CIRP*, Vol. 36, pp 199-202, 1987.

32. Rogers, R.W., and Anderson, W.A., Effect of Plastic Anisotropy on Drawing characteristics of Aluminium Alloy sheet, *Metal Forming-Interrelation between theory and practice*, Edited by A.L. Hoffmanner, 1971, Plenium Press, New York, London.

33. Schuler, *Metal Forming HandBook*, Springer, 1998.

34. Sing, W.M., and Rao, K.P., Knowledge-Based Process Layout System For Axisymmetrical Deep Drawing Using Decision Tables, *Computers ind. Engng.*, Vol. 32, pp 299-319, 1997.

35. Sitaram, S.K., Kinzel, G.L., and Altan T., A Knowledge Based System for Process Sequence Design in Axisymmetric Sheet Metal Forming, *J. of Mat. Processing Tech.*, Vol.25, pp 247 -271, 1991.

36. Sonis, P., Reddy, N.V., Lal, G.K., *On Multistage Deep Drawing of Axisymmetric Components*, ASME J. of Manuf. sci.&Engg., 2003, Vol 125, (In Press).

37. Tisza, M. Expert Systems for Metal Forming, *J. of Mat. Processing Tech.*, Vol. 53, pp 423 -432, 1995.

38. Wallace, J.W., Improvement In Punches For Cylindrical Deep Drawing, *Sheet Metal Industries*, pp 901-904, Dec 1960.

39. Wilson, D.V., Sunter, B.J., and Martin D.F., *Sheet Metal Industries*, Vol. 43, pp 465-476, 1966.

40. Wright J.C., Relationship Between Mechanical Properties, Deep Drawablity and Stretch-Formability for some non-ferrous Sheet Materials, *Sheet Metal Industries*, pp 887-901, Dec 1962.

41. Woo, D.M., On The Complete Solution The Deep Drawing Problem, *Int. J. of Mech. Science*, Vol. 10, 1968.

42. Yu, T.X. and Johnson, W., The Buckling of Annular Plates in Relation to the Deep Drawing Process, *Int. J. of Mech. Science*, Vol. 24, No. 3, pp 175-188, 1982.

Appendix

Appendix A

Solutions of the Integral Terms

I

$$\int_{r_{cd}}^{r_0}\left(ln\frac{R}{r}\right)^n\frac{dr}{r}=\int_{r_{cd}}^{r_0}\left[1+(ln\frac{R}{r}-1)\right]^n\frac{dr}{r}$$

$$=\int_{r_{cd}}^{r_0}\left[1+n\Big(ln\frac{R}{r}-1\Big)\right]\frac{dr}{r}$$

$$=n\int_{r_{cd}}^{r_0}ln\frac{R}{r}\frac{dr}{r}+(1-n)ln\frac{r_0}{r_{cd}} \tag{A.1}$$

The integral term at the right side of the Eq. ?? can also be approximated as :

$$\int_{r_{cd}}^{r_0}ln\frac{R}{r}\frac{dr}{r}=\int_{r_{cd}}^{r_0}2\Big[\frac{\frac{R}{r}-1}{\frac{R}{r}+1}\Big]\frac{dr}{r}=2\int_{r_{cd}}^{r_0}\Big(1-\frac{2r}{R+r}\Big)\frac{dr}{r}$$

$$=2ln\frac{r_0}{r_{cd}}-4\int_{r_{cd}}^{r_0}\frac{1}{R+r}dr \tag{A.2}$$

Based on the volume constancy of the plastic deformation in the flange region of the cup-drawing, i.e. $R_0^2-r_0^2=R^2-r^2=R_2^2-r_{cd}^2=C^2$ =constant, Eq. A.2 can be expressed as

$$\int_{r_{cd}}^{r_0}ln\frac{R}{r}\frac{dr}{r}=2ln\frac{r_0}{r_{cd}}-\frac{4}{C^2}\int_{r_{cd}}^{r_0}(R-r)dr$$

$$=2ln\frac{r_0}{r_{cd}}-\frac{4}{C^2}\Big(\int_{r_{cd}}^{r_0}\sqrt{C^2+r^2}dr-\frac{r_0^2-r_{cd}^2}{2}\Big)$$

$$=2\Big[ln\frac{r_0}{r_{cd}}-\frac{1}{C^2}\Big(R_0r_0-R_2r_{cd}+C^2ln\frac{R_0+r_0}{R_2+r_{cd}}$$

$$-r_0^2+r_{cd}^2\Big)\Big] \tag{A.3}$$

Sustituting the above terms in Eq. A.3, one can get the following equation.

$$\int_{r_{cd}}^{r_0}\left(ln\frac{R}{r}\right)^n\frac{dr}{r}=(1+n)ln\frac{r_0}{r_{cd}}-2n\Big(ln\frac{R_0+r_0}{R_2+r_{cd}}+\frac{r_0}{R_0+r_0}-\frac{r_{cd}}{R_2+r_{cd}}\Big) \tag{A.4}$$

$$\int_{r_{cd}}^{r_{c_0}} ln\frac{R}{r}\frac{dr}{r} = \int_{r_{cd}}^{r_{c_0}} 2\Big[\frac{\frac{R}{r}-1}{\frac{R}{r}+1}\Big]\frac{dr}{r} = 2\int_{r_{cd}}^{r_{c_0}} \Big(1-\frac{2r}{R+r}\Big)\frac{dr}{r}$$

$$= 2ln\frac{r_{c_0}}{r_{cd}} - 4\int_{r_{cd}}^{r_{c_0}} \frac{1}{R+r}dr \tag{A.5}$$

Let R_{i+1} be the intermediate radius on the base of the cup after I pass. From the volume constancy, $R^2 - r^2 = R_{i+1}^2 - r_{cd}^2 = C^2$ =constant

$$4\int_{r_{cd}}^{r_{c_0}} \frac{1}{R+r}dr = 4\int_{r_{cd}}^{r_{c_0}} \frac{R-r}{C^2}dr$$

$$= \frac{4}{C^2}\int_{r_{cd}}^{r_{c_0}} \sqrt{C^2+r^2}dr - \int_{r_{cd}}^{r_{c_0}} rdr$$

$$= \frac{2}{C^2}\Big[\Big(r\sqrt{C^2+r^2} + C^2 ln(r+\sqrt{C^2+r^2})\Big)_{r_{cd}}^{r_{c_0}} - (r_{c_0}^2 - r_{cd}^2)\Big]$$

$$= \frac{2}{C^2}\Big[r_{c_0}\sqrt{R_{i+1}^2 - r_{cd}^2 + r_{c_0}^2} - r_{cd}\,R_{i+1} - (r_{c_0}^2 - r_{cd}^2) + (R_{i+1}^2 - r_{cd}^2)\Big[ln\frac{r_{c_0} + \sqrt{R_{i+1}^2 - r_{cd}^2 + r_{c_0}^2}}{r_{cd} + R_{i+1}}\Big]\Big]$$

Equation becomes

$$\int_{r_{cd}}^{r_{c_0}} ln\frac{R}{r}\frac{dr}{r} = 2\Big[ln\frac{r_{c_0}}{r_{cd}} - \frac{1}{R_{i+1}^2 - r_{cd}^2}\Big[r_{c_0}\sqrt{R_{i+1}^2 - r_{cd}^2 + r_{c_0}^2} - r_{cd}R_{i+1} - (r_{c_0}^2 - r_{cd}^2)$$

$$+(R_{i+1}^2 - r_{cd}^2)\Big[ln\frac{r_{c_0} + \sqrt{R_{i+1}^2 - r_{cd}^2 + r_{c_0}^2}}{r_{cd} + R_{i+1}}\Big]\Big]\Big] \tag{A.6}$$

Appendix B

Product and Process Design Rules for Deep Drawing

Introduction

Process design for deep drawn components is composed of both analytical and empirical techniques. Analytical methods are usually based on specified mathematical models. The results obtained are sometimes far from satisfactory due to the change of process conditions or some unpredictable variables. As the analytical methods have some limitations, it can be applied only to specialized types of cups. Hence an aid of experimental knowledge and experience is a must in deep drawing. In the present work, guidelines for deep drawing [Jones, 1951; Eshel et al, 1986; Sitaraman et al.,1991; Eshe et al, 1996; Sing et al.,1998] are collected from the literature and are arranged in the form of design rules. These rules are implemented in the form of *if-then-else* statements.

Rules for Die and Punch Geometries

Die and punch profile radii have significant effect on the LDR. It has been experimentally proved [] that die corner radius has more effect on the LDR than frictional effects. In the present work following guidelines are used to select the punch, die profile radii and die clearance.

Die Corner Radius

The radius of the draw die corner should be as large as possible to aid the flow of metal. If the die arc radius is too small, the material will rupture while it is bending around the die edge. Further, small die arc radius increases bending stresses and leads to lesser limiting drawing ratios. A sharp die corner radius produces heat buildup in the corner making it difficult to maintain lubrication and making galling more troublesome. This causes the die to weaken and erode. However, if the die arc radius is too large, the material will be released by the blank

holder too soon and wrinkling will result. Therefore a recommended safe region for die corner radius is between 4 to 10 times the sheet thickness [Lange, 1985]. After reducing the radius in each subsequent operation to a minimum value a smaller corner radius can be obtained in the sizing operation as the last forming process.

Punch Corner Radius

The punch nose radius should be sufficiently large enough to avoid both punching out the bottom of the cup and tilting the part during forming. The suggested safe limit for the punch corner radius is 4 to 10 times sheet thickness [ASM Hand book, 1992]. The punch corner radius should be larger than the die corner radius by a factor of 3 to 5 and should never be smaller than the die corner radius otherwise the punch may shear the material [Lange, 1985]. Ideally, the punch corner radius should be same as the corner radius of the required cup, because it takes its form. It is not possible in deep drawing to obtain the final cup size in a single drawing operation. For the initial draws, larger punch corner radii are used and for the final draw the required radius is used and this pass is generally called as sizing pass.

Die Clearance

The clearance between the punch and die must be sufficiently large in order to avoid ironing. The amount of clearance actually used in deep drawing depends upon the part requirements and the sheet material. Clearances upto 20% greater than blank thickness are generally used, yielding a cup which is slightly ironed at the top. Although ironing adds additional force to the total punch load, it occus late in the draw cycle after the maximum punch force is reached. However, if there is severe ironing then the punch force may cross the limiting value during ironing stage. Hence severe ironing will reduce the limiting drawing ratio and also leads to higher tool pressures and shorter tool life. Redrawing operation requires greater clearance, in relation to blank thickness, than the first draw in order to compensate for the increase in sheet thickness during previous draws. Table B.1 lists clearances for cupping, redrawing and sizing draws of cylindrical parts from sheet metal of various thicknesses. The clearance between punch and die for the first draw can also be calculated form

$$Clearance = t_0 \sqrt{\frac{D_0}{d}}$$

where t_0 is the sheet thickness, D_0 is the blank diameter and d is the punch diameter[Sing et al, 1998].

Rules for Geometric Sequence

The geometric sequence rules are concerned with generating a sequence backwards from final product to initial blank. Starting from the bottom of the final part, a set of deformed elements

Blank thickness(mm)	First Draws	Redraws	Sizing draw
Up to 0.38	1.07-1.09t_0	1.08-1.10t_0	1.04-1.05t_0
0.41-1.27	1.08-1.10t_0	1.09-1.12t_0	1.05-1.06t_0
1.29-3.18	1.10-1.12t_0	1.12-1.14t_0	1.07-1.09t_0
3.2 and up	1.12-1.14t_0	1.15-1.20t_0	1.08-1.10t_0

Table B.1: Punch to die clearance for drawing operations, ASM Handbook [1992]

is identified which can be formed from a cup consisting of a fillet while disregarding the remaining elements. After that, all remaining elements are appended to this cup. Then, this resulting geometry and the rules are applied recursively until the current geometry is a flat circular blank. Fig.B.1 shows the principle of backward sequencing. The assumptions have

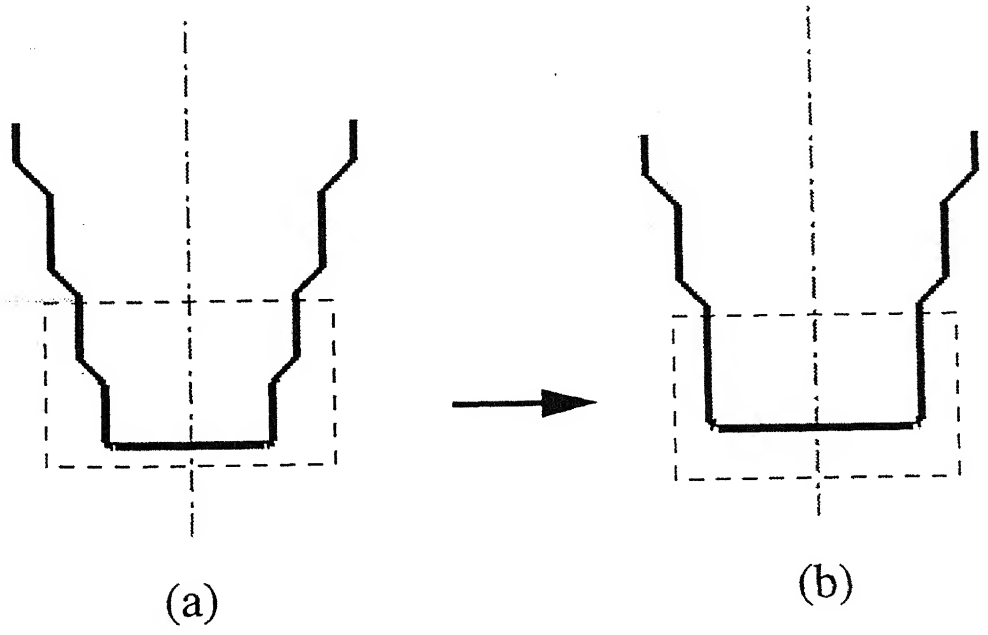

Figure B.1: Generation of Geometric Sequence, (a) Current deformation zone (b) Previous deformation zone

been made for designing the initial process sequence to simplify the sequence calculations are.

1. The sheet thickness is assumed to be constant during the drawing, therefore surface area of the final cup is equal to the surface area of the initial blank.

2. All fillets on the part and tool (punch and die) are assumed to be circular arcs.

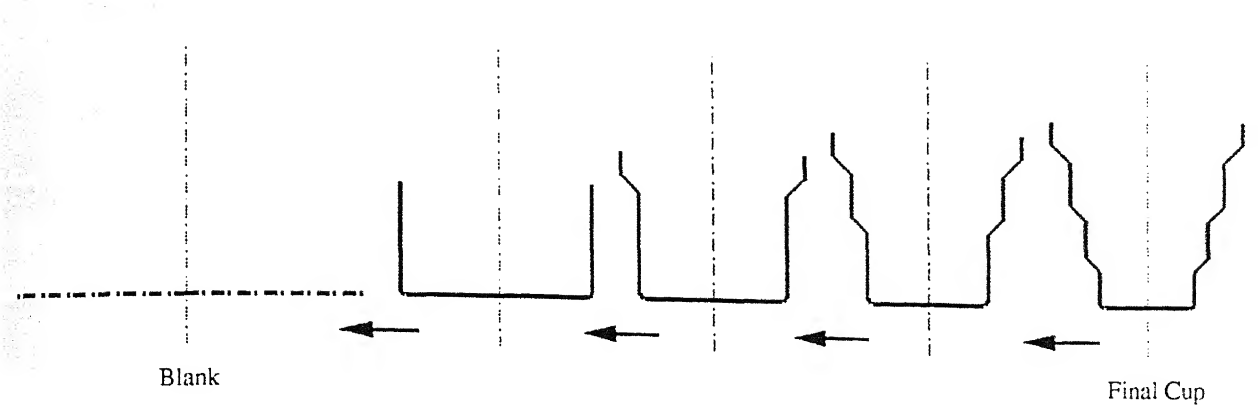

Figure B.2: Backward generation of geometric sequence

To compensate the above assumptions a trimming allowance is added interactively by the designer to the surface area of the final cup. Esche et al, [1996] presented the sequence of steps involved in the geometric sequencing are listed below

1. Starting from the bottom, identify the current deformed set of elements in the final cup (portion of the cup with in the rectangular box shown in Fig. B.1 a).
2. Compute the surface area of the current deformed set.
3. Select the previous deformed set as a straight non-flanged cup of diameter equal to the maximum diameter of the current deformed set (portion of the cup with in the rectangular box shown in Fig. B.1 b).
4. Calculate the fillet radius connecting the cup bottom and wall as a function of the sheet thickness in the previous deformed set.
5. Compute the surface areas of the fillet and the flat bottom of previous deformed set.
6. Compute the cup height of the previous deformed set by equating it with the surface area of the current deformed set.
7. Replace the current deformed set with previous deformed set in the final cup to get the previous geometric shape (Fig. B.1 b) for the final cup.
8. Repeat the same procedure for the previous geometric shape until the previous deformed set is a blank (Fig. B.2).

The rules presented by Eshel et al, [1986] are implemented in the present system to generate geometric sequence and are given below.

Rule 1: If a stepped cup is required then it should be produced by a sequence of operations, where each operation produces one new deformation zone.

Rule 2: If available processes can produce a set of elements of monotonically nondecreasing diameters and distances from the bottom, then deformation-zone$_{current}$ is identified in the set of the bottommost elements of the cup.

Rule 3: If the deformation-zone$_{current}$ is to be identified then it should include a combination of elements such that it is producible by one of the participating processes for example straight-cupping, direct-redrawing, tapered-cupping.

Rule 4: If deformed-zone$_{previous}$ is to be designed then deformation-zone$_{current}$ should be one that is producible in one operation.

Rule 5: If the set of elements, starting from the bottom, is

E4,E3,E2,E1 or E3,E2,E1 or E2,E1 where:

E4 is an element of type: v,

E3 is an element of type: h;i;c;r,

E2 is an element of type: v;i;c;r,

E1 is an element of type: h

then the set can constitute one deformation-zone$_{current}$.

Rule 6: If deformation-zone$_{previous}$ is to be designed then it should be straight, vertical non-flanged cup, i.e., one that consists of a wall, a recess radius and a bottom, or a blank only.

Rule 7: If shape$_{current}$ is a cup having two or three elements, then shape$_{previous}$ is a circular blank.

Rule 8: The total material volume of a set of deformed elements, before and after deformation, is constant (or the meridional surface area of a set of deformed elements, for all practical purposes is constant).

Rule 9: If the angle between adjacent elements in the cross section of the cup is less than πradians (measured between the cross section of the main portion of the closer-to-orifice element and the main portion of the adjacent element) then the bend radius of the deformation-zone is determined by the punch.

Rule 10: If the angle between adjacent elements in the cross section of the cup is greater than π radians then the bend radius of the deformation-zone is determined by the die.

Rules for Rectification

The process sequence generated using the geometric sequence may not be feasible, as the formability of the material is not taken into consideration. Process analysis model developed during the present work is used to test the formability of the process sequence generated by the geometric sequence module. Process sequence is modified by adding new intermediate stages to the process sequence generated by the geometric design module wherever the process analysis predicted formability violation (Fig.B.3). The sequence of steps [Esche et al, 1996] to introduce intermediate stages are listed below.

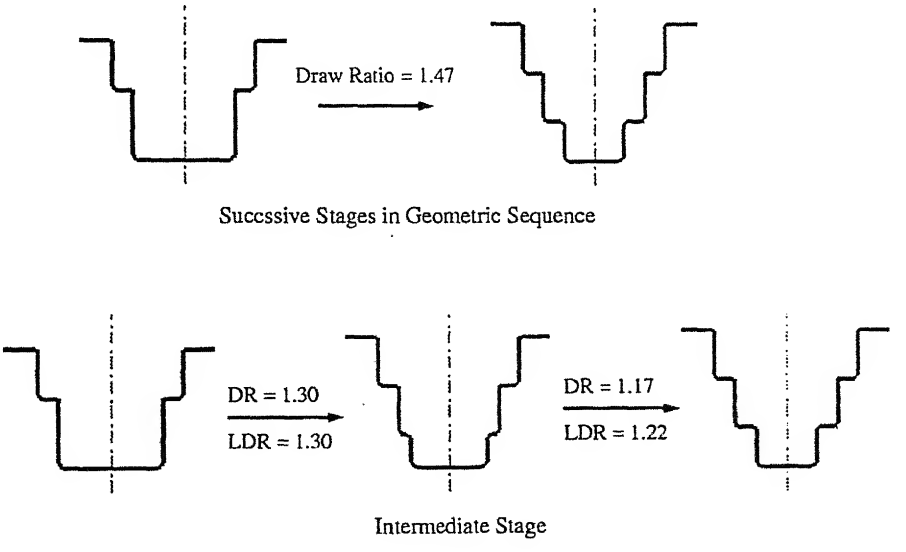

Figure B.3: Rectification of geometric sequence by adding intermediate stage

1. Determine the drawing ratio required between two successive stages in geometric sequence.
2. Select the punch corner, die corner radii and then compute the possible LDR using the analysis model presented in chapter 2.
3. Compare the drawing ratio required and determined LDR.
4. Add intermediate stages between the successive stages in geometric sequence if LDR is less than the required drawing ratio.
5. Set the cup diameter according to LDR and set the fillet radius connecting the cup bottom and wall.
6. Compute the surface areas of the fillet and the flat bottom.
7. Compute the cup height from the surface area of the deformed set of elements.

There are rules for the intermediate stages to select the fillet radii, finishing stages and other considerations. Some important rules used for rectification of geometric sequence are presented below.

Rule 11: If a horizontal element cannot be completed in one draw then by adding portions of the element in a series of redraws, build it up towards the center (the axis of rotational symmetry).

Rule 12: If the sizes of the geometrical features of the cup are the required finished ones and final sizing is to be employed then it is necessary to design the intermediate shape so that each of the volumetric elements, within the zone to be sized will undergo a minimal possible plastic deformation.

Rule 13: If the sizes of the geometrical features of the cup are the required finished ones and final sizing is not employed then it is necessary to design the intermediate shape such that those features assume their final values.

Rule 14: If the sizes of the geometrical features of the cup are not the required finished ones then it is necessary to design the intermediate shape with optimal bend radii.

Rule 15: If multistage drawing is introduced and the difference between $wall_{current}$ and $wall_{nextpass}$ is less than the sum of optimal die and punch profile radii then the intermediate pass should be designed such that the outcoming cup will have a zero-length sloped recess element and optimal die and punch profile radii.

Rules for Cups having Tapered Elements

Cups having tapered elements can be drawn through conical dies. These dies generally incorporate half-angles anywhere between 15^o to 45^o and the upper and lower edges of the beveled surfaces are typically rounded to required radius. In case of conical cups the zone between the die and the punch where the work is not supported is crucial as it may leads to the formation of puckers (wrinkles at the bottom). In this unsupported region the tangential compressive stresses may cause puckering. In order to minimize the formation of puckering, the blank holder pressure must be increased or draw beads must be implemented, but this will reduce the possible LDR [Lange, 1985]. One stage tapering is possible when the height of the tapered cup to diameter of the open end ratio is ≤ 0.25 and the corresponding limiting drawing ratio should not exceed 2. However, for conical parts with a wall angle of $\leq 15^o$, drawing can proceed analogous to that of cylindrical draws. If a tapered cup cannot be produced in a single stage then it is generally formed by producing a stepped cup then using a final forming stage to produce the tapered wall [Jones, 1951 and Eshel et al, 1986] as shown in Fig.B.4. The rules for producing tapered cups are presented below.

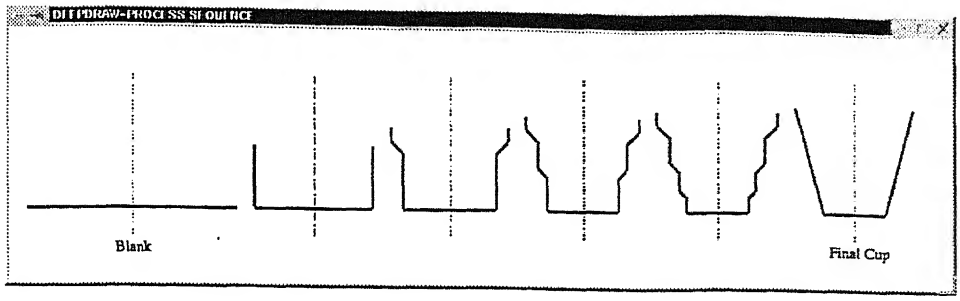

Figure B.4: Drawing of conical cup

Rule 16: If a redrawing operation has to produce an intermediate tapered recess element then simultaneously increase the length of the tapered element and deepen the vertical portion of the cup.

Rule 17: If a tapered element cannot be drawn in one draw then by adding portions of the element in a series of redraws, build it up towards the bottom.

Rule 18: If a severe cone or a deep-concave cup cannot be drawn in one tapering operation then draw it from an intermediate stepped cup.

Rule 19: If an intermediate stepped cup is to be drawn, as a means of producing a severe cone then design it such that each step is drawn to the smallest possible diameter (final cone not intersected), the optimal recess element angle (15^o tapered), maximal depth and optimal recess radii, provided that the accumulated height does not exceed the required finished height.

Rule 20: Limiting drawing ratio for tapered cups is approximately equal to Limiting drawing ratio for straight cup/conicity severity [Eshel et al., 1986]. Where conicity severity is the ratio between height to diameter ratio of vertical cup and height to diameter ratio of tapered cup.

Rules for Flanged Cups

In the case of flange formation, the blank is not completely pushed into the die cavity but some material between die and blank holder which forms the flange portion. Jones, [1951] classified the flanges into two categories namely wide flange and narrow flange. Although there is no exact distinction between these two categories, some rules can be separately used for flange formation in these two cases.

For narrow flange category an angular flange is formed partially in various stages of drawing. Conical dies are used till the prefinal draw with increasing cone angle. In the final step of drawing the flange is flattened and sized to its final dimensions. For wide flange category the

flange is formed to its final diameter from the beginning itself and its inner diameter is reduced step by step in further reductions [Jones, 1951].

Rule 21: If the final cup geometry has a flat flange, and the outer diameter of the flange is less than 1.45 times cup diameter then form the flange as an angular element and size it in the last stage of deep drawing [Jones, 1951 and Sitaraman, 1991].

Rule 22: If the final cup geometry has a flat flange, and the outer diameter of the flange is more than 1.45 times cup diameter then one should employ the first draw to obtain the outside diameter of the finished flange [Jones, 1951].

Miscellaneous Rules

Rule 23: Severity of wrinkling is predicted by relative sheet thickness ($\frac{t_0}{D_0} \times 100$). Eary et al, [1974] presented requirement of blank holding force according to the severity of wrinkling same is shown in Table B.2.

$\frac{t_0}{D_0} \times 100$	Wrinkling	Blank holding force
< 0.50	severe	A substantial blank holding force is required
0.50 to 1.50	moderate	Sufficient blank holding force is required
1.5 to 2.5.	slight	A blank holding force may be required if reduction is severe
> 2.5	No wrinkling	No blank holding force is required

Table B.2: Severity of wrinkling [Eary et al, 1974]

Rule 24: For cupping, annealed metals, medium and thin walled blanks, the blank holding force should not be less than one third of the punch force.

Rule 25: For shallow drawings, low-carbon steels, thin-walled blanks, the blank holding force is selected as a percentage of the punch-force and is a function of the wall-thickness of the blank, as given in table B.3.

Rule 26: If a material responds to heat-treatment (annealing, tempering) the it should be introduced whenever the total strain reached to a limiting value or the Max. allowed number of redraws is reached.

Sheet thickness t_0 (in.)	Blank holder force (%)	Sheet thickness t_0 (in.)	Blank holder force (%)
0.005	85.00	0.050	23.00
0.010	67.00	0.070	14.00
0.015	57.00	0.100	09.00
0.020	50.00	0.125	08.50
0.025	44.00	0.187	08.25
0.030	39.00	0.250	08.00

Table B.3: Blank holding force as a percentage of punch force [Eshel et al, 1986]

Rule 27: If interstage heat-treatment (annealing, tempering) is performed then strain history is nullified.